

Aus der Klinik für Neurologie  
(Prof. Dr. D. Kömpf)  
und dem Interdisziplinären Zentrum für Genetisch Bedingte Bewegungsstörungen  
(Prof. Dr. C. Klein)  
vertreten in der Technisch-Naturwissenschaftlichen Fakultät  
durch das Institut für Biologie der Universität zu Lübeck  
(Direktor: Prof. Dr. E. Hartmann)

---

**Molecular characterisation of  
*SGCE*-associated myoclonus-dystonia and  
*PINK1*-associated Parkinson's disease**

Inauguraldissertation  
zur  
Erlangung der Doktorwürde  
der Universität zu Lübeck  
- Aus der Technisch-Naturwissenschaftlichen Fakultät -

Vorgelegt von  
**Anne Grünewald**  
aus Chemnitz

Lübeck, 2008

- |                        |                                     |
|------------------------|-------------------------------------|
| 1. Berichterstatter:   | Prof. Dr. rer. nat. E. Hartmann     |
| 2. Berichterstatterin: | Prof. Dr. med. C. Klein             |
| 3. Berichterstatterin: | Prof. Dr. rer. nat. B. Royer-Pokora |

Tag der mündlichen Prüfung: 16.12.2009  
zum Druck genehmigt.

Lübeck, den 16.12.2009

gez. Prof. Dr. rer. nat. J. Prestin  
- Dekan der Technisch-Naturwissenschaftlichen Fakultät -

This thesis is dedicated to my family.

**LIST OF CONTENT**

<b>1</b>	<b>INTRODUCTION.....</b>	<b>1</b>
<b>1.1</b>	<b>Movement disorders – dystonia and parkinsonism.....</b>	<b>1</b>
<b>1.2</b>	<b>Dystonia.....</b>	<b>3</b>
1.2.1	<i>SGCE</i> -associated myoclonus-dystonia.....	4
1.2.2	Detection of microdeletions .....	6
1.2.3	Maternal imprinting in myoclonus-dystonia .....	7
<b>1.3</b>	<b>Parkinsonism and Parkinson’s disease.....</b>	<b>7</b>
1.3.1	<i>PINK1</i> -associated Parkinson’s disease.....	9
1.3.2	Heterozygous mutations in Parkinson’s disease .....	11
1.3.3	A common pathway in Parkinson’s disease? .....	12
1.3.4	Nonsense-mediated mRNA decay as a disease mechanism.....	13
<b>1.4</b>	<b>Mitochondria in Parkinson’s disease.....</b>	<b>13</b>
1.4.1	The electron transport chain .....	13
1.4.1.1	Complex I.....	14
1.4.1.2	Complex II+III .....	14
1.4.1.3	Complex IV .....	15
1.4.1.4	Complex V .....	15
1.4.2	Implications of complex I deficiency in Parkinson’s disease .....	16
<b>1.5</b>	<b>Hypotheses.....</b>	<b>18</b>
<b>2</b>	<b>PATIENTS, MATERIAL AND METHODS .....</b>	<b>19</b>
<b>2.1</b>	<b>Patients .....</b>	<b>19</b>
2.1.1	M-D patients with mutations in <i>SGCE</i> and family members.....	19
2.1.2	PD patients with mutations in <i>PINK1</i> and controls.....	20
2.1.2.1	Family W.....	20
2.1.2.2	Other <i>PINK1</i> mutants.....	20
2.1.2.3	Healthy controls included in the <i>PINK1</i> studies .....	20
<b>2.2</b>	<b>Material .....</b>	<b>23</b>
2.2.1	Chemicals .....	23
2.2.2	Solutions .....	25
2.2.3	Kits .....	26
2.2.4	Antibodies .....	26
2.2.5	Oligonucleotides.....	27

2.2.6	Equipment .....	27
2.2.7	Software.....	28
<b>2.3</b>	<b>Methods .....</b>	<b>28</b>
2.3.1	Extraction of nucleic acids .....	28
2.3.1.1	DNA extraction from whole blood .....	28
2.3.1.2	DNA extraction from fibroblasts .....	28
2.3.1.3	RNA extraction from whole blood.....	28
2.3.2	Polymerase chain reaction.....	29
2.3.2.1	Standard PCR.....	29
2.3.2.2	PCR with fluorescence-labelled primers: Genotyping and sequencing.....	29
2.3.2.3	Real-time PCR: Gene dosage studies.....	30
2.3.2.4	Real-time PCR: Gene expression studies.....	32
2.3.2.5	Multiplex ligation-dependent probe amplification.....	32
2.3.3	Gel electrophoresis .....	33
2.3.3.1	Agarose gel electrophoresis .....	34
2.3.3.2	Denaturing polyacrylamide gel electrophoresis for DNA .....	34
2.3.4	Determination of reduced cellular glutathione .....	35
2.3.4.1	Reverse-phase HPLC .....	35
2.3.4.2	Sample Preparation .....	36
2.3.5	Tissue culture .....	36
2.3.5.1	Fibroblast culture .....	36
2.3.5.2	Passage of fibroblasts.....	36
2.3.5.3	Treatment with toxins .....	36
2.3.6	Mitochondrial preparation.....	37
2.3.7	Protein determination .....	37
2.3.8	Mitochondrial enzyme assays .....	37
2.3.8.1	Citrate synthase assay .....	38
2.3.8.2	Malate dehydrogenase assay .....	38
2.3.8.3	Complex I assay (NADH dehydrogenase).....	38
2.3.8.4	Complex II+III assay (succinate cytochrome c reductase) .....	39
2.3.8.5	Complex IV assay (cytochrome c oxidase).....	39
2.3.9	Cellular ATP concentration.....	40
2.3.10	Mitochondrial membrane potential .....	40

2.3.11	Western blotting .....	41
2.3.11.1	Sample preparation.....	41
2.3.11.2	Denaturing PAGE for proteins.....	41
2.3.11.3	Non-denaturing PAGE for proteins .....	42
2.3.11.4	Protein transfer .....	43
2.3.11.5	Antibody staining of Western blots.....	43
2.3.12	Staining of the mitochondrial network .....	43
2.3.13	Electron microscopy.....	44
2.3.13.1	Sample preparation.....	44
2.3.13.2	Microscopic analysis.....	44
2.3.14	Review of the literature .....	45
<b>3</b>	<b>RESULTS.....</b>	<b>46</b>
<b>3.1</b>	<b>Myoclonus-dystonia: Significance of large <i>SGCE</i> deletions .....</b>	<b>46</b>
3.1.1	Patients .....	46
3.1.2	Quantitative mutational screening.....	50
3.1.3	Determination of the extent of the large deletions .....	52
3.1.4	Qualitative mutational screening.....	54
3.1.5	Review of mutations in <i>SGCE</i> .....	54
<b>3.2</b>	<b>Parkinson's disease: Gene expression in patients with <i>PINK1</i> mutations .....</b>	<b>56</b>
3.2.1	<i>PINK1</i> genomic and cDNA sequencing analysis .....	56
3.2.2	Haplotype analysis .....	58
3.2.3	<i>PINK1</i> gene expression .....	58
3.2.4	Review of mutations in <i>PINK1</i> .....	59
<b>3.3</b>	<b>Parkinson's disease: Mitochondrial function and morphology in patients with <i>PINK1</i> mutations .....</b>	<b>62</b>
3.3.1	Mitochondrial respiratory chain enzyme complexes.....	62
3.3.2	Mitochondria content and mtDNA levels .....	63
3.3.3	Assembly of respiratory chain enzyme complexes .....	64
3.3.4	Mitochondrial membrane potential .....	65
3.3.5	Cellular ATP content.....	66
3.3.6	Oxidative stress in <i>PINK1</i> mutant fibroblasts.....	67
3.3.7	Mitochondrial network.....	68
3.3.8	Electron microscopy studies.....	68

<b>4</b>	<b>DISCUSSION .....</b>	<b>70</b>
<b>4.1</b>	<b>Myoclonus-dystonia: Significance of large <i>SGCE</i> deletions .....</b>	<b>70</b>
4.1.1	Frequency and type of <i>SGCE</i> mutations .....	70
4.1.2	Comparison of phenotype and genotype .....	71
4.1.3	Clinical relevance of deletion mutations in <i>SGCE</i> .....	73
4.1.4	Deviation from paternal transmission .....	73
<b>4.2</b>	<b>Parkinson's disease: Gene expression in patients with <i>PINK1</i> mutation.....</b>	<b>74</b>
4.2.1	Frequency and significance of heterozygous <i>PINK1</i> mutations .....	74
4.2.2	Genetic origin of the <i>PINK1</i> c.1366C>T mutation .....	74
4.2.3	Influence of the c.1366C>T mutation on the <i>PINK1</i> gene expression....	75
4.2.4	Genotype-phenotype correlation in Family W .....	76
<b>4.3</b>	<b>Parkinson's disease: Mitochondrial function and morphology in patients with <i>PINK1</i> mutations .....</b>	<b>77</b>
4.3.1	Mutations in <i>PINK1</i> alter respiratory chain enzyme activities .....	77
4.3.2	Reductions in membrane potential and ATP level .....	78
4.3.3	Elevated oxidative stress in <i>PINK1</i> mutant cells .....	79
4.3.4	Mitochondrial fusion in <i>PINK1</i> mutant cells .....	80
<b>4.4</b>	<b>Conclusions .....</b>	<b>82</b>
<b>5</b>	<b>PERSPECTIVES.....</b>	<b>85</b>
<b>6</b>	<b>SUMMARY.....</b>	<b>87</b>
<b>7</b>	<b>ZUSAMMENFASSUNG .....</b>	<b>89</b>
<b>8</b>	<b>REFERENCES .....</b>	<b>92</b>
<b>9</b>	<b>APPENDIX .....</b>	<b>109</b>
<b>9.1</b>	<b>List of abbreviations.....</b>	<b>109</b>
<b>9.2</b>	<b>Supplementary material .....</b>	<b>112</b>
<b>9.3</b>	<b>Curriculum vitae .....</b>	<b>115</b>
<b>9.4</b>	<b>Publications .....</b>	<b>117</b>
<b>9.5</b>	<b>Acknowledgements .....</b>	<b>119</b>
<b>9.6</b>	<b>Declaration .....</b>	<b>121</b>

## LIST OF FIGURES

Fig 1	<i>Projects and levels of investigation in the present thesis. ....</i>	1
Fig 2	<i>Scheme of neuronal traces in the basal ganglia for motor control. ....</i>	2
Fig 3	<i>Potential connection between environmental and genetic factors, and PD. ....</i>	17
Fig 4	<i>Pedigree of Family W. ....</i>	22
Fig 5	<i>Principle of the MLPA analysis. ....</i>	33
Fig 6	<i>Scheme to illustrate the apparatus used to determine GSH by reverse-phase HPLC and electrochemical detection. ....</i>	35
Fig 7	<i>Projects and levels of investigation in the present thesis [Project A]. ....</i>	46
Fig 8	<i>(previous page) Relevant pedigrees of families with M-D of index patients (A) IP15916; (B) IP16535; (C) IP15624; (D) IP15251 and (E) IP2141. ....</i>	50
Fig 9	<i>(previous page) Screening for exon rearrangements. ....</i>	52
Fig 10	<i>Scheme of the genomic region, surrounding SGCE, with relevant markers and qPCRs. ....</i>	53
Fig 11	<i>Schematic representation of the SGCE gene and identified mutations. ....</i>	55
Fig 12	<i>Projects and levels of investigation in the present thesis [Project B]. ....</i>	56
Fig 13	<i>Electropherograms of genomic DNA and cDNA. ....</i>	57
Fig 14	<i>PINK1 haplotype analysis. ....</i>	58
Fig 15	<i>Histograms displaying results of the quantitative PINK1 mRNA analysis. ....</i>	59
Fig 16	<i>Box-and-Whisker Plot showing clustered results of the mRNA expression analysis for each mutational status in Family W. ....</i>	60
Fig 17	<i>The human PINK1 gene and identified mutations. ....</i>	61
Fig 18	<i>Projects and levels of investigation in the present thesis [Project C]. ....</i>	62
Fig 19	<i>Respiratory chain enzyme complexes I-IV. ....</i>	63
Fig 20	<i>Mitochondria content and mtDNA levels. ....</i>	64
Fig 21	<i>Protein expression of the respiratory chain enzyme complexes. ....</i>	65
Fig 22	<i>Membrane potential under basal and stress conditions. ....</i>	66
Fig 23	<i>ATP levels under normal conditions. ....</i>	66
Fig 24	<i>Indicators of oxidative stress. ....</i>	67
Fig 25	<i>Mitochondrial network in primary fibroblasts. ....</i>	68
Fig 26	<i>Mitochondrial morphology in fibroblasts. ....</i>	69
Fig S1	<i>Determination of the optimal number of control genes for normalization. ....</i>	112
Fig S2	<i>Average expression stability values (M) of reference genes calculated by the geNorm VBA applet. ....</i>	112

**LIST OF TABLES**

<i>Table 1</i>	<i>Genetic causes of dystonia .....</i>	<i>4</i>
<i>Table 2</i>	<i>Genetic causes of parkinsonism .....</i>	<i>8</i>
<i>Table 3</i>	<i>Classification criteria of M-D phenotypes in the SGCE study.....</i>	<i>19</i>
<i>Table 4</i>	<i>Genotypic and phenotypic characterization of Family W.....</i>	<i>21</i>
<i>Table 5</i>	<i>Demographic, clinical and genetic data of index patients and affected family members investigated in the M-D study .....</i>	<i>48</i>
<i>Table 6</i>	<i>Summary of the mitochondrial function and morphology data.....</i>	<i>69</i>
<i>Table S1</i>	<i>Primer for PCR-amplification of SGCE genomic fragments .....</i>	<i>113</i>
<i>Table S2</i>	<i>Primer for gene dosage quantification of SGCE exons .....</i>	<i>113</i>
<i>Table S3</i>	<i>Primer for PCR-amplification of PINK1 genomic fragments.....</i>	<i>113</i>
<i>Table S4</i>	<i>Primer for the quantification of the PINK1 expression level.....</i>	<i>114</i>

## 1 INTRODUCTION

The present thesis investigates two different movement disorders: *Epsilon-sarcoglycan* (*SGCE*)-associated myoclonus-dystonia (M-D) and *PTEN-induced putative kinase 1* (*PINK1*)-associated Parkinson's disease (PD). The spectrum of investigation spans the genomic, mRNA, protein, and functional level (see Fig 1).

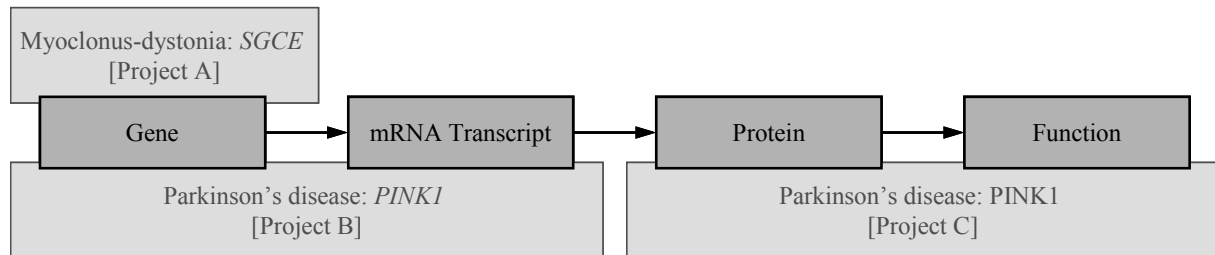


**Fig 1** Projects and levels of investigation in the present thesis. The scheme shows the three research projects (A, B and C) included in this thesis according to their level of investigation: Gene, mRNA transcript, protein and function.

In this introduction the clinical features of dystonia and PD, their physiological commonalities and differences are described (1.1). Furthermore, the current state of knowledge regarding genetic causes of both diseases is given (1.2 and 1.3) focussing on *SGCE* and *PINK1* as the genes involved in M-D and PD, respectively (1.2.1 and 1.3.1). In the fourth section, findings supporting a link between mitochondrial function and PD are summarized (1.4).

### 1.1 Movement disorders – dystonia and parkinsonism

Both diseases investigated in this thesis are movement disorders sharing the common features of impaired planning, control or execution of movement.

Parkinsonism belongs to the class of akinetic rigid syndromes, it is neurodegenerative and occurs in advanced age in the majority of cases. In contrast, dystonias are classified as hyperkinetic syndromes. Dystonia patients do usually not show neurodegeneration and their symptoms start often during childhood or early adulthood (Klein, 2005).

There are ‘overlap syndromes’ which combine signs of both diseases, such as the dystonia-parkinson syndromes DYT3, DYT5 and DYT12. Another link between dystonia and parkinsonism is that in some forms of parkinsonism dystonias occur as the first clinical feature. This overlap can be explained as both diseases are caused by alterations within the same neuronal circuit, the extrapyramidal system (EPS) (Herrero *et al.*, 2002).

The EPS has been implicated in a number of important motor functions, especially the initiation of motor responses. The EPS is a complex neuronal network, encompassing the cerebral cortex, thalamus, basal ganglia, brain stem nuclei and cerebellum, which provides the execution of voluntary movements, innately involuntary movements and learnt automatic movements. All regulatory components considered part of the extrapyramidal system modulate motor activity without directly innervating motor neurons.

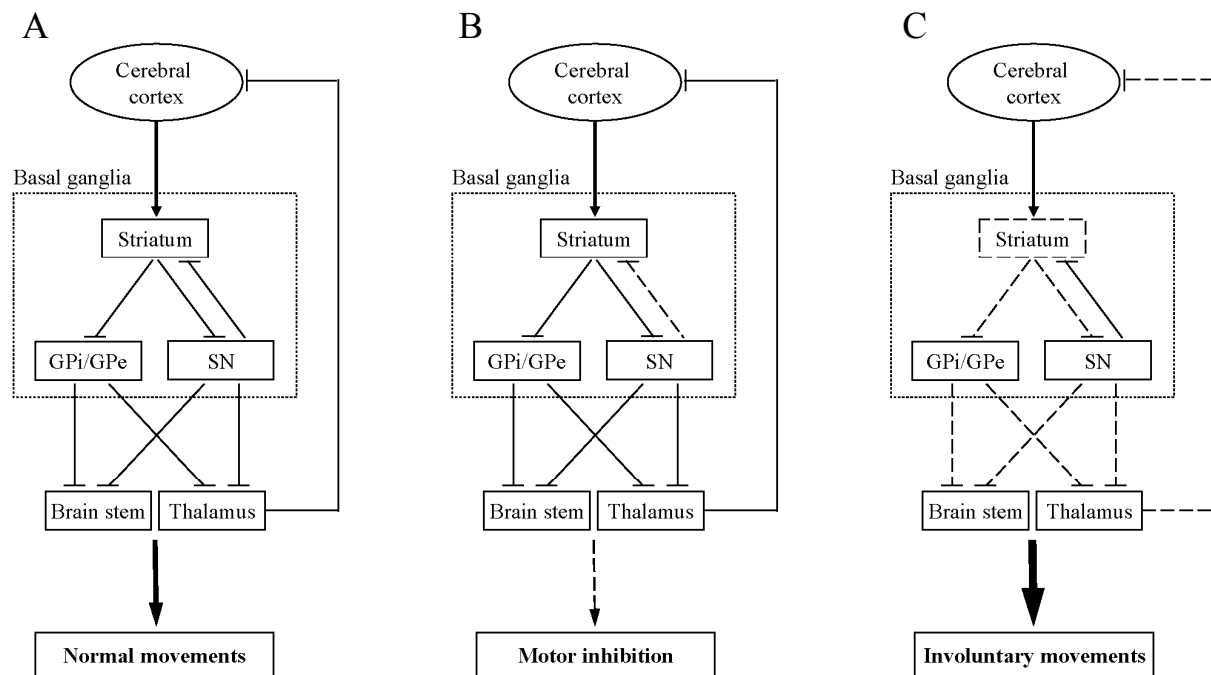


**Fig 2** Scheme of neuronal traces in the basal ganglia for motor control. (A) Signalling under healthy conditions. (B) Alterations of signalling in PD. Decreased inhibition of the striatum by the SN leads to motor inhibition. (C) Alterations for dystonias. Malfunction of the striatum results in additional, involuntary movements. Arrows stand for activating signals, crossbars indicate inhibitory signals. Bold lines highlight increasing signal intensity, discontinuous lines emphasize a reduction of the signal intensity. Regions of the basal ganglia are surrounded by a dotted line. GPi/e – internal/external globus pallidus, SN – substantia nigra. Scheme modified analogue to the literature (Herrero *et al.*, 2002; Todd and Perlmutter, 1998).

The basal ganglia are a group of interconnected subcortical nuclei. They comprise one input structure, the striatum, and two output structures, the substantia nigra (SN) and the globus pallidus (GP). The excitatory signals entering the basal ganglia originate from the cerebral cortex. In the basal ganglia they are processed and transmitted as inhibitory signals to the brain stem, partially to the motor thalamus and from there back to the cortex (Fig 2). In parkinsonism a decreased inhibition of the striatum leads to motor inhibition (Herrero *et al.*, 2002). In dystonias and dyskinesias, however a malfunction of the striatum itself is thought to cause involuntary movements (Todd and Perlmutter, 1998).

## 1.2 Dystonia

In 1897, Lluís Barraquer-Roviralta described a patient with generalized dystonia under the term of athetosis (Barraquer-Roviralta, 1897), a term which was used earlier by William Alexander Hammond. He had identified abnormalities in the structure of the basal ganglia in his athetosis patients when he investigated their brain post-mortem (Hammond, 1871). These findings and the twisting, sustained character and action exacerbation observed in dystonia as well as athetosis aroused a first interest of clinicians and researchers for the peculiar brain area. Focal dystonias were appreciated earlier than generalized dystonia and were categorized as cramps or “occupational spasms.” In 1836 Johann Heinrich Kopp described the features of writer’s cramp in his German medical monograph (Kopp, 1830-45). In 1908 the clinical picture of dystonia was further expanded by Markus Walter Schwalbe who described the hereditary pattern and progression of generalized torsion dystonia (Schwalbe, 1908). The term “dystonia” was introduced by Hermann Oppenheim in 1911 to reflect his conclusion that the disorder was associated with a generalized abnormality of tone with coexistent hypo- and hypertonia (Oppenheim, 1911).

To date, the prevalence of dystonia is estimated to be at least 10 per 100,000 persons in different populations (Butler *et al.*, 2004; Matsumoto *et al.*, 2003). Several different classification schemes have been used to categorize the various forms of dystonia. The simplest classification of dystonia distinguishes primary and secondary forms: In the primary form, dystonia (with the exception of tremor) is the only symptom of the disease, and the cause is either unknown or genetic. In the secondary form, dystonia is usually one of several disease manifestations and the cause is identifiable (e. g. lesion, drugs/toxins, metabolic disorders). From those two a third form denominated as dystonia-plus syndromes is distinguished. There are uncertainties about placing the dystonia-plus group that is considered a special subcategory associated with, but not secondary to other types of movement disorders (Klein, 2005).

In the past decade, monogenic defects have been found to underlie many forms of primary dystonia and dystonia-plus syndromes. These monogenetic forms have recently been classified according to the gene or gene loci involved. Currently, 15 different types of dystonia are distinguished genetically, which are designated DYT1-13, DYT15 and DYT16 (Table 1). Six of these 15 dystonias are primary forms (DYT1, 2, 4, 6, 7, and 13). While three types of the dystonias represent recessive or X-linked forms (DYT2, 3 and 5b), the majority are inherited in an autosomal dominant fashion. Genes have been identified for seven (DYT1, 3, 5, 8, 11, 12 and 16), and the chromosomal location is known for another six forms (DYT6,

7, 9, 10, 13, and 15). However, despite the identification of several genes linked to dystonia and the observation of a positive family history in a considerable subset of patients, a monogenic cause can currently only be detected in a minority.

**Table 1** Genetic causes of dystonia

Acronym	Mode of inheritance	Locus	Gene	Mutations	Exemplary references
DYT1	AD	9q34	<i>DYT1</i>	GAG deletion in all known cases, except for a 18bp deletion in a single family	Ozelius <i>et al.</i> , 1997 Leung <i>et al.</i> , 2001
DYT2	AR	Unknown	Unknown		
DYT3	XR	Xq13	<i>DYT3/TAF1</i>	DSC3 prevailing in affected; SVA retrotransposon insertion in intron 32	Evidente <i>et al.</i> , 2004 Makino <i>et al.</i> , 2007
DYT4	AD	Unknown	Unknown		
DYT5/	AD	14q22	<i>GCHI</i>	>100 small mutations and 8 large deletions	Ichinose <i>et al.</i> , 1994 Hagenah <i>et al.</i> , 2005
DYT14	AR	11p	<i>TH</i>	<20 mutations (small sequence changes and repeat variations)	Swaans <i>et al.</i> , 2000 Furukawa <i>et al.</i> , 2001
DYT6	AD	8p	Unknown		
DYT7	AD	18p	Unknown		
DYT8	AD	2q33-q35	<i>MR-1</i>	2 missense mutations in <20 families	Lee <i>et al.</i> , 2004 Rainier <i>et al.</i> , 2004
DYT9	AD	1p21	Unknown		
DYT10	AD	16p11-q12	Unknown		
DYT11	AD	7q21	<i>SGCE</i>	>60 mutations (small sequence changes and a few large deletions)	Zimprich <i>et al.</i> , 2001 Asmus <i>et al.</i> , 2005 Grünewald <i>et al.</i> , 2008
DYT12	AD	19q12-q13	<i>ATPIA3</i>	6 missense/nonsense mutations in 7 families	de Carvalho Aguiar <i>et al.</i> , 2004
DYT13	AD	1p36-p35	Unknown		
DYT15	AD	18p	Unknown		
DYT16	AR	2q31	<i>PRKRA</i>	1 missense mutation in a single family	Camargos <i>et al.</i> , 2008

Note: AD – autosomal dominant, AR – autosomal recessive, *ATPIA3* – *ATPase alpha 3*, *DSC3* – disease-specific sequence changes, *GCHI* – *GTP cyclohydrolase 1*, *MR-1* – *myofibrillogenesis regulator 1*, *PRKRA* – *protein kinase, interferon-inducible double stranded RNA dependent activator*, *SGCE* – *epsilon-sarcoglycane*, *SVA* – *SINE-VNTR-Alu*, *TAF1* – *TAF1 RNA polymerase II*, *TH* – *tyrosine hydrolase*, XR – X-chromosomal recessive

This project focuses on DYT11 dystonia which is often also referred to as M-D. *SGCE* is the sole gene unequivocally connected with the disease. Mutations in this gene account for about a quarter of the M-D index patients (Grünewald *et al.*, 2008). An overview summarizing the current knowledge about M-D is given below.

### 1.2.1 *SGCE*-associated myoclonus-dystonia

There is not much known about the incidence, prevalence, and distribution of M-D in the general population. According to a study performed in Olmsted County, Minnesota the average annual incidence rate of myoclonus amounts to 1.3 cases per 100,000 person-years. But no case or family with M-D was ascertained through this study (Caviness *et al.*, 1999).

However, M-D may be underdiagnosed because of clinical misinterpretation (Caviness *et al.*, 1999; Quinn, 1996). Since the penetrance of the autosomal dominantly inherited disease is reduced it may appear sporadic rather than familial if only a partial pedigree is available (Daube and Peters, 1966).

M-D patients present with a predominantly myoclonic syndrome that is combined with dystonic features. In rare cases dystonia occurs as the only manifestation of the disease. The symptoms are responsive to alcohol and psychiatric disturbances are frequently found as an additional clinical feature in affected (Klein, 2003a). For the majority of cases the disorder starts within the first or second decade of life.

Independently of M-D, SGCE was first described by Ettinger *et al.* (1997). The authors showed that SGCE is a membrane-associated glycoprotein that is widely expressed in both muscle and nonmuscle cells, and in embryos as well as adults. They suggested that sarcoglycans may be important for embryonic development and/or for integrity of nonmuscle tissues.

Subsequently, McNally *et al.* (1998) localized the human *SGCE* gene which contains 12 exons to chromosome 7q21-q22 by use of radiation hybrid mapping.

Three years later, Zimprich *et al.* identified five different heterozygous loss-of-function mutations in the *SGCE* gene, which they mapped to a refined critical region of 3.2 Mb for M-D. Among them there were two nonsense mutations (c.209C>T/ p.R97X and c.304C>T/ p.R102X), two small deletions (c.565delA/ p.N189fsX196 and c.391\_406del/ p.I132fsX144) and one intronic sequence change (c.825+1:IVS6+1G>A). Pedigree analysis showed a marked difference in penetrance depending on the parental origin of the disease allele. This was indicative of a maternal imprinting mechanism, which had been demonstrated in the mouse *SGCE* gene (Piras *et al.*, 2000).

In 24 patients from 9 families with M-D, Asmus *et al.* (2002) identified one previously known (c.304C>T) and 6 novel mutations (c.233-1:IVS2-1G>A, c.276delG/ p.M92fsX131, c.463+6:IVS4+6T>C, c.733\_737delAATT/ p.Q245fsX254, c. 856C>T/ p.Q286X, and c.1037+5: IVS7+5G>A) in *SGCE*.

In 2003, an interstitial deletion of chromosome 7q encompassing the entire *SGCE* gene has been reported in one patient with a phenotype combining a variety of dysmorphic features and language delay with myoclonus (DeBerardinis *et al.*, 2003). The authors estimated the size of the deletion to 9.0 to 15 Mb by means of fluorescent in situ hybridization (FISH). PCR analysis of polymorphic markers in the region revealed that the paternally inherited

chromosome contained the deletion, consistent with a model of maternal *SGCE* imprinting. The patient appeared to represent a new contiguous gene disorder.

Later, heterozygous deletions of single exons have been detected in two patients (Asmus *et al.*, 2005). In one index case they identified a deletion of exon 5. The deletion was paternally inherited in all affected members of the family. In the other index patient exon 6 was deleted. Like in the first case he also received the mutation from his father, who himself inherited the deletion maternally. The father did not have motor symptoms, but suffered from alcohol dependence. The authors suggested nonhomologous end joining as the molecular mechanism for both deletions.

### 1.2.2 Detection of microdeletions

The results of DeBeradinis *et al.* (2003) and Asmus *et al.* (2005) riveted the attention of geneticists on deletions as a possible cause of M-D for the first time. However, microdeletions were known in several other genes before. Historically, patients with microdeletion syndromes were identified by a number of key clinical features which were received from the examination of large collections of individuals with similar abnormalities. The cytogenetic cause of these syndromes was not known. Due to the development of G-banding and other chromosomal banding techniques in the 1970s the identification of light- and dark-staining bands on the human chromosomes allowed the detection of large structural rearrangements, such as deletions, duplications and translocations. For example Langer-Giedion syndrome (LGS) was characterized by its conspicuous phenotype already in 1969. However, the cytogenetic basis of the disease was elusive until high-resolution banding identified interstitial deletions in the long arm of chromosome eight with LGS (Pfeiffer, 1980). The invention of FISH at the beginning of the 1980s facilitated the visualization of nucleic acids once more (Bauman *et al.*, 1980). This technique uses fluorescent probes that exclusively bind to parts of the chromosome with which they show a high degree of sequence similarity. Until now chromosome analyses by FISH have led to marked progress in cytogenetic research of microdeletions. However, the resolution of FISH for the detection of deletions is restricted. The location of deletion breakpoints can only be defined in the range of megabases (Lengauer *et al.*, 1993). To overcome those limitations more precise techniques like multiplex ligation-dependent probe amplification (MLPA) are applied. MLPA is a variation of the polymerase chain reaction that permits the simultaneous detection of DNA rearrangements in multiple targets. A detailed description of principles underlying MLPA is given in the methods section.

The technique was only recently invented by Schouten *et al.* (2002). It allows the quantitative detection of single exon changes.

### 1.2.3 Maternal imprinting in myoclonus-dystonia

As mentioned earlier, M-D is inherited in an autosomal dominant fashion with variable expressivity and incomplete penetrance (Grünewald *et al.*, 2008; Klein, 2003a). This pattern of disease transmission is caused by maternal imprinting of *SGCE* (Müller *et al.*, 2002). Imprinting is an epigenetic phenomenon and results in the selective silencing of one of the two parental alleles.

In 2002 Müller *et al.* presented an apparently sporadic M-D case and 2 patients from a family with seemingly autosomal recessive inheritance. In both families, they detected an *SGCE* mutation (c.625insG/ p.G209fsX216 and c.966delT/ p.A322fsX333) that was inherited from the patients' clinically unaffected fathers in an autosomal dominant fashion. In the first family, RNA expression studies revealed expression of only the mutated allele in affected individuals and expression of the normal allele exclusively in unaffected mutation carriers, whereas the affected individual of the second family expressed both alleles. The authors identified differentially methylated regions in the promoter region of *SGCE* as a characteristic feature of imprinted genes. With help of a rare polymorphism in the promoter region in a family unaffected with M-D, they demonstrated methylation of the maternal allele, in keeping with maternal imprinting of *SGCE*. Loss of imprinting in the patient with M-D who had biallelic expression of *SGCE* was associated with partial loss of methylation at several CpG dinucleotides.

### 1.3 Parkinsonism and Parkinson's disease

In 1817 James Parkinson (1755–1824) published his historic study “An essay on the shaking palsy”. For decades his work did not receive any scientific attention until the renowned French neurologist Jean-Martin Charcot (1825–1893) defined the syndrome, and named it “maladie de Parkinson” (PD) after its first discoverer. Leroux and Lhironde, two of Charcot's students at the “Hôpital de la Salpêtrière” in Paris, first described a familial component to PD, “a true cause of paralysis agitans, and may be the only true cause, is heredity” (Leroux, 1880). Since this publication enormous reports dealing with hereditary “parkinsonism” appeared in the literature.

PD is the most common form of “parkinsonism”, an umbrella term which is used to describe all movement disorders with parkinsonian features independent of their (unknown) etiology. The denomination “parkinsonism” has been suggested for the symptom triad of bradykinesia, rigidity and rest tremor with a therapeutic response to levo-dopa (L-dopa) and the frequent development of motor complications. Loss of dopamine in the corpus stratum is the primary defect in parkinsonism. Dopamine is one of three major neurotransmitters known as catecholamines, which play a role in the physiological response to stress in the organism. More than 1% of the population over the age of 65 years are affected by parkinsonism. Presumably, about 75% of all these patients show a negative family history. In 25%, however, at least one additional affected family member can be found, likely pointing to a direct, genetic cause of the disease. In case of clinically classic parkinsonism with a known genetic origin, the condition is often denoted as, for example, *PINK1*-linked PD.

**Table 2** Genetic causes of parkinsonism

Acronym	Mode of inheritance	Locus	Gene	Mutations	Exemplary references
PARK1/ PARK4	AD	4q21-q23	<i>SNCA</i>	Whole gene duplications/ triplications in <10 families, 3 missense mutations	Singleton <i>et al.</i> , 2003 Nishioka <i>et al.</i> , 2006 Polymeropoulos <i>et al.</i> , 1997 Kruger <i>et al.</i> , 1998 Zarranz <i>et al.</i> , 2004
PARK2	AR	6q25-q27	<i>Parkin</i>	>100 mutations (gene dosage alterations, small sequence changes)	Hedrich <i>et al.</i> , 2004a Kitada <i>et al.</i> , 1998
PARK3	AD	2p13	Unknown		
PARK5	AD	4p14	<i>UCH-L1</i>	1 mutation in a single family	Leroy <i>et al.</i> , 1998
PARK6	AR	1p36-p35	<i>PINK1</i>	40 small sequence changes, Rarely large deletions	Marongiu <i>et al.</i> , 2006 Valente <i>et al.</i> , 2004a
PARK7	AR	1p36	<i>DJ-1</i>	10 mutations (point mutations, large deletions)	Bonifati <i>et al.</i> , 2003 Bonifati <i>et al.</i> , 2004
PARK8	AD	12p11-q13	<i>LRRK2</i>	>50 variants, >16 of them pathogenic	Zimprich <i>et al.</i> , 2004 Paisan-Ruiz <i>et al.</i> , 2004
PARK9	AR	1p36	<i>ATP13A2</i>	3 nonsense mutations	Ramirez <i>et al.</i> , 2006
PARK10	AR	1p32	Unknown		
PARK11	Unknown	2q36-q37	Unknown		
PARK12	X	Xq21-q25	Unknown		
PARK13	Unknown	2p12	<i>Omi/HtrA2</i>	1 mutation in 4 families; 1 disease-associated variant	Strauss <i>et al.</i> , 2005

Note: AD – autosomal dominant, AR – autosomal recessive, *ATP13A2* – *ATPase type 13A2*, *DJ-1* – *amyotrophic lateral sclerosis-parkinsonism/dementia complex 2*, *LRRK2* – *Leucine-rich repeat kinase 2*, *Omi/HtrA2* – *HtrA serine peptidase 2*, *PINK1* – *PTEN-induced putative kinase 1*, *SNCA* – *alpha-synuclein*, *UCH-L1* – *ubiquitin C-terminal hydrolase-L1*, X – X-chromosomal; Table modified after Klein and Schlossmacher (2007).

To date, 13 genetic loci, PARK1-13, have been suggested for rare forms of PD. These loci include five autosomal dominant (PARK1 (=4), 3, 5, 8 and 13), four autosomal recessive (PARK2, 6, 7, and 9), one X-linked (PARK12) and two forms with still unknown mode of transmission (PARK10, 11). At eight of these loci, genes have been identified and reported by

several groups to carry mutations that are linked to affected family members: *α-synuclein* (*SNCA*) at PARK1, *Parkin* at PARK2, *ubiquitin C-terminal hydrolase-L1* (*UCH-L1*) at PARK5, *PINK1* at PARK6, *amyotrophic lateral sclerosis-parkinsonism/dementia complex 2* (*DJ-1*) at PARK7, *Leucine-rich repeat kinase 2* (*LRRK2*) at PARK8, *ATPase type 13A2* (*ATP13A2*) at PARK9 and *HtrA serine peptidase 2* (*Omi/HtrA2*) at PARK13 (see Table 2, Klein *et al.*, 2007).

For the present thesis the PARK6 gene *PINK1* is of particular interest. Details about *PINK1*-associated PD are summarized in the following chapter.

### 1.3.1 *PINK1*-associated Parkinson's disease

The frequency of *PINK1* mutations varies within a range of 1 to 8% in patients of different ethnicities (Bonifati *et al.*, 2005; Healy *et al.*, 2004; Klein *et al.*, 2005; Li *et al.*, 2005; Rogaeva *et al.*, 2004; Tan *et al.*, 2006). Several homozygous mutations have been detected in patients with familial PD, supporting the hypothesis that loss of function underlies the pathogenesis. *PINK1* mutation carriers are clinically indistinguishable from *Parkin* mutation carriers with the possible exception of a higher rate of psychiatric symptoms (Abou-Sleiman *et al.*, 2006a; Criscuolo *et al.*, 2006; Steinlechner *et al.*, 2007). Most of the affected have a disease onset in their fourth decade of life, presenting with features typical for PD: good response to levodopa, slow progression of the disease and early motor complications.

The PARK6 locus for a rare familial form of PD was first mapped to chromosome 1p36 due to a common haplotype in 8 families from 4 different European countries (Valente *et al.*, 2002).

In 2003, Nakajima *et al.* described the protein structure of BRPK, which eventually turned out to be identical with *PINK1*. The authors determined that BRPK cDNAs are well conserved among species and that the human cDNA sequence encodes 581 amino acids (AA). The protein was found to contain a putative serine-threonine protein kinase catalytic domain spanning from AA 156 to 509 which is capable of autophosphorylation (Nakajima *et al.*, 2003).

One year later, Valente *et al.* (2004a) identified a gene within the promising 9cM region on chromosome 1. The *PINK1* transcript has a length of 2,659 bp with an open reading frame of 1,746bp and comprises eight exons. Initially, two homozygous mutations affecting the *PINK1* kinase domain were identified in three consanguineous PARK6 families. A Spanish family carried a c.926G>A missense mutation in exon 4 at a highly conserved amino acid (p.G309D). Two Italian families carried the same c.1311G>A transitions in exon 7 which

results in a p.W437X substitution, truncating the last 145 AA encoding the C terminus of the kinase domain (Valente *et al.*, 2004a). Following this publication Valente *et al.* (2004b) reported a 60-year-old woman, compound heterozygote for missense mutations c.275G>T (Cys92Phe) and c.1391G>A (Arg464His). The presenting sign was resting tremor of the right upper limb at age 37 years. Progression was slow and response to L-dopa sustained.

In the same year six additional *PINK1* mutations have been identified in families from different Asian countries (Japan, Taiwan and Philippines), indicating that mutations in the gene cause PD in a wide range of populations. Hatano *et al.* identified four homozygous point mutations (c.736C>T/ p.R246X, c.813C>A/ p.H271Q, c.1040T>C/ p.L347P and c.1250C>T/ p.E417G) involving exons 3, 4, 5, and 6 in *PINK1* of patients from five unrelated families. They also detected two nonsense mutations (c.715C>T/ p.Q239X and c.1474C>T/ p.R492X) as a compound heterozygote (c.1474C>T/ p.R492X) in a sixth family (2004).

Phenotypical consequences of an insertion (c.1573\_1574insTTAG/ p.D525fsX562) were then described by Rohé *et al.* (2004).

The first large homozygous deletion including exon six to eight was identified in a cohort of Asian and European patients (Li *et al.*, 2005). A deletion of exons six to eight was reported in a 62 years old Japanese female again by Atsumi *et al.* (2006). Recently, the mutational spectrum has been expanded by the identification of a deletion of approximately 50 kb including the entire *PINK1* gene and partly also neighbouring genes (Marongiu *et al.*, 2007).

A first splicing mutation (g.15445\_15467del23), identified by Marongiu *et al.* in 2007, generates five aberrantly spliced transcripts resulting from exon 7 skipping, intron 6 retention and the activation of three distinct cryptic splice sites within exon 7 (p.V418\_L496del, p.V418\_Q456del, p.V418fsX461, p.V418fsX421 and p.T420fsX444).

A pathogenic effect of heterozygous mutations in *PINK1* related recessively inherited PD was first discussed by Hedrich *et al.* (2006). The clinical phenotype in the presented family (Family W) was compatible with “benign” idiopathic PD with a mean age of onset of 50 years, slow disease progression, excellent response to treatment, and minimal motor complications. Overall, signs of PD in the reported heterozygous cases were milder than in homozygous patients but their current mean age was almost a decade younger than the average onset age of their homozygous parents. Although UPDRS III scores (Unified Parkinson's Disease Rating Scale, see: Fahn *et al.*, 1987; Olanow *et al.*, 2001) were overall low in the heterozygous carriers, they reflected unequivocal clinical signs that are not obtained in healthy individuals, such as unilaterally reduced or absent arm swing with flexion of the arm at the wrist and elbow, and unilaterally delayed shoulder shrug.

Signs of PD in individuals with heterozygous mutations in recessively inherited genes are a common clinical observation. An abridgement of the literature is given below.

### 1.3.2 Heterozygous mutations in Parkinson's disease

To date, the most common familial forms of PD are considered to be inherited in an autosomal dominant fashion (one mutated allele) or in a recessive manner (two mutated alleles) (see Table 2). In 2000, researchers began questioning this simple applicability of the established Mendelian concepts to the inheritance of PD in humans for the first time. Experience from large mutational screenings in the recessively inherited *Parkin* gene revealed that more than half of the affected patients carried only one mutated allele (rather than the expected two). Similar observations were later reported for *PINK1*. Those findings raised the question as to whether the much more frequent heterozygous mutations in 'recessive' genes might contribute to the development of PD under some (but not all) circumstances, thereby constituting a susceptibility factor (Klein *et al.*, 2007).

Family studies can serve as a valuable tool to investigate the role of heterozygous mutations in PD genes. They allow the detailed neurological assessment of heterozygous relatives of index patients that are known to carry two mutations. There are several reports that employed careful clinical examinations; these demonstrated that some relatives with heterozygous *Parkin* or *PINK1* mutations may indeed be affected by mild signs of classical parkinsonism. Importantly, the nature of the pedigrees examined (i.e., the identification of affected individuals in successive generations) made it unlikely that a second mutation in the respective gene had been missed (Klein *et al.*, 2007).

Khan *et al.* reported on a large Brazilian kindred with young-onset PD due to either a homozygous or heterozygous deletion in exon 4 of *Parkin*. One heterozygous mutation carrier presented with poor arm swing, mild bilateral bradykinesia of the limbs especially on the left, minimal rigidity, and a mild postural tremor of the right hand. She fulfilled the above-mentioned criteria for PD but was not as severely affected as her homozygous siblings (Khan *et al.*, 2005).

A similar case was depicted for *PINK1* by Criscuolo *et al.* (2006). The authors analyzed the *PINK1* gene in 58 patients with early-onset parkinsonism and detected the homozygous mutation p.W437X in one patient. The parents of this index patient were both heterozygous for the mutation. Like her son, the mother was classified as definitely affected from PD. She had an onset of the disease at 53 years of age, with left arm rest tremor and bradykinesia. She

showed good response to L-Dopa. By contrast, the neurological examination of the proband's father at age 79 was entirely normal.

Since the role of heterozygous mutations in so-called recessive genes in PD disease development remains elusive this thesis deals with the effect of heterozygous mutations in *PINK1* at the gene expression level.

### 1.3.3 A common pathway in Parkinson's disease?

Besides the mutational analysis of PD-linked genes the search for potential interactions between the protein products of these genes has recently gained increasing importance. This research focuses not only on proteins known to be involved in PD but also on novel interactors. Since the identification of the second monogenetic PD gene product (Parkin) a common pathway leading to dopaminergic neurodegeneration has been discussed. First, Shimura *et al.* (2001) hypothesized that Parkin plays a role in the co-regulation of SNCA. The group identified a protein complex in normal human brain that included the E3 ubiquitin ligase parkin, UBCH7 as its associated E2 ubiquitin-conjugating enzyme, and a novel form of SNCA as its substrate. Later an early-onset parkinsonism patient with a heterozygous missense mutation in both the *DJ-1* and the *PINK1* genes has been described. Additionally, overexpression of DJ-1 and PINK1 in SHSY-5Y cells revealed that the wildtype as well as the mutant forms of both proteins interact, and DJ-1 stabilised PINK1 (Tang *et al.*, 2006). Furthermore, the knockdown of Parkin or PINK1 in *Drosophila* flies results in a similar phenotype, which is accompanied with a motor-deficit, a shorter life span, non-functional flight muscle, disorganised mitochondrial morphology, lower ATP-levels and a reduction of dopaminergic neurons. Interestingly, the PINK1-related abnormalities can be rescued by Parkin overexpression but not vice versa. Overexpression of both genes does not exacerbate the phenotype. Both results suggest that PINK1 acts upstream of Parkin in a common pathway (Clark *et al.*, 2006; Park *et al.*, 2006). There is also evidence that PINK1 regulates the phosphorylation of the mitochondria-associated stress-protective protease HtrA2. HtrA2 is phosphorylated at a residue adjacent to the residue G399S that is mutated in patients with PD. The phosphorylation of HtrA2 is decreased in the brains of PD patients with *PINK1* mutations (Plun-Favreau *et al.*, 2007). The TNF receptor-associated protein 1 (TRAP1), a mitochondrial molecular chaperone, has been identified as another cellular substrate of PINK1. Recent findings support that PINK1 protects the cell against oxidative-stress-induced cell death and that this effect depends on its kinase activity to phosphorylate TRAP1 (Pridgeon *et al.*, 2007).

Taking all these data together, it is tempting to speculate that DJ-1, PINK1, Parkin, HtrA2 and TRAP1 function in the same pathway to protect the cell against oxidative-stress-induced apoptosis.

### **1.3.4 Nonsense-mediated mRNA decay as a disease mechanism**

In the present thesis a PD-positive family with a mutation in *PINK1* leading to a premature stop codon was studied. In this context nonsense-mediated mRNA decay (NMD) was taken into consideration as a possible disease causing factor.

NMD is a cellular mechanism of mRNA surveillance. It enables the cell to detect nonsense mutations and to prevent the expression of truncated or incorrect proteins. NMD is triggered by exon-junction complexes (EJC). During pre-RNA processing (splicing) these complexes are formed and disposed 5' of exon-exon junctions. Normally, EJCs are removed during the first round of translation of the mRNA. If the translating ribosome encounters a premature termination codon upstream of at least one EJC, however, NMD is triggered. Consequently, mRNA degradation is initiated (Noensie and Dietz, 2001).

## **1.4 Mitochondria in Parkinson's disease**

Mitochondria are the main source of energy for the eukaryotic cell under aerobic conditions. Their core function is maintained by the electron transport chain, which is located on the inner mitochondrial membrane. In recent years, the role of mitochondria in neurodegeneration has come under intense scrutiny. Dysfunction of the mitochondrial electron transport chain has been reported in several neurological disorders such as PD and Huntington's disease (Gu *et al.*, 1996; Schapira *et al.*, 1990a). This link is of particular interest in the present thesis since PINK1 is also known to localize on the mitochondrial membrane.

### **1.4.1 The electron transport chain**

The electron transport chain (ETC) is comprised of more than 80 polypeptides grouped together into four enzyme complexes (Schapira, 2006). It facilitates the transfer of electrons from NADH and FADH<sub>2</sub>, to oxygen, which is reduced to water at complex IV (Michel *et al.*, 1998). The reduction of oxygen is coupled to the synthesis of ATP (oxidative phosphorylation) by ATP synthase (complex V) (Mitchell, 1961). Complexes I–IV contain bound redox centres (e.g., iron-sulphur complexes, FAD), which transfer electrons

sequentially from one to another via increasing reduction potentials (Michel *et al.*, 1998; Zhang *et al.*, 1998). Ubiquinol transfers two electrons from both complex I and complex II to complex III, while cytochrome c transfers one electron from complex III to complex IV (Crofts *et al.*, 1999; Tormo and Estornell, 2000). The free energy generated by the transfer of electrons is conserved by the pumping of protons from the mitochondrial matrix into the intermembrane space by complexes I, III, and IV (Crofts *et al.*, 1999; Michel *et al.*, 1998; Mitchell, 1961). This process results in an electrochemical gradient across the inner membrane, and a mitochondrial membrane potential ( $\Delta\psi_m$ ) of 150 mV (Scheffler, 2001). This proton motive force is dissipated through the membrane domain of ATP synthase leading to the phosphorylation of ADP (Mitchell, 1961).

#### 1.4.1.1 Complex I

With 43 subunits and a molecular mass of approximately 900 kDa the mitochondrial NADH dehydrogenase (complex I) is the largest enzyme in the ETC (Grigorieff, 1999; Sazanov *et al.*, 2000). Seven subunits of complex I are coded for by the mitochondria, with the remainder coded for by the nucleus (Sazanov *et al.*, 2000). Complex I removes two electrons from NADH and transfers them to a lipid-soluble carrier, ubiquinone (CoQ1). The reduced product, ubiquinol (CoQH<sub>2</sub>) is free to diffuse within the membrane. At the same time, complex I moves four protons (H<sup>+</sup>) across the membrane, producing a proton gradient.

Complex I activity has been considered difficult to assay, mainly due to the inaccessibility of the complex in the inner mitochondrial membrane and the insolubility of its natural substrate, CoQ1. Though, the accessibility of soluble short chain CoQ1 analogues as substrates, along with improved methods of sample preparation, has enhanced the reliability of the assay. Complex I is inhibited by rotenone, but there is considerable rotenone-insensitive background activity in many tissues and cultured cells (Birch-Machin *et al.*, 1994). Only the use of hypotonic lysis in the preparation of isolated mitochondria from cultured cells achieved a marked reduction of this effect (Lowerson *et al.*, 1992).

#### 1.4.1.2 Complex II+III

Succinate dehydrogenase (SDH), generally known as respiratory complex II is composed of the four subunits SDHA, SDHB, SDHC, and SDHD and contains a flavin (FAD), non-heme iron centre and a b-type cytochrome as prosthetic groups. Unlike the other complexes in the electron transport chain, the polypeptides of complex II are all coded for by nuclear genes (Hirawake *et al.*, 1999). It is the only enzyme that serves as a direct link between the citric

acid cycle and the electron transport chain (Ackrell, 2000). Complex II oxidises succinate to fumarate, transferring the electrons to CoQ1.

The cytochrome bc<sub>1</sub> complex (complex III) transfers electrons from CoQH<sub>2</sub> to cytochrome c. This electron transfer is coupled to proton pumping from the matrix to the inner membrane space contributing to the proton gradient required for ATP synthesis. The mechanism by which electrons are transferred through complex III has been termed the Q cycle. The protein exists as a homodimer with each monomer consisting of 11 different subunits with a total molecular mass of approximately 240 kDa (Zhang *et al.*, 1998). Only one of these subunits (cytochrome b) is coded for by the mitochondria (Taanman, 1999). The protein contains four redox centres: two b-type haem groups, one c-type haem of cytochrome c<sub>1</sub>, and an iron-sulphur centre bound to the Rieske iron-sulphur protein (Zhang *et al.*, 1998).

#### 1.4.1.3 Complex IV

Cytochrome c oxidase (complex IV) is the terminus for electron transfer in the respiratory chain. The enzyme removes four electrons from four molecules of cytochrome c and transfers them to molecular oxygen (O<sub>2</sub>), producing two molecules of water (H<sub>2</sub>O). At the same time, it moves four protons across the membrane, producing a proton gradient. Crystallisation of bovine heart complex IV by Tsukihara *et al.* (1996) revealed that the mammalian enzyme has 13 different subunits, and several prosthetic groups including two haems (a and a<sub>3</sub>) and two copper atoms. The protein exists in the inner membrane as a dimer with each monomer having a molecular mass of 211 kDa (Tsukihara *et al.*, 1996). Subunits I, II and III are mitochondrially encoded and form the core of the protein (Michel *et al.*, 1998). The remaining ten subunits of mitochondrial cytochrome c oxidase are nuclear encoded.

#### 1.4.1.4 Complex V

ATP synthase (complex V) uses the proton motive force generated across the inner mitochondrial membrane by electron transfer through the ETC to drive ATP synthesis. Bovine heart ATP synthase is comprised of 16 different subunits and is divided into three domains (Abrahams *et al.*, 1994). The matrix globular domain (F<sub>1</sub>) containing the catalytic site is linked to the intrinsic membrane domain (F<sub>0</sub>) by a central stalk (Karrasch and Walker, 1999). Proton flux through F<sub>0</sub> causes the subunit to rotate, which is transferred to the central stalk, and is utilised by F<sub>1</sub> domain to synthesise ATP (Tsunoda *et al.*, 2000).

The F<sub>1</sub> catalytic domain contains three  $\alpha$  subunits and three  $\beta$  subunits with the nucleotide binding sites located at the interfaces between the  $\alpha$  and  $\beta$ -subunits (Boyer, 2001). Rotation of the stalk changes the conformation of the active sites making the synthesis of ATP more

favourable (Boyer, 2001). A stator prevents the F<sub>1</sub> domain following the rotation of the stalk and F<sub>0</sub> domains (Karrasch and Walker, 1999).

#### **1.4.2 Implications of complex I deficiency in Parkinson's disease**

Mitochondrial dysfunction has long been implicated in the pathogenesis of PD. Evidence first emerged when 1-methyl-4-phenyl-1,2,3,4-tetrahydropyridine (MPTP), an environmental toxin, was discovered to produce parkinsonian features in drug abusers (Langston *et al.*, 1983). The active metabolite of MPTP, the 1-methyl-4-phenylpyridinium ion (MPP<sup>+</sup>) is an inhibitor of complex I of the mitochondrial electron transport chain and a substrate for the dopamine transporter (DAT). As a consequence it accumulates in dopaminergic neurons where it confers toxicity and leads to neuronal death due to inhibition of complex I (Nicklas *et al.*, 1985).

This finding was further supported by the detection of a complex I deficiency in the substantia nigra of PD patients (Schapira *et al.*, 1989). Subsequently, NADH dehydrogenase dysfunction has also been observed in platelets (Benecke *et al.*, 1993; Krige *et al.*, 1992; Parker *et al.*, 1989) as well as in fibroblasts of patients (Hoepken *et al.*, 2007; Winkler-Stuck *et al.*, 2004). Furthermore, rats administered the complex I inhibitor rotenone developed a PD-like syndrome characterized by neuronal degeneration and the formation of alpha-synuclein-rich inclusion bodies (Betarbet *et al.*, 2000).

The complex I depletion results in increased free radical production, and it contributes to the oxidative mediated damage seen the in PD nigra (Beal, 2003). This relationship is bi-directional (for details see Fig 3). The enhanced release of free radicals causes a decrease in the activity of the respiratory chain enzymes, particularly of complex I and IV (Genova *et al.*, 2004). The mitochondrial dysfunction contributes then to the dysfunction of the energy-dependent ubiquitin proteasomal system (UPS) and consequently leads to enhanced dopaminergic cell damage and death (Hoglinger *et al.*, 2003).

Except for by environmental factors (such as MPTP), mitochondrial function can also be influenced by genetic defects. Several studies showed evidence that SNCA inhibits mitochondrial activity (Hsu *et al.*, 2000; Lee, 2003). *Parkin* knockout mice had decreased mitochondrial respiratory chain function in the striatum and reductions in the specific respiratory chain and antioxidant proteins (Palacino *et al.*, 2004). *Parkin* knockout flies developed mitochondrial abnormalities and apoptotic cell death (Greene *et al.*, 2003). As another example, *DJ-1* knockout mice have increased sensitivity to MPTP and oxidative stress. Of particular interest for this study, the protein product of *PINK1* localizes to the

mitochondrion (Valente *et al.*, 2004a). However, it can also be found in the cytosol (Unoki and Nakamura, 2001). Recent studies provided evidence that PINK1 has an impact on mitochondrial morphology. Swollen and ruptured mitochondria were observed in *Drosophila* and human *PINK1* null mutant cells (Clark *et al.*, 2006; Park *et al.*, 2006; Yang *et al.*, 2006). The exact role of PINK1 in PD still remains elusive, however it functions as a protein kinase and mutations in the gene increase the cellular sensitivity to oxidative stress resulting in a lower threshold to apoptotic death (Schapira, 2006). Hoepken and colleagues observed elevated levels of oxidative stress, a mild decrease in complex I activity and a trend to superoxide elevation in lymphoblasts from three patients homozygous for G309D-PINK1 (2007). As a conclusion from their data the authors claim that PINK1 is critical to prevent oxidative damage. These findings, implying a role of PINK1 involved in respiratory chain function, however could not yet be confirmed in a larger group of patients.

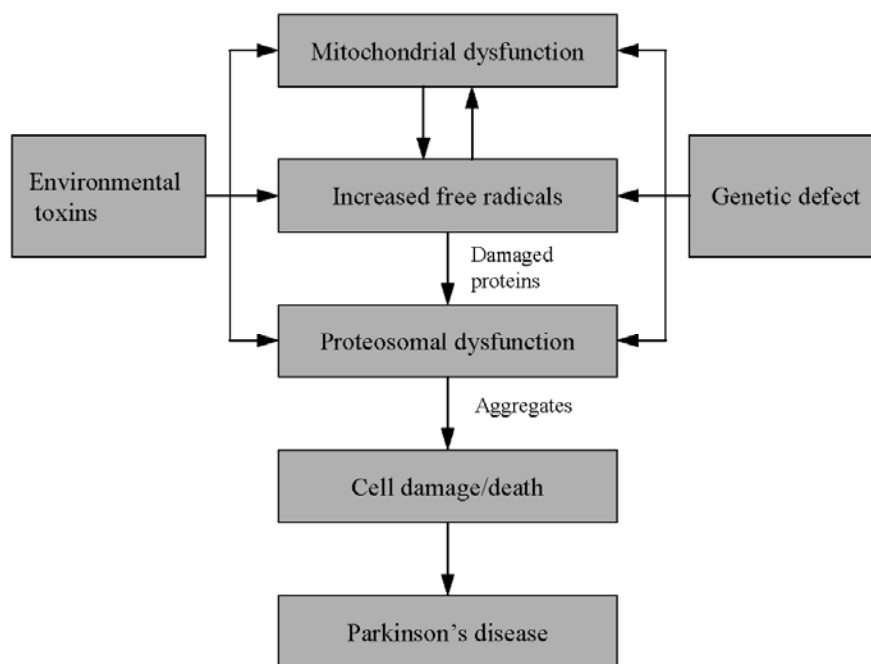


**Fig 3** Potential connection between environmental and genetic factors, and PD. Scheme adapted from Schapira, 2006.

## 1.5 Hypotheses

The general aim of the present thesis was to correlate clinical features of M-D and PD patients with their genetic variations in *SGCE* and *PINK1*, respectively. For the M-D cases this attempt was performed considering genomic data only. By contrast, for the PD cases the effect of mutations in *PINK1* were investigated at mRNA, protein and functional level. The intention was to gain a better understanding of the cause of the disease and the phenotypic variability of affecteds. Specifically, the following hypotheses were addressed:

- Project A:
- *Deletions in the SGCE gene are an underestimated cause of M-D.*
  - *There is a link between genotype and phenotype in M-D patients.*

- Project B:
- *The c.1366C>T mutation in PINK1 influences the expression of the gene.*
  - *The variable phenotype of patients with heterozygous mutations in PINK1 is explained by the expression level of the gene.*

- Project C:
- *Mutant PINK1 exerts its pathogenic effect by inhibition of the respiratory chain function.*
  - *Loss of PINK1 function leads to oxidative stress in the cell.*
  - *PINK1 plays a role in the process of mitochondrial fission.*

## 2 PATIENTS, MATERIAL AND METHODS

This thesis was carried out at the Neurology department at the University of Lübeck. However, a number of methods mentioned in this chapter have been established during a one-month research study in Professor Bonifati's Department of Clinical Genetics at the Erasmus MC, Rotterdam, The Netherlands (Project B) and a seven-month internship in Professor Schapira's Department of Clinical Neurosciences at the University College London (Project C), London, UK. This includes all experiments related to *PINK1* gene expression and the methods to investigate the mitochondrial function and morphology in PD patient fibroblast cultures. The learned techniques were set up in Lübeck afterwards.

### 2.1 Patients

In the present study patients suffering from two different movement disorders (M-D and parkinsonism) were investigated at the genetic level. The diagnosis was made by movement disorders specialists based on published criteria (for parkinsonism see Gibb and Lees, 1988; clinical features of M-D are reviewed in Klein, 2003b). All patients and control individuals gave informed consent and the study was approved by the local Ethics Committee.

#### 2.1.1 M-D patients with mutations in *SGCE* and family members

Based on a provisional diagnosis of M-D, 45 DNA samples were newly referred for genetic testing of *SGCE* from different international clinical centres to the laboratory at the University of Lübeck. The index patients were classified according to criteria summarized in Table 3.

**Table 3** *Classification criteria of M-D phenotypes in the SGCE study*

Notation	Operator	Phenotype
<b>Definite M-D</b>		Early-onset myoclonus and dystonia
	OR	Isolated myoclonus predominantly in upper body half
	AND	Positive family history
<b>Probable M-D</b>		Early-onset myoclonus and dystonia
	OR	Isolated myoclonus predominantly in upper body half
<b>Possible M-D*</b>		“Jerky dystonia” of neck
	OR	Isolated jerky movements of variable distribution
	OR	Signs of dystonia and/or myoclonus in lower body half
	OR	No response to alcohol

Note: \* Used to describe a number of different phenotypes with some features possibly consistent with but not entirely typical of classic M-D

Ten of the referred samples did not meet these rigorous inclusion criteria or lacked detailed clinical information and, thus, were not included in the mutational analysis.

Demographic, clinical and genetic data of M-D index patients and affected family members are given in Table 5. For related pedigrees see Fig 8.

### 2.1.2 PD patients with mutations in *PINK1* and controls

The investigations regarding PD included one German, one Italian and one French family of healthy and diseased members. In addition single individuals from Germany (one affected) and Italy (two affected) were involved. The data were compared to those of four controls with British origin.

#### 2.1.2.1 Family W

Family W consists of three generations. Among the members there were four patients with a homozygous c.1366C>T, p.Q456X (cp. Fig 17) nonsense mutation (one male, mean age: 70.0 years [ $\pm 4.8$ ], mean age at onset: 50.0 years [ $\pm 9.3$ ]). Eleven relatives were tested heterozygous (nine male, mean age: 46.2 years [ $\pm 5.9$ ]). Five healthy members were also included (two male, mean age: 44.6 [ $\pm 10.0$ ]). For phenotypic features of the family see Table 4. A pedigree is given in Fig 4. A detailed clinical report has been published when the family was first identified (Hedrich *et al.*, 2006).

#### 2.1.2.2 Other *PINK1* mutants

Four families with a segregating c.1366C>T mutation came from Italy (MI-002, two heterozygous and two homozygous samples; NE-166, one homozygous sample; Roma-360, one heterozygous sample) and France (FPD; one homozygous and one compound heterozygous case with the c.373T>C, [p.C125G] mutation). Clinical details concerning these samples were published earlier (Bonifati *et al.*, 2005; Ibanez *et al.*, 2006).

In addition, one patient (female, age: 70 years, age at onset: 31 years) harbouring a homozygous missense mutation c.509T>G, p.V170G (cp. Fig 17) was studied. Clinical details of this case are published elsewhere (Moro *et al.*, 2008). No relatives of this individual were available.

#### 2.1.2.3 Healthy controls included in the *PINK1* studies

Five independent age-matched healthy individuals of British origin served as controls (four male, mean age: 64.8 years [ $\pm 13.1$ ]).

**Table 4** Genotypic and phenotypic characterization of Family W

Mutational status	Identifier	Code	Sex	Age (yr)	Age of Onset (yr)	Clinical status
Homo-zygous	II:1	IP2123	M	71	39	Definite
	II:8	F2122	F	72	61	Definite
	II:10	F2124	F	63	53	Definite
	II:12	F2126	F	74	47	Definite
<b>Mean</b>				<b>70.0+/-4.8</b>	<b>50.0+/-9.3</b>	
<b>Range</b>				<b>63-74</b>	<b>39-61</b>	
Heterozygous	III:1	F2129	M	53	—	Probable
	III:2	F2130	M	34	—	Unaffected
	III:3	F2152	M	46	—	Probable
	III:4	F2153	M	51	—	Possible
	III:11	F2125	M	42	—	Possible
	III:12	F2121	M	38	—	Unaffected
	III:13	F2127	M	50	—	Possible
	III:14	F2151	M	48	—	Unaffected
	III:15	F2149	F	51	—	Possible
	III:16	F2150	F	48	—	Unaffected
III:19	F2128	M	47	—	Unaffected	
<b>Mean</b>				<b>46.2+/-5.9</b>		
<b>Range</b>				<b>34-53</b>		
Wildtype	II:5	F2131	M	61	—	—
	III:5	F2135	M	39	—	—
	III:6	F2133	F	46	—	—
	III:7	F2132	F	35	—	—
	III:8	F2134	F	42	—	—
<b>Mean</b>				<b>44.6+/-10.0</b>		
<b>Range</b>				<b>35-61</b>		

Note: The index patient is denoted by IP whereas family members are marked by an F. Sex: F – female, M – male. For definition of the clinical status see Hedrich *et al.* (2006).

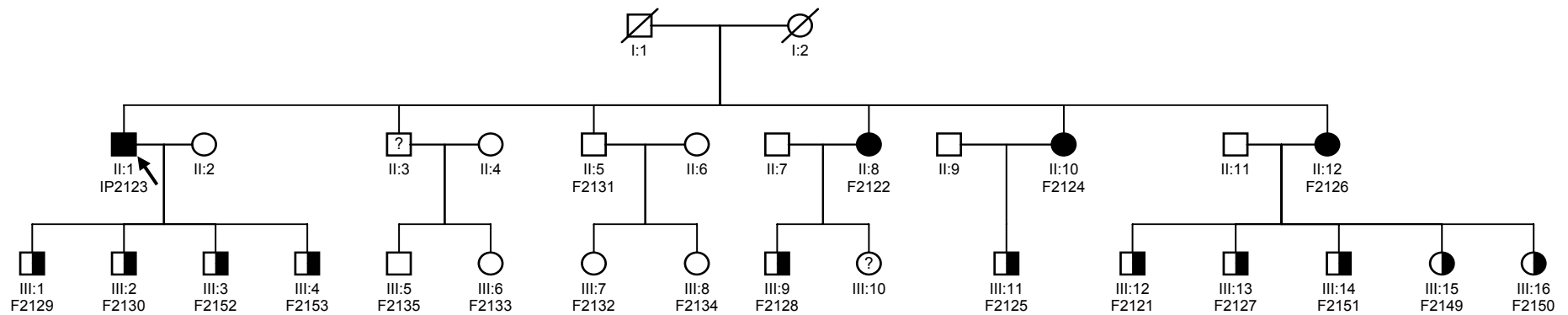


**Fig 4** Pedigree of Family W. Circles represent female subjects; squares represent male subjects; deceased individuals are slashed; the individual pedigree number is below each symbol. A black arrow points to the index patient (IP). Family members (F) included in the clinical and molecular genetic studies are denoted by their code number. The clinical status of the remaining family members is obtained by history. Filled symbols indicate members with a homozygous *PINK1* c.1366C>T mutation. Half filled symbols indicate heterozygous mutation carriers. Individuals with unknown genetic statuses are highlighted by a question mark.

## 2.2 Material

Materials used in the three sections of the study are classified below with manufacture's name.

### 2.2.1 Chemicals

Acetyl-CoA (trilithium)	Sigma-Aldrich
Acrylamide (C <sub>3</sub> H <sub>5</sub> NO)	Roth
Acrylamide	LongRanger
Acrylamide 30% / Bisacrylamide 0.8%	BioRad
Agarose	Biozym
6-Aminocaproic acid (C <sub>6</sub> H <sub>13</sub> NO <sub>2</sub> )	Sigma-Aldrich
Ammonium chloride (NH <sub>4</sub> Cl)	Sigma-Aldrich
Ammonium persulfate (APS)	Sigma-Aldrich
Antimycin A (C <sub>28</sub> H <sub>40</sub> N <sub>2</sub> O <sub>9</sub> )	Sigma-Aldrich
Ascorbic acid (C <sub>6</sub> H <sub>8</sub> O <sub>6</sub> )	Sigma-Aldrich
Betaine	Sigma-Aldrich
Bis-tris propane (C <sub>11</sub> H <sub>26</sub> N <sub>2</sub> O <sub>6</sub> )	Invitrogen
Boric acid (H <sub>3</sub> BO <sub>3</sub> )	Merck
Bovine serum albumin (BSA)	Sigma-Aldrich
Bromphenol blue	Sigma-Aldrich
ChemiBlocker	Chemicon International
Cytochrome c (horse heart)	RocheDiagnostics
Cycloheximide (C <sub>15</sub> H <sub>23</sub> NO <sub>4</sub> )	Alomone labs
Cytofluor mounting medium	Applied biosystems
Dimethyl sulfoxide (DMSO)	Sigma-Aldrich
Dipotassium hydrogen phosphate (K <sub>2</sub> HPO <sub>4</sub> )	BDH
5, 5'-Dithiobis-(2-nitrobenzoic acid) (DTNB)	Sigma-Aldrich
Desoxyribonucleotides (dNTPs)	Amersham Biosciences
Dithiothreitol (DTT; C <sub>4</sub> H <sub>10</sub> O <sub>2</sub> S <sub>2</sub> )	Sigma-Aldrich
Dulbeccos Modified Eagle Medium (DMEM)	PAA Laboratories GmbH
Durcupan	Fluka
Ethanol (C <sub>2</sub> H <sub>5</sub> OH)	J.T. Baker
Ethidium bromide (C <sub>21</sub> H <sub>20</sub> BrN <sub>3</sub> )	Sigma-Aldrich

Ethylenediaminetetraacetic acid (EDTA)	Merck
Foetal Bovine Serum (FBS)	PAA Laboratories GmbH
Formamide (HCONH <sub>2</sub> )	Fluka
Glucose (C <sub>6</sub> H <sub>12</sub> O <sub>6</sub> )	Sigma-Aldrich
Glutaraldehyde (C <sub>5</sub> H <sub>8</sub> O <sub>2</sub> )	Sigma-Aldrich
Glycerol (C <sub>3</sub> H <sub>5</sub> (OH) <sub>3</sub> )	Sigma-Aldrich
Hydrochloric acid (HCl)	Merck
Lauryl maltoside (C <sub>24</sub> H <sub>46</sub> O <sub>11</sub> )	Sigma-Aldrich
Leupeptin	Sigma-Aldrich
Loading dye (sequencing)	Amersham Biosciences
Low-melting point agarose	BRL
2-Mercaptoethanol (C <sub>2</sub> H <sub>6</sub> OS)	Sigma-Aldrich
Magnesium Chloride (MgCl <sub>2</sub> )	Sigma-Aldrich
Methanol (CH <sub>3</sub> OH)	J.T. Baker
MitoTracker Green FM	Molecular Probes
Monopotassium phosphate (KH <sub>2</sub> PO <sub>4</sub> )	BDH
Nicotinamide adenine dinucleotide (NADH)	RocheDiagnostics
Nitric acid (HNO <sub>3</sub> )	Merck
Osmium tetroxide (OsO <sub>4</sub> )	TAAB
Oxaloacetic acid (C <sub>4</sub> H <sub>4</sub> O <sub>5</sub> )	Sigma-Aldrich
Paraformaldehyde	Sigma-Aldrich
Paraquat (Methylviologen hydrate; C <sub>12</sub> H <sub>14</sub> C <sub>12</sub> N <sub>2</sub> )	Sigma-Aldrich
Penicillin/Streptomycin (P/S)	PAA Laboratories
Pepstatin A (C <sub>34</sub> H <sub>63</sub> N <sub>5</sub> O <sub>9</sub> )	Sigma-Aldrich
Phenylmethylsulphonyl fluoride (PMSF; C <sub>7</sub> H <sub>7</sub> FO <sub>2</sub> S)	Sigma-Aldrich
Phosphate buffered saline (PBS)	PAA Laboratories
PIPES	Sigma-Aldrich
Poly-lysine	Sigma-Aldrich
Potassium bicarbonate (KHCO <sub>3</sub> )	Sigma-Aldrich
Potassium chloride (KCl)	Merck
Potassium cyanide (KCN)	BDH
Potassium ferricyanide (K <sub>3</sub> [Fe(CN) <sub>6</sub> ])	Sigma-Aldrich
Propylene oxide (C <sub>3</sub> H <sub>6</sub> O)	VWR
Proteinase K	Sigma-Aldrich

Rotenone (C <sub>23</sub> H <sub>22</sub> O <sub>6</sub> )	Sigma-Aldrich
Tris/Glycine (blotting) buffer 10x	BioRad
Tris/Glycine/SDS (protein running) buffer 10x	BioRad
Serva blue G	Sigma-Aldrich
Sodium borohydride (NaBH <sub>4</sub> )	BDH
Sodium chloride (NaCl)	Merck
Sodium dodecyl sulphate (SDS)	Fluka
Sodium hydrogencarbonate (Na <sub>2</sub> HPO <sub>4</sub> )	Merck
Sodium succinate (Na <sub>2</sub> C <sub>4</sub> H <sub>16</sub> O <sub>10</sub> )	BDH
Sucrose (C <sub>12</sub> H <sub>22</sub> O <sub>11</sub> )	BDH
Taq-DNA-Polymerase and buffer	Qbiogene
5,5',6,6'-Tetrachloro-1,1',3,3'-tetraethyl- benzimidazolylcarbocyanine iodide (JC1)	Molecular Probes
N,N,N',N'-Tetramethylethylenediamine (TEMED)	Fluka
Tricine (C <sub>6</sub> H <sub>13</sub> NO <sub>5</sub> )	Sigma-Aldrich
Tris (C <sub>4</sub> H <sub>11</sub> NO <sub>3</sub> )	BDH
Tris-Borate-EDTA buffer (TBE) 10x	Sigma-Aldrich
Tris-Buffered-Saline (TBS) 10x	BioRad
Tris(hydroxymethyl)aminomethane (H <sub>2</sub> NC(CH <sub>2</sub> OH) <sub>3</sub> )	MP-Biomedicals
Triton-X100	Sigma-Aldrich
Tween	Merck
Trypsin	Invitrogen
Ubiquinone (CoQ1)	EISAI
Urea ((NH <sub>2</sub> ) <sub>2</sub> CO)	Merck
Valinomycin (C <sub>54</sub> H <sub>90</sub> N <sub>6</sub> O <sub>18</sub> )	Sigma-Aldrich
Versene	PAA Laboratories

### 2.2.2 Solutions

Anode buffer:	50mM bis-tris propane
Cathode buffer:	50mM tricine, 15mM bis-tris propane, 0.02% Serva blue G
Formamide:	47.5ml formamide, 2.0ml 0.5M EDTA, 0.01g bromphenol blue, pH 8.0

Homogenization buffer:	10mM Tris, 1mM EDTA, 250mM sucrose, 1mM PMSF, 1µg/ml pepstatin A, 1µg/ml leupeptin, pH 7.4
Gel buffer 3x:	1.5M 6-aminocaproic acid, 150mM bis-tris propane, pH 7.0
GSD-buffer 3x:	12ml 100% glycerol, 12ml 20% SDS, 1.852 DTT; 0.1g bromphenol blue, ad 36ml H <sub>2</sub> O
Isolation medium:	320mM sucrose, 10mM Tris, 1mM EDTA, pH 7.4
Leidener solution:	155mM NH <sub>4</sub> Cl, 10mM KHCO <sub>3</sub> , 0.1mM EDTA, pH 8.0
Loading buffer:	1M 6-aminocaproic acid, 5% Serva blue G
Lysis buffer:	10mM Tris, 400mM NaCl, 0.2mM EDTA, pH 8.0
Phosphate buffer (10mM):	10 mM KH <sub>2</sub> PO <sub>4</sub> , 10 mM K <sub>2</sub> HPO <sub>4</sub> , pH 7.0
Phosphate buffer (20mM):	20mM KH <sub>2</sub> PO <sub>4</sub> , 20mM K <sub>2</sub> HPO <sub>4</sub> , 8mM MgCl <sub>2</sub> , pH 7.2
Phosphate buffer (100mM):	100 mM KH <sub>2</sub> PO <sub>4</sub> , 100 mM K <sub>2</sub> HPO <sub>4</sub> , pH 7.4
Protein solubilising solution:	1M 6-aminocaproic acid, 50mM bis-tris propane, pH 7.0
Tris-Cl/SDS 4x:	0.5M Tris, 0.4% SDS, pH 6.8
Tris-Cl/SDS 4x:	1.5M Tris, 0.4% SDS, pH 8.8

### 2.2.3 Kits

ATP Bioluminescence Assay Kit HS II	RocheDiagnostics
BCA Protein Assay Kit	Pierce
iTaq SYBR Green Supermix with ROX	RocheDiagnostics
Native IgG Detection Kit	Pierce
Nucleon I Kit	Scotlab
Pax gene blood kit	Pax gene
SALSA P099B kit	MRC Holland
SuperScript	Invitrogen
SYBR Green I Mix	RocheDiagnostics

### 2.2.4 Antibodies

Mouse anti-NDUFA9, subunit of complex I (1:1000)	Mitosciences
Mouse anti-SDHA, subunit of complex II (1:250)	Mitosciences
Mouse anti-Core 2, subunit of complex III (1:2000)	Mitosciences
Mouse anti-MTCO2, subunit of complex IV (1:20000)	Mitosciences

Mouse anti-Alpha, subunit of complex V (1:30000)	Mitosciences
Mouse anti-GAPDH (1:1000)	Abcam
Rabbit anti-SOD2 (1:250)	Santa Cruz Biotechnology
Goat anti-mouse, HRP-conjugated (1:1000)	Dako
Goat anti-rabbit, HRP-conjugated (1:1000)	Dako
Goat anti-mouse, Alexa 488-conjugated (1:100)	Amersham Biosciences

### 2.2.5 Oligonucleotides

Oligonucleotide (primer)	Biometra; MWG Biotech
Oligonucleotide, labelled	MWG Biotech
Probes	TIB Molbiol
Size standard (100bp)	Invitogen

### 2.2.6 Equipment

Automatic sequencer Long Read IR2-DNA	LI-COR
Centrifuge	Eppendorf, Neolab, Sorvall
Column heater	Jones Chromatography
Confocal microscope Axioplan	Zeiss
DEG-1033 degasser	Kontron Instruments
ESA 5010 analytical cell	ESA Analytical
Filter papers	Whatman
Homogeniser	Eurostar IKA Werke
Jade luminometer	Labtech International
Kontron HPLC 360 autosampler	Watford
Mini-transblot unit	BioRad
Mini-gel system	BioRad
Octadecasilyl column	Techsphere
Pax gene blood tubes	Pax gene
PD <sub>10</sub> column	Pharmacia Biotech
Spectrophotometer	Hitachi
PU-1580 pump	Jasco
PVDF HyperbondP membrane	Amersham Biosciences
Scale	Satorius

Synergy HT plate reader	BIOTEK
Thermocycler - LightCycler	RocheDiagnostics
- Mastercycler	Eppendorf
- 7300 Real-Time PCR System	Applied Biosystems
Thermoseparation Products chromejet integrator	Anachem
Upstream and downstream electrode	ESA Analytical

### 2.2.7 Software

geNorm program	VBA applet10
Image processing program	TotalLab
RQ Study Application	7300 SDS Software

## 2.3 Methods

This methodical description is especially focussed on techniques which were established in the neurogenetics laboratory of Professor Klein as a part of the present thesis.

### 2.3.1 Extraction of nucleic acids

During the experimental phase of this thesis DNA was gained from human blood and fibroblast cell cultures. RNA was only extracted from blood samples.

#### 2.3.1.1 DNA extraction from whole blood

Genomic DNA was prepared from leucocytes of peripheral blood by means of a salting out method (Miller *et al.*, 1988). Cells are lysed by adding of a hypertonic solution. Proteins are digested by proteinase K and the DNA is isolated by precipitation.

By means of this method between 100 and 1000µg genomic DNA can be retained.

#### 2.3.1.2 DNA extraction from fibroblasts

For DNA extraction from fibroblast the Nucleon I kit was used. Cell pellets were processed according to manufacture's protocol.

#### 2.3.1.3 RNA extraction from whole blood

Blood for RNA extraction from patients was collected in Pax gene tubes and extracted with the respective Pax gene blood kit.

### 2.3.2 Polymerase chain reaction

The polymerase chain reaction (PCR) is an enzymatic method to amplify DNA *in vitro* (Saiki *et al.*, 1985). The specificity of the amplification is achieved by use of two chemically synthesized primers which bind complementary to a certain target sequence. A temperature stable polymerase synthesises the DNA region between the primers. The reaction is divided in three repeating steps: denaturing, annealing, extension. Exponential amplification of the target sequence provides high DNA concentrations for further analysis.

#### 2.3.2.1 Standard PCR

A PCR under standard conditions is run as follows.

Reaction mixture:

Substance	Stock concentration	Volume	Final concentration
dH <sub>2</sub> O		ad 15,00µl	
Betaine	5mM	0,70µl	0,23mM
Puffer	10x	1,50µl	1x
dNTPs	1mM	3,00µl	0,2µl
Primer +	10µM	0,60µl	0,4µl
Primer -	10µM	0,60µl	0,4µl
Taq polymerase	5U/µl	0,07µl	0,23U/µl
DNA	~ 5ng/µl	5,00µl	~ 1,67ng/µl

Cycling conditions:

95°C 5min // 35 cycles: 95°C 30s; 55-72°C 30s; 72°C 30s-4min // 72°C 10min // 4°C ∞

The annealing temperature is depending on the structure of the primers used. The extension time is adjusted to the expected product size.

For the M-D study (3.1) all coding *SGCE* exons except for a rare splicing variant of exon 10 were sequenced as described (primer sequences are shown in Table S1). The finding of an exon 2 deletion was investigated by sequencing at the cDNA level in F2454 (father of IP15624) with primers in exons 1 and 3 (Fig 8C inset).

In the *PINK1* expression study (3.2) the eight exons of the gene were amplified using PCR conditions and intronic primers as described above (for primer sequences see supplement: Table S3).

#### 2.3.2.2 PCR with fluorescence-labelled primers: Genotyping and sequencing

Genotype analysis and sequence analysis was performed by means of an automatic sequencer. Therefore, fluorescence-labelled primers are needed.

Before the actual sequencing procedure can be started the target DNA is amplified in a basic PCR reaction. The amplification is achieved by the help of primers which are extended for a

specific M13-sequence at their 5' end (M13F nucleic sequence for forward primer and M13R for reverse primer).

For the sequencing reaction primers complement to the M13F or M13R sequence are added to the first PCR product. These primers are labelled with the fluorescence dye IRD-700 or IRD-800. During this second PCR reaction specific products are generated which are elongated by the M13F or M13R sequence and which carry the fluorophore IRD-700 at the forward sequence and IRD-800 at the reverse sequence.

For genotyping only the forward primer including the M13F sequence is used in the first PCR step. In a second PCR a M13F primer either labelled with IRD-700 or IRD-800 plus a standard primer is used. Therefore PCR products are obtained which carry an extension of the M13F sequence and a fluorophore in forward transcription orientation only.

In the M-D study (3.1) a haplotype analysis of the *SGCE* region on chromosome 7q was performed with polymorphic markers (positions are given in Fig 8B; see also UniSTS database at PubMed). Whenever it was impossible to differentiate between homo- and hemizygoty at certain polymorphic DNA markers, gene dosage (2.3.2.3) at these marker positions was additionally determined by quantitative PCR. For IP16535, paternity was confirmed with seven polymorphic DNA markers on different chromosomes.

For haplotype analysis in the *PINK1* expression study (3.2), four intragenic SNPs and six flanking microsatellite markers were genotyped using primer sequences which were also taken from the UniSTS database. The haplotypes were constructed manually.

#### 2.3.2.3 Real-time PCR: Gene dosage studies

Gene dosage analysis was performed in a quantitative SYBR Green PCR on the LightCycler. Each individual target sequence was amplified by use of appropriate primers. In addition to this target reaction, the expression of the nuclear single copy gene was quantified for each investigated sample serving as an external standard.

The following reagents were used for amplification in a 10 $\mu$ l reaction: 2 $\mu$ l SYBR Green I Mix, 0.5–1.0 $\mu$ M of each primer and 1–15ng of DNA. PCR conditions were as follows: 95°C for 10min, 95°C for 5s, 65°C for 10s, 72°C for 15s (40 cycles); measurement of fluorescence in each cycle according to the amplification product.

During the log-linear phase, amplification can be described as:

$$N=N_0(1+E_{\text{const}})^n$$

N - Number of amplified molecules

$N_0$  - Initial number of molecules

E - Amplification efficiency

n - Number of cycles

Since amplification efficiency during the log-linear phase is constant, the initial concentration of the sample was calculated based on the above formula, using a standard curve. This standard curve was generated using human genomic DNA in concentrations of 20, 4 and 0.8ng/ $\mu$ l, respectively. All standards were amplified in duplicate and a regression curve was calculated. Sample concentrations were inferred based on this regression curve. Concentrations not within the range of the standard templates were disregarded and adjusted. All samples were also measured in duplicate and results were accepted only within a range of <10% of the standard deviation of the two inferred sample concentrations. After each PCR, a melting curve was performed between 40 and 80°C to analyze the purity of the amplification product.

In the M-D study (3.1) the MLPA results of selected *SGCE* exons (3, 4, 6, 8, 9, 11 and 12; for primer sequences see Table S2) were confirmed by quantitative real-time PCR (qPCR) (data not shown). The expression of the target exons were quantified with *beta globin* serving as an external standard. A ratio between 0.8 and 1.2 was considered as normal, a heterozygous deletion was expected at a ratio between 0.4 and 0.6, a heterozygous duplication between 1.3 and 1.7, and a homozygous duplication or a triplication at a ratio between 1.8 and 2.2. In addition, the final narrowing of the deletion breakpoints in the families of IP15916 and IP16535 was achieved by quantification of two different DNA fragments within the remaining undefined regions surrounding *SGCE* on chromosome 7q using qPCR on the LightCycler with SYBR Green (qPCR1 and qPCR2, Fig 10).

In the functional approach for *PINK1* (3.3) mitochondrial DNA concentration was measured with the help of primers against the mitochondrial displacement loop (D-loop) (for sequences see Bai and Wong, 2005). In this region in the mitochondrial DNA no polymorphisms are known and it is not prone to mutations or deletions. Using the external nuclear control gene *thymidine kinase 2* (*TK2*; forward primer: 5'-TCC TGC AGA TGC CAC TTT GA-3'; reverse primer: 5'-CCC CAA GTC TGA AGA AAA CG-3') provided a relative ratio of concentration target/concentration reference (amplification of the nuclear gene in a separate reaction form the target sequence). Thus, this ratio corresponded to the gene dosage of both DNA fragments.

#### 2.3.2.4 Real-time PCR: Gene expression studies

To investigate the gene expression of *PINK1* (3.2), patient mRNA was transferred into cDNA by means of the Superscript kit. On basis of the generated cDNA quantitative real-time PCR was performed. Real-time PCR amplification mixtures (25µl) contained 2µl cDNA, 12.5µl 2X iTaq SYBR Green Supermix with ROX and 200nM forward and reverse primer. Reactions were performed in duplicate and run on an ABI 7300 Real-time PCR System; cycling conditions: 10' 95°C initial denaturation followed by 40 cycles 15" 94°C denaturation and 1' 68°C annealing/extension/data-collection. This was followed by a dissociation curve analysis. In a first step, we determined the stability of ten control genes for normalization of the real-time PCR. They were tested in a four-point relative standard curve analysis (cDNA standards from a pool of tested samples diluted over a 10-fold range). To determine the linearity and efficiency of PCR amplification of each reference gene,  $C_T$  values were plotted versus log [initial cDNA] using the RQ Study Application of the 7300 SDS Software.

The eight genes with the highest efficiency (close to 100%) were *ACTB* (*actin, beta*), *B2M* (*beta 2-microglobulin*), *HMBS* (*hydroxymethylbilane synthase*), *HPRT1* (*hypoxanthine phosphoribosyltransferase 1*), *SDHA* (*succinate dehydrogenase complex, subunit A*), *LOC644604* (*similar to eukaryotic translation elongation factor 1 alpha 2*), *UBE2D2* (*ubiquitin-conjugating enzyme E2D 2*), and *YWHAZ* (*tyrosine 3-monooxygenase/tryptophan 5-monooxygenase activation protein, zeta polypeptide*) (for details see supplementary material: Table S4). These were studied for their average expression stability in six randomly chosen cDNA samples from Family W. From these real-time raw data, both the optimal number of control genes for normalization and the most stable genes out of the pool were determined by using the geNorm VBA applet<sup>10</sup> (cp. Fig S1 and Fig S2).

The PCR amplification efficiency was additionally evaluated for three *PINK1* fragments spanning exons 3 to 4, 5 to 6 or 7 to 8 (primer sequences shown in Table S4).

Based on the evaluation of *PINK1* and the reference genes, we decided to use four different real-time assays to perform the quantification of *PINK1* mRNA levels (*PINK1* exon 5-6 or exon 7-8 relative to *SDHA* or *YWHAZ*). All of these combinations were applied to the 20 cDNA samples of Family W, whereas for Family MI-002, only two assays were carried out (*PINK1* exon 5-6 or exon 7-8 relative to *SDHA*) in four members.

#### 2.3.2.5 Multiplex ligation-dependent probe amplification

For MLPA analysis the SALSA P099B kit (MRC Holland; Amsterdam, The Netherlands; [<http://www.mrc-holland.com/pages/p099pag.html>]) was applied. Probes were amplified in a

PCR reaction according to the manufacturer's protocol (Fig 5). Amplification products were separated by polyacrylamide gel electrophoresis (PAGE, see 2.3.3.2) and visualized on an automated sequencing machine. For all samples, a specific pattern of bands, varying in size and intensity, was observed. Each of these bands represented one amplified pair of probes from the kit. The MLPA gel images were analyzed with the help of an image processing program (TotalLab), employing a "nearest neighbour" model (Djarmati *et al.*, 2007), which allows calculating the relative initial concentration of the specific DNA fragment. Normalized value ratios between 0.8 and 1.2 were considered normal, a heterozygous deletion was expected at a ratio between 0.3 and 0.7, and a heterozygous duplication between 1.3 and 1.7. MLPA was performed for all exons of *SGCE* except the rare splicing variant, exon 10, in the M-D approach (Fig 9).

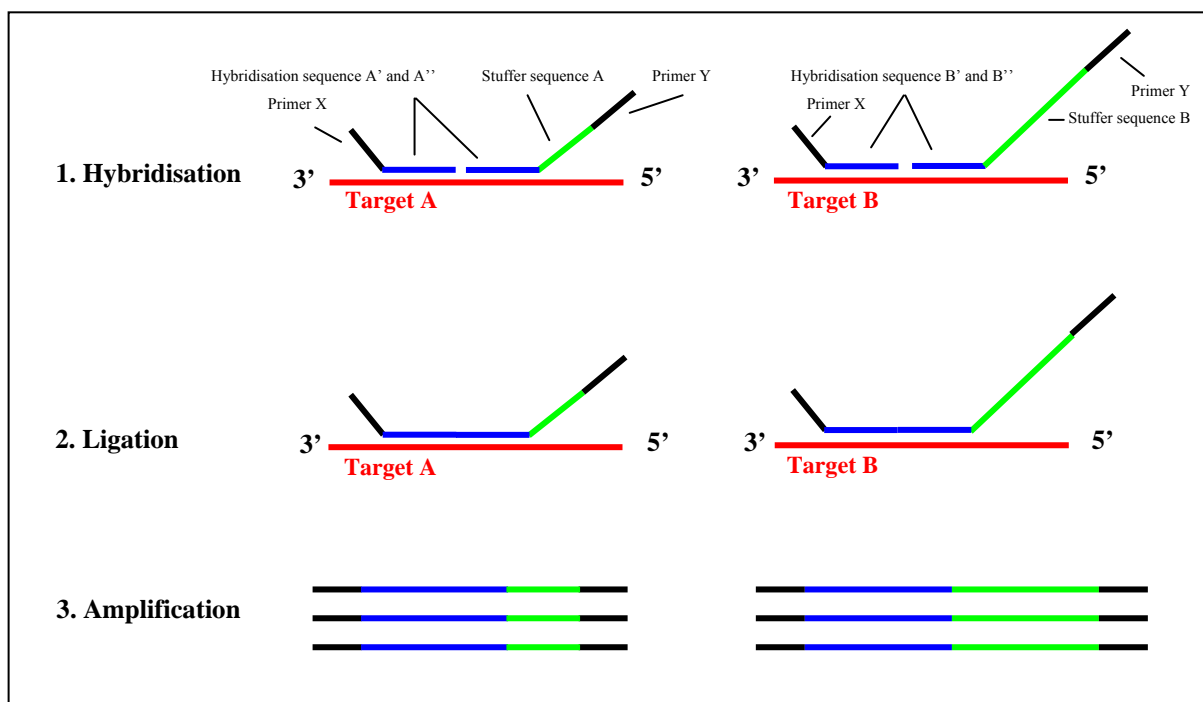


**Fig 5** Principle of the MLPA analysis. For each target a specific pair of probes is needed. The included primer sequences X and Y are constant whereas the stuffer sequence varies for each pair of probes. Two parts of each probe hybridise to adjacent target sequences and are ligated by a thermostable ligase. In a next step all probe ligation products are amplified by PCR using only one primer pair. If one of the two probes can not bind to their target because of a mutation or a lack of target sequence a ligation is abolished and no amplification will occur. The amount of probes binding to a target can be quantified after the amplification (Schouten *et al.*, 2002).

### 2.3.3 Gel electrophoresis

Three different types of electrophoresis were applied here: agarose gel electrophoresis and polyacrylamide gel electrophoresis in a denaturing as well as a non-denaturing form.

### 2.3.3.1 Agarose gel electrophoresis

Agarose powder is mixed with electrophoresis buffer to the desired concentration and then heated in a microwave oven until completely melted. Ethidium bromide is added to the gel (final concentration 0.5µg/ml) at this point to facilitate visualization of DNA after electrophoresis. After cooling the solution to about 60°C, it is poured into a casting tray containing a sample comb and allowed to solidify at room temperature.

Formamide dye is added in ratio 1:3 (vol/vol) to the samples before loading. With each set of samples a molecular weight standard (100bp ladder) is loaded. The electrophoresis is processed at 120V for 30-60min in 1x TBE buffer.

### 2.3.3.2 Denaturing polyacrylamide gel electrophoresis for DNA

Denaturing PAGE uses the anionic detergent sodium dodecyl sulfate (SDS) to transfer samples into linear monomers, rendering their charge proportional to their length so that migration is a function of size.

For sequencing, genotyping and MLPA an automated sequencer is employed. This sequencer is equipped with two infrared lasers which allow simultaneous detection at 500 and 700nm.

Gel composition:

Substance	Genotyping	MLPA	Sequencing
30% Acrylamid (vol/vol)	6ml	—	—
Acrylamid (Long Ranger)	—	2.4ml	3.3ml
10xTBE	3ml	2.4ml	3.0ml
Urea	3g	8.4g	12.6g
dH <sub>2</sub> O	Ad 30ml	Ad 20ml	ad 30ml
10% APS (wt/vol)	180µl	134µl	200µl
TEMED	25µl	13.4µl	20µl

The SDS-PAGE is performed for DNA samples as follows:

- Pouring of gel
  - genotyping: 25cm x 22.5cm x 0.4mm
  - MLPA: 25cm x 22.5cm x 0.2mm
  - sequencing: 25cm x 41cm x 0.2mm
- Polymerisation and adjusting to the LI-COR
- System prerun (focussing of the lasers) for 20min
- Addition of formamide to the samples
  - genotyping: 2 vol.
  - MLPA: 5 vol.
  - sequencing: 4µl loading dye
- Denaturing of samples at 95°C for 3min, then cooling to 4° C

- Loading

- genotyping: 0.7 – 1.5 $\mu$ l
- MLPA: 0.7 $\mu$ l
- sequencing: 1 $\mu$ l

- Electrophoresis in 1x TBE as running buffer

- genotyping: for about 3h at 45°C, 25W and 40mA
- MLPA: for about 3h at 45°C, 25W and 40mA
- sequencing: for about 6h at 50°C, 31.5W and 35mA

### 2.3.4 Determination of reduced cellular glutathione

The concentration of reduced cellular glutathione (GSH) was determined by reverse-phase high-performance liquid chromatography (HPLC) coupled to a dual-electrode electrochemical detector as previously described by Riederer *et al.* (1989).

#### 2.3.4.1 Reverse-phase HPLC

A scheme of the reverse-phase HPLC system is shown in Fig 6. Sample (20 $\mu$ l) was injected by an autosampler through a guard column (octadecasilyl; 3mm x 10mm) to remove debris, and resolved using a reverse-phase octadecasilyl column (particle size 5 $\mu$ m, 4.6mm x 250mm) maintained at 30°C by a column heater. The mobile phase was 15mM orthophosphoric acid prepared in 18.2M $\Omega$  H<sub>2</sub>O (pH 2.5) and degassed. The flow rate was maintained at 0.5ml/min.

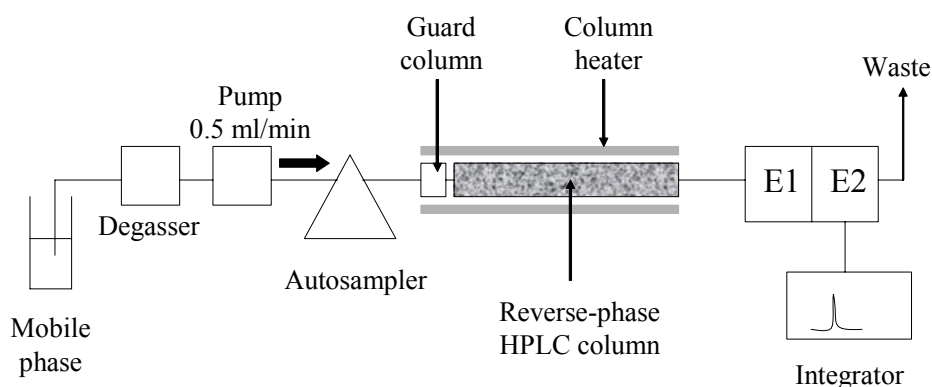


**Fig 6** Scheme to illustrate the apparatus used to determine GSH by reverse-phase HPLC and electrochemical detection. E1, upstream electrode; E2, downstream electrode.

Following separation by the column, GSH was electrochemically detected by an analytical cell containing an upstream and downstream electrode. The magnitude of current generated

by the oxidation of GSH at the downstream electrode was proportional to the amount of GSH and was recorded as a chromatogram on a Thermoseparation Products chromejet integrator at a chart speed of 0.25cm/min. Note that prior to detection of samples, the mobile phase was circulated through the column and electrode for 18h. This allows the electrochemical detector to settle and yield a low baseline current (0.02-0.1 $\mu$ A).

#### *2.3.4.2 Sample Preparation*

GSH standards (1-10 $\mu$ M) were prepared in 15mM orthophosphoric acid and stored at  $-70^{\circ}\text{C}$ . The levels of GSH in fibroblasts were determined by trypsinizing the cells, resuspending in isolation medium, and extracting into 15mM orthophosphoric acid (1:1 vol/vol). Samples were then centrifuged at room temperature for 5min at 14000 x g to pellet protein. The supernatant was used for injection onto the HPLC column. The current generated by samples was converted into sample concentration using a GSH standard calibration graph (1-10 $\mu$ M).

### **2.3.5 Tissue culture**

The tissue culture necessary for the collection of the results described in chapter 3.3 was restricted to fibroblasts.

#### *2.3.5.1 Fibroblast culture*

Fibroblasts were plated in 100mm dishes and T-175 flasks and cultured in Dulbecco's Modified Eagle Medium (DMEM) plus 10% foetal bovine serum albumin (vol/vol), 10mg/l sodium pyruvate, 4.5g/l glucose and 10ml/l penicillin/streptomycin in an incubator (95% air/5% CO<sub>2</sub>) at 37 °C (media changed every 3-7 days).

#### *2.3.5.2 Passage of fibroblasts*

Fibroblast were passaged when 80% confluent. Cell media was removed, the cells washed with phosphate buffered saline (PBS), and incubated at 37°C with 5ml to 10ml trypsin/versene (0.5% (wt/vol) trypsin) for 5min. Trypsinisation was terminated by the addition of 10% (vol/vol) foetal bovine serum, and the fibroblasts pelleted by centrifugation at 1000rpm for 5min. Fibroblasts were resuspended in culturing medium composed as above.

#### *2.3.5.3 Treatment with toxins*

To study the presence of NMD, fibroblast cell cultures from one mutant member of Family W were cultured with and without treatment with cycloheximide (100 $\mu$ g/ml for 8h), a known NMD inhibitor, before mRNA isolation and cDNA synthesis.

To study consequences of oxidative stress several fibroblast cultures of Family W were treated with the superoxide generator paraquat (0.5mM for 48h).

### **2.3.6 Mitochondrial preparation**

Mitochondria were isolated from fibroblasts as previously described by Almeida and Medina (1997). Cells were removed from flasks by incubating the cells with 0.5% (wt/vol) trypsin resuspended in versene for 5min. Trypsinisation was stopped by addition of an equal volume of isolation medium supplemented with 10% (vol/vol) foetal bovine serum. The cells were pelleted by centrifugation at 1000rpm for 5min. (The pellet can be frozen at -80°C at this point.) To proceed, cells were resuspended in 1ml ice-cold homogenization buffer. Cells were then centrifuged at 4000 x g for 5min and the supernatant was discarded. The pellet was again resuspended in 2ml ice-cold homogenisation buffer. Cells were optimally homogenised on ice by 20 strokes of a tight fitting glass-teflon homogeniser revolving at 1000rpm. Cell homogenates were centrifuged at 1500 x g for 10min at 4 °C, the supernatant placed on ice, and the pellet resuspended in 2ml homogenisation buffer, homogenised and centrifuged as above. The supernatants were then combined and centrifuged once more at 1500 x g (10min, 4°C). The pellet was discarded, and the supernatant centrifuged at 11500 x g for 12min at 4°C. The received mitochondria pellet was resuspended in 75µl homogenization buffer, frozen in liquid nitrogen, and stored at -80°C until required. The activity of the mitochondrial marker enzyme citrate synthase was enriched approximately 3-fold between the initial cell homogenate and the final mitochondrial pellet.

### **2.3.7 Protein determination**

Sample protein concentration was determined by use of the BCA protein assay kit according manufacture's protocol. Absorbance was measured on a plate reader at 562nm. Sample protein concentration was calculated from the BCA standard calibration curve (0-1500µg/ml).

### **2.3.8 Mitochondrial enzyme assays**

The activities of complexes I to IV, of citrate synthase and of malate dehydrogenase were determined in mitochondrial preparations by means of a spectrophotometrical approach. The data of the complexes were expressed against citrate synthase.

### 2.3.8.1 Citrate synthase assay

The enzyme citrate synthase exists in nearly all living cells and stands as a pace-making enzyme in the first step of the Citric Acid Cycle. Citrate synthase is localized within eukaryotic cells in the mitochondrial matrix, but is encoded by nuclear DNA rather than mitochondrial (Wiegand and Remington, 1986). It is therefore used as a cellular marker for mitochondrial integrity and content. Citrate synthase activity (CS) was determined using a Hitachi U-3310 spectrophotometer as described by Coore *et al.* (1971). Sample (10-20 $\mu$ g protein; freeze-thawed three times in liquid nitrogen) was mixed with 100mM Tris (pH 8.0), 0.1mM acetyl coenzyme A, 0.1% (wt/vol) Triton-X100, and 0.1mM DTNB in a cuvette (total volume 1ml, path length 1cm). The reaction was started by the addition of 0.1mM oxaloacetate, and activity measured at 412nm for 5min at 30°C (DTNB extinction coefficient =  $13.6 \times 10^3 \text{ M}^{-1} \text{ cm}^{-1}$ ). Samples were run against a reference cuvette that contained sample and all substrates except oxaloacetate. Citrate synthase activity was linear between 5 and 25 $\mu$ g protein.

### 2.3.8.2 Malate dehydrogenase assay

Like citrate synthase, malate dehydrogenase is an enzyme of the Citric Acid Cycle where it catalyzes the conversion of malate into oxaloacetate and vice versa. In eukaryotes two different isoforms of the enzyme can be found – a mitochondrial and a cytoplasmic version (Davidson and Cortner, 1967). The activity of the mitochondrial malate dehydrogenase (MDHM) is used to determine the mitochondrial content in cells. MDHM was measured according to the method of Lai and Clark (1976). The reaction mixture contained 100mM potassium phosphate buffer, pH7.4, 0.16mM NADH, 0.16% (v/v) Triton X-100, 133pM oxaloacetate and about 10 $\mu$ l of the cellular homogenates (cp. 2.3.6). After controlling the flattening of the baseline for 1-2min the reaction was commenced with the addition of oxaloacetate and the NADH oxidation was measured at 340nm for 5min at 30°C (NADH extinction coefficient =  $6.81 \times 10^3 \text{ M}^{-1} \text{ cm}^{-1}$ ; total volume = 1ml; path length = 1cm). Homogenates were measured against a reference cuvette that contained all components except oxaloacetate.

### 2.3.8.3 Complex I assay (NADH dehydrogenase)

Complex I activity (CI) was determined spectrophotometrically using a Hitachi U-3310 spectrophotometer as described by Ragan *et al.* (1987). Sample (10-20 $\mu$ g protein; freeze-thawed three times in liquid nitrogen) was mixed with 20mM phosphate buffer (pH 7.2), 2.5mg/ml BSA, 0.15mM NADH, and 1mM KCN in a cuvette. The reaction was started by the

addition of 0.25mM CoQ1. Enzyme activity was measured at 30°C by following the oxidation of NADH to NAD<sup>+</sup> at 340nm for 5min (NADH extinction coefficient =  $6.81 \times 10^3 \text{M}^{-1} \text{cm}^{-1}$ ; total volume = 1ml; path length = 1cm). After 5min, 10 $\mu$ M rotenone was added, and rotenone insensitive NADH oxidation was measured for 5min. Complex I activity was calculated by subtracting the rotenone insensitive NADH oxidation rate from total NADH oxidation rate (units = nmol/min/mg protein). Note that all cuvettes were run against a reference cuvette that contained sample and all the substrates except CoQ1. Complex I activity was proportional to protein between 5 and 25 $\mu$ g protein.

#### 2.3.8.4 Complex II+III assay (succinate cytochrome c reductase)

Complex II+III activity (CII+III) was determined spectrophotometrically as described by King (1967). Sample (10-20 $\mu$ g protein; freeze-thawed three times in liquid nitrogen) was mixed with 100mM phosphate buffer (pH 7.4), 0.3mM EDTA, 1mM KCN, and 0.1mM oxidised cytochrome c (from horse heart) in a cuvette. The reaction was started by addition of 20mM succinate and enzyme activity measured at 30°C by following the reduction of cytochrome c at 550nm for 5min (cytochrome c extinction coefficient =  $19.2 \times 10^3 \text{M}^{-1} \text{cm}^{-1}$ ; total volume = 1ml; path length = 1cm). After 5min, 20 $\mu$ M antimycin A was added, and the antimycin A insensitive rate of cytochrome c reduction was followed for a further 5min. Complex II+III activity was calculated by subtracting the antimycin A insensitive cytochrome c reduction rate from total cytochrome c reduction rate (units = nmol/min/mg protein). Note that all cuvettes were run against a reference cuvette that contained sample and all the substrates except succinate. Complex II+III activity was proportional to protein between 5 and 35 $\mu$ g protein.

#### 2.3.8.5 Complex IV assay (cytochrome c oxidase)

The determination of the enzyme kinetic of complex IV requires reduced cytochrome c as a substrate.

##### 2.3.8.5.1 Reduction of oxidised cytochrome c

Ascorbate crystals were added to oxidised cytochrome c (0.8mM) until a colour change was observed from dark to light red. The reduced cytochrome c was then passed through a PD<sub>10</sub> gel filtration column (column equilibrated by washing column with 30ml of 10mM phosphate buffer, pH 7.0) to remove the ascorbate from the reduced cytochrome c. The concentration of reduced cytochrome c was determined by mixing 50 $\mu$ l reduced cytochrome c with 950 $\mu$ l H<sub>2</sub>O in both a sample and reference cuvette. The sample cuvette was 'zeroed' against the reference

cuvette at an absorbance of 550nm. 1mM ferricyanide was then added to the reference cuvette to oxidise the reduced cytochrome c, and the absorbance of the sample cuvette noted (cytochrome c extinction coefficient =  $19.2 \times 10^3 \text{M}^{-1} \text{cm}^{-1}$ ; total volume = 1ml; path length = 1cm).

#### 2.3.8.5.2 Measurement of complex IV activity

Complex IV activity (CIV) was determined spectrophotometrically using a Hitachi U-3310 spectrophotometer as described by Wharton and Tzagoloff (1967). In a sample and reference cuvette, 10mM phosphate buffer (pH 7.0) and 50 $\mu$ M reduced cytochrome c was mixed, and the sample cuvette zeroed against the reference. To the reference cuvette, 1mM ferricyanide was added to oxidise the cytochrome c, yielding an absorbance of approximately 1.0 at 550nm in the sample cuvette prior to addition of sample. Sample (10-20 $\mu$ g protein; freeze-thawed three times in liquid nitrogen) was then added to the sample cuvette and the oxidation of cytochrome c at 550nm was measured for 5min at 30°C against the reference cuvette (cytochrome c extinction coefficient =  $19.2 \times 10^3 \text{M}^{-1} \text{cm}^{-1}$ ; total volume = 1ml; path length = 1cm). Complex IV activity is expressed as the first order rate constant k per min per mg protein and was determined by noting the highest positive absorbance following sample addition ( $t = 0$ min), and the absorbance every minute after that for 3min. k was calculated by:  $(\ln(A_{550t=0}/A_{550t=n})/\text{number of min})/\text{protein concentration}$ . The rate constant for each sample was taken as the mean of k at 1, 2 and 3min. Complex IV activity was proportional to protein between 2 and 20 $\mu$ g protein.

### 2.3.9 Cellular ATP concentration

ATP levels were determined with the ATP Bioluminescence Assay Kit HS II. Prior to the measurement with a luminometer the samples were corrected for cell number. The experiment was performed with  $1 \times 10^5$  cells per ml PBS. The standard curve ranged from  $4.15 \times 10^{-13}$  to  $8.3 \times 10^{-9}$  moles of ATP.

### 2.3.10 Mitochondrial membrane potential

$\Delta\psi_m$  was analysed with the sensitive fluorescent probe 5,5',6,6'-tetrachloro-1,1',3,3'-tetraethylbenzimidazolylcarbocyanine iodide. This lipophilic cation changes reversibly its emitted light from 530nm to 590nm as membrane potentials increase. Therefore about  $5 \times 10^5$  cells were plated per 12-well. One well per culture was treated with 1 $\mu$ g/ml JC-1 for 15min at

37°C. To detect basal fluorescence emission an additional well per culture was treated with the ionophore valinomycin in the presence of JC-1. As a blank, one well per sample remained untreated. For detection at 590nm a plate reader was used.  $\Delta\psi_m$  was expressed relative to the protein concentration per well and calculated by:

$$\Delta\psi_m = \frac{FL_{\text{Target}}/[Protein]_{\text{Target}} - FL_{\text{Blank}}/[Protein]_{\text{Blank}}}{FL_{\text{Valinomycin}}/[Protein]_{\text{Valinomycin}} - FL_{\text{Blank}}/[Protein]_{\text{Blank}}}$$

$FL_x$  - Fluorescence emission of a certain well

[x] - Protein concentration of cells of a certain well

### 2.3.11 Western blotting

The Western blotting procedure involves sample preparation, PAGE, protein transfer and antibody detection of target proteins on the resulting blot.

#### 2.3.11.1 Sample preparation

For the preparation of blue native gels whole cell homogenates in isolation medium were used. The protein concentration per sample was determined according to the protocol given in 2.3.7. Five to 10 $\mu$ g protein were loaded per well on the PAGE gel.

#### 2.3.11.2 Denaturing PAGE for proteins

For protein separation a mini-gel system was used. The two gel solutions applied are composed as follows:

Substance	10% separating gel	Stacking gel
30% acrylamid/ 0.8% bisacrylamid (vol/vol)	5ml	650 $\mu$ l
4x Tris-Cl/SDS, pH 6.8	—	1.25ml
4x Tris-Cl/SDS, pH 8.8	3.75ml	—
dH <sub>2</sub> O	6.25ml	3.05ml
10% APS (wt/vol)	50 $\mu$ l	25 $\mu$ l
TEMED	10 $\mu$ l	5 $\mu$ l

A 10% separating gel was poured up to 4/5 of the total height of the prepared glass plates. After polymerisation (~30min) the stacking gel was added (Laemmli, 1970). GSD-buffer in ratio 1:3 (vol/vol) was added to the samples and boiled for 5min at 95°C. 5-10 $\mu$ l of sample mixture were loaded on the bottom of each well. A molecular weight standard was run on the same gel. The electrophoresis was performed in protein running buffer for about 2h at ~100V and 10mA.

### 2.3.11.3 Non-denaturing PAGE for proteins

"Native" or "non-denaturing" gel electrophoresis is run in the absence of SDS. While in SDS-PAGE the electrophoretic mobility of proteins depends primarily on their molecular mass, in native PAGE the mobility depends on both the protein's charge and its hydrodynamic size.

The electric charge driving the electrophoresis is governed by the intrinsic charge on the protein at the pH of the protein running buffer. This charge is depending on the AA composition of the protein as well as post-translational modifications such as addition of sialic acids. In contrast to a normal PAGE gel for the separation of proteins a 5 to 14% gradient gel was needed. The gel solutions necessary for native PAGE are composed as follows:

Substance	4% separating gel	14% separating gel	3% stacking gel
48% acrylamid/ 1.5% bisacrylamid (vol/vol)	0.99ml	2.44ml	0.38ml
3x gel buffer, pH 7.0	3.96ml	3.3ml	2.0ml
dH <sub>2</sub> O	6.85ml	2.51ml	3.12ml
Glycerol	—	1.98g	—
10% APS (wt/vol)	70µl	35µl	50µl
TEMED	7µl	3.5µl	5µl

The separating gel was poured in between prepared glass plates which were assembled per BioRad protocol (as above). To gain the desired gradient, a mixing apparatus consisting of two connected chambers (including one stirring rod each) was used. Dispersion of the gel solutions was achieved by an external pump. After polymerisation of the separation gel the stacking gel is added. The protein samples were prepared for loading according to the following protocol:

Substance	Volume or time
Protein solubilising solution + inhibitors	15µl
10% Lauryl maltoside (wt/vol)	5µl
Protein sample	5µg
Incubation on ice	15min
Centrifugation (13,000rpm; 4°C)	20min
Loading buffer	2.5µl

For the electrophoresis cathode buffer was filled in the inner chamber of the mini-gel system and anode buffer into the cell to cover the anode. The samples were mixed with loading buffer in ratio 1:6 (vol/vol). The gel was run at 100V until the front entered the stacking gel. The electrophoresis was changed to 4-8mA fixed current until the front had started running out of the gel.

#### 2.3.11.4 Protein transfer

A piece of PVDF membrane was cut and wet for about 30min in methanol on a rocker at room temperature. Then the membrane was washed three times in blotting buffer and finally equilibrated in blotting buffer for about 15min.

Sponges and filter papers were prewet in 1x blotting buffer before assembling of the mini-transblot unit. The Western blot “sandwich” was built in the following order:

1. Sponge
2. Filter paper
3. PAGE gel
4. PVDF membrane
5. Filter paper
6. Sponge

The transfer is run at 100V for 1hr in blotting buffer at 4°C.

#### 2.3.11.5 Antibody staining of Western blots

The blot was blocked in 0.1%TBS-Tween/ChemiBlocker (1:1, vol/vol) for 1h. The primary antibody was added into 0.1%TBS-Tween/ChemiBlocker (1:1, vol/vol) in an appropriate concentration (according to manufacture’s protocol) and the blot was incubated over night at 4°C. This was followed by three washings in 0.1%TBS-Tween for 10min each. The blot was then incubated with a horseradish-peroxidase (HRP)-conjugated secondary antibody in 0.1%TBS-Tween/ChemiBlocker (1:1, vol/vol) in an appropriate ratio (according to manufacture’s protocol). This is followed by another three washing steps. The bands were detected by enhanced chemiluminescence. Equal loading was assessed by use of an antibody against a standard protein. Band density was measured using Alpha DigiDoc software.

### 2.3.12 Staining of the mitochondrial network

Fibroblasts were removed from flasks with trypsin as above (2.3.5.2), and  $1.5 \times 10^4$  cells in 0.5ml of culturing medium (2.3.5.1) were seeded onto poly-lysine (10 $\mu$ g/ml) coated glass coverslips (5.3cm<sup>2</sup>) placed in 6-well plates. The cells were then incubated for approximately 24h. The medium was removed and replaced by prewarmed medium containing MitoTracker Green MF (250nM, for further details see manufacturer’s protocol). After an incubation of 45min the cells were washed for three times with 1ml of PBS. Fibroblasts were fixed by adding 2ml pre-chilled 3.7% paraformaldehyde permeabilised in methanol (-20°C) per well and incubating on ice for 5min. The methanol was then removed and washed three times with

1ml PBS. Finally, the coverslips were mounted on glass microscope slides (76 x 26mm) with 10µl Cytofluor. Fluorescence was detected using a confocal microscope at 516nm.

### **2.3.13 Electron microscopy**

Before the samples of interest can be studied by electron microscopy complex processing of the material is necessary.

#### *2.3.13.1 Sample preparation*

Cells of one T-175 flask were harvested as above (2.3.5.2). For fixation the pellet was treated with 2% glutaraldehyde/0.1M PIPES (vol/vol) buffer (pH 7.4) for 1h. This was followed by centrifugation (2000rpm) and resuspension of the cells in 2% sucrose/0.1M PIPES (wt/vol) buffer for 15min. After centrifugation 1% OsO<sub>4</sub>/0.1M PIPES buffer (wt/vol) was added and incubated for 40min. To finish, the incubation cells were centrifuged at 2000rpm, the supernatant was taken off and the pellet was resuspended in 0.1M PIPES buffer. This washing was repeated another two times. Following the washes 3% low-melting point agarose in 0.1M PIPES buffer was warmed up and poured onto the pellets. This step was followed by a spin at 2000rpm for 5min.

By adding of 30% ethanol (vol/vol) the gel containing the cells was released from the tube. Additional gel of the block was eliminated. The remaining part of gel including the cells was cut in pieces of about 3mm<sup>3</sup>. These pieces were dehydrated in 30% ethanol (vol/vol) for 15min. After incubation, the alcohol was replaced by 50% ethanol (vol/vol) and incubated for additional 15min. This step was then repeated with 70% ethanol (vol/vol) for 15min. In the following, the samples were incubated three times in 100% ethanol for 10min. Next, samples were transferred into propylene oxide for 10min. After that the samples were incubated in 1:1 propylene oxide/durcupan (vol/vol) for 1h and in 1:3 propylene oxide/durcupan (vol/vol) for 3h. In a last step cells were left in absolute durcupan at -20°C O/N. The day after, the samples are stored at RT for 3h.

For embedding of the fixed cells the samples were transferred into a malt form containing pure durcupan. Covered by durcupan the samples were stored for another 3h on RT. Then the malt forms were baked in an oven (65°C, 58KPa). After 2h the oven is set under vacuum O/N.

#### *2.3.13.2 Microscopic analysis*

Electron microscopy was performed on ultrathin sections of the embedded samples by a specialist of the Department of Clinical Neurosciences, UCL, London. Sections were

contrasted with uranyl acetate and lead citrate. Images were captured with a digital camera attached to a Zeiss 902C electron microscope. Images were analysed blinded.

#### **2.3.14 Review of the literature**

The Medline database (via PubMed, online at <http://www.ncbi.nlm.nih.gov>) was screened for articles concerning M-D and *SGCE* mutational screening as well as PD and *PINK1* mutation analysis. The search terms “epsilon-sarcoglycan AND myoclonus-dystonia” and “PTEN-induced putative kinase 1 AND Parkinson’s disease” were used. At the end of March 2008 this data-base analysis resulted in 51 and 67 citations, respectively. Furthermore, all related publications, which were additionally mentioned at the Leiden Muscular Dystrophy pages<sup>©</sup> ([http://www.dmd.nl/sgce\\_seqvar.html](http://www.dmd.nl/sgce_seqvar.html)) or the Human Gene Mutation Database<sup>©</sup> (<http://www.hgmd.cf.ac.uk>), were included. We avoided double counts when families were described in different articles.

### 3 RESULTS

This thesis is concerned with two different movement-disorders: M-D and parkinsonism. First, a mutational screen in *SGCE* was performed in a large group of patients with particular emphasis on whole exon deletions (3.1). Second, different PD-causing mutations in *PINK1* were tested for their influence on the expression of the gene. The study included a large German family which was particularly interesting as the heterozygous mutation carriers presented with a phenotype varying from definitely to possibly affected (3.2). As a third part, the effect of mutations in *PINK1* on the respiratory chain function and mitochondrial morphology was investigated in fibroblast cells (3.3).

#### 3.1 Myoclonus-dystonia: Significance of large *SGCE* deletions

This study aimed at the identification of new M-D-causing mutations in *SGCE* (see Fig 7, Project A). First, clinical features of the individuals examined were collected (3.1.1). To test for whole exons alterations an MLPA screen was performed in the available patients (3.1.2). The extent of the detected deletions was then determined by means of genotyping and real-time PCR (3.1.4). Finally, the *SGCE* mutational spectrum was reviewed in the published M-D literature (3.1.5).

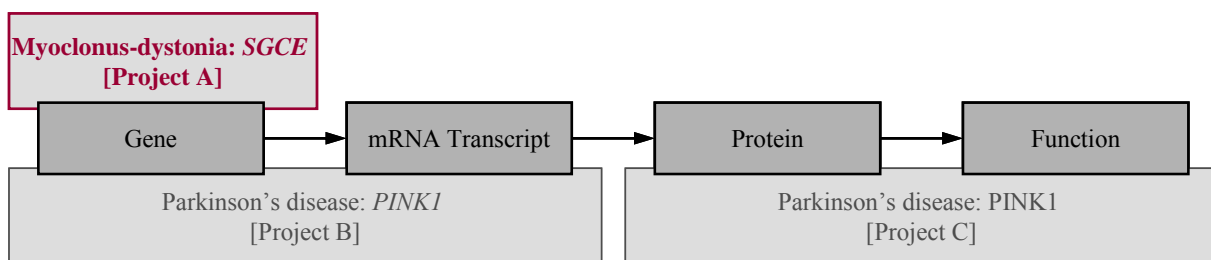


**Fig 7** Projects and levels of investigation in the present thesis [Project A]. The scheme shows the three research projects (A, B and C) included in this thesis according to their level of investigation: Gene, mRNA transcript, protein and function. The part of the thesis described in the current section is highlighted in red.

##### 3.1.1 Patients

A total of 35 index patients (19 female; mean age: 29.6+/-16.7 years; range: 4-68 years), nine of whom (25.7%) carried a mutation, were examined by neurological specialists. For calculation of the mean age of onset (9.5+/-9.5 years; range: 0-46 years), a reported age of onset in 'early childhood' was set to 4 years and 'early teens' to 13. Ten of the 35 patients

showed characteristic clinical features of definite M-D (7 female). Fifteen individuals were diagnosed as probable M-D cases (7 female), and ten patients as possibly affected (5 female). Age of onset was not significantly different in these three groups ( $p > 0.05$ ; independent t-test with unequal sample size). Only when comparing mutation carriers (mean age of onset:  $3.5 \pm 3.9$  years) and non-mutation carriers (mean age of onset:  $11.5 \pm 10.1$  years), a significant difference was found ( $p = 0.027$ ; independent t-test with unequal sample size). Demographic, clinical, genetic information and additional features are summarized in Table 5. Selected special features are detailed below:

In the mutation-positive families, paternal transmission of the disease prevailed (Table 5). However, in the family of IP15251, the mode of transmission was compatible with paternal expression with the exception of one affected female (V:7) who inherited the disorder from her mother (Fig 8D). Though, a transmission of the disease through individual III:1 and the patient's father (IV:1) can not be excluded in this case.

Two patients carried large deletions, including the entire *SGCE* gene and the *collagen type I alpha 2 gene (COL1A2)*. In both families, additional phenotypes were observed beyond the motor syndrome. IP16535 had delayed skeletal development and later presented with severe generalized osteoporosis, necrosis of the femoral head, and cartilage defects of the condyli leading to hip and knee replacement in his twenties. There were no abnormalities of the skin and eyes. Neither of his mutation-negative parents showed any signs of bone and joint disease. The four-year old index patient IP15916 had no other features, however, two mutation carriers including the patient's father, as well as at least three other obligate mutation carriers, reported joint problems (Fig 8A). More detailed information was unavailable for these family members.

**Table 5** Demographic, clinical and genetic data of index patients and affected family members investigated in the M-D study

	Patient	Mutational status	Novel mutation	Sex	Age (Yr)	Age of onset (Yr) (motor symptoms)	Myoclonus	Dystonia	Response to alcohol	Family history	Additional features
Definite	IP15916 <sup>a</sup>	c.exon1_12del(7q21.3-q22.1) <sup>c</sup>	Yes	f	4	1.5	+	+	?	+ (Fig 8)	Joint problems reported by several family members
	F46 <sup>a</sup>	c.exon1_12del(7q21.3-q22.1) <sup>c</sup>	Yes	f	37	Early adulthood	+	-	?		Unknown
	IP15624 <sup>a</sup>	c.exon2del	Yes	f	5	4	+	+	?	+	Unknown
	F2454 <sup>a</sup>	c.exon2del	Yes	m	45	34	+	+	+		Unknown
	IP16099	c.771_772delAT, p.C258X	Yes	f	47	0	+	+	+	+	Unknown
	IP1601 <sup>b</sup>	c.289C>T; p.R97X	No	m	8	2	+	+	?	+	Unknown
	F2354	c.289C>T; p.R97X	No	m	36	6	+	+	+		Unknown
	IP15251 <sup>a</sup>	c.304C>T; p.R102X	No	f	46	4	+	+	?	+ (Fig 8)	Depression; maternal M-D transmission from IV:3 to V:7
	IP2141 <sup>a</sup>	c.1114C>T, p.R372X	No	f	6	4	+	-	?	+ (Fig 8)	Unknown
	F2142 <sup>a</sup>	c.1114C>T, p.R372X	No	f	11	2	+	-	?		Unknown
	F2144 <sup>a</sup>	c.1114C>T, p.R372X	No	f	51	12	+	-	+		Unknown
	IP2140	No mutation found		f	45	24	+	+	+	+	Unknown
	IP2433	No mutation found		f	21	Early childhood	+	+	?	+	Unknown
IP2624	No mutation found		m	20	0.5	+	+	+	+	Aggressive periods and emotional lability	
IP15668	No mutation found		m	43	16	+	-	?	+	Unknown	
	<b>Mean</b>				<b>24.5+/-18.8</b>	<b>6.0+/-7.8</b>					
	<b>Range</b>				<b>4-47</b>	<b>0-24</b>					
Probable	IP16535 <sup>a</sup>	c.exon1_12del(7q21.3-q22.1) <sup>d</sup> , <i>de novo</i>	Yes	m	28	3	+	+	+	-	Severe generalized osteoporosis: hip & knee placement
	IP2625	c.304C>T, p.R102X	No	m	47	Early teens	+	+	+	-	Unknown
	IP15039	c.709C>T; p.R237X	No	f	53	0	+	+	+	-	Jerks of the fetus reported by the mother; panic attacks
	IP2136	No mutation found		m	34	13	+	+	+	?	Unknown
	IP2225	No mutation found		f	17	12	+	+	?	-	Unknown
	IP2446	No mutation found		m	36	16	+	+	+	?	Depression
	IP10841	No mutation found		f	42	11	+	-	?	-	Depression
	IP14574	No mutation found		m	20	Early childhood	+	-	?	?	Unknown
	IP14741	No mutation found		m	10	5	+	-	?	-	Unspecified psychiatric features
	IP14838	No mutation found		f	11	Early childhood	+	-	?	-	Unknown
	IP15356	No mutation found		m	31	12	+	-	?	?	Unknown
	IP15386	No mutation found		m	40	12	+	+	+	-	Head tremor
	IP15582	No mutation found		f	51	46	+	+	?	-	Psychosis; schizoaffective disorder
IP15731	No mutation found		f	5	2	+	+	?	-	Unknown	
IP15747	No mutation found		f	23	2	+	+	+	-	Unknown	
	<b>Mean</b>				<b>29.9+/-15.3</b>	<b>10.3+/-11.1</b>					
	<b>Range</b>				<b>5-53</b>	<b>0-46</b>					
Possible	IP1559	No mutation found		f	43	Early childhood	+	+	-	+	Unknown
	IP2093	No mutation found		f	17	5	+	+	-	-	Unknown
	IP2139	No mutation found		m	45	18	+	+	-	-	Unknown
	IP14079	No mutation found		m	22	Early childhood	+	+	-	-	Unknown
	IP15118	No mutation found		m	25	22	-	+	+	-	Head tremor
	IP15914	No mutation found		f	17	Early childhood	-	+	+	+	Myoclonic epilepsy
	F15915	No mutation found		f	14	Early childhood	-	+	+		Myoclonic epilepsy
	IP16242	No mutation found		m	46	15	-	-	-	+	Hand tremor
	IP16281	No mutation found		f	40	15	-	+	?	+	Head tremor; depression
	IP16354	No mutation found		f	68	25	-	+	?	+	Head tremor; unspecified psychiatric features
IP16483	No mutation found		m	19	Early childhood	-	+	+	+	Head tremor; hand tremor	
	<b>Mean</b>				<b>34.2+/-16.9</b>	<b>11.6+/-8.3</b>					
	<b>Range</b>				<b>17-68</b>	<b>4-25</b>					

Note: Mean age and age range are given for index patients only. Data of family members (F) is shown below the respective index patients (IP).

+ positive, - negative, ? unknown

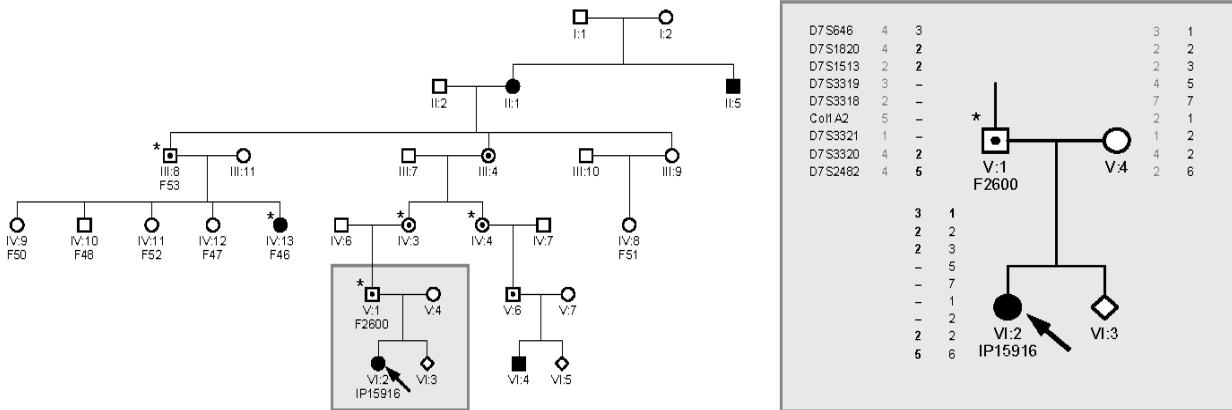
<sup>a</sup> Subjects are shown in a pedigree.

<sup>b</sup> Patient previously described as mutation-negative (Kock *et al.*, 2004); resequencing of a fresh DNA sample revealed mutation

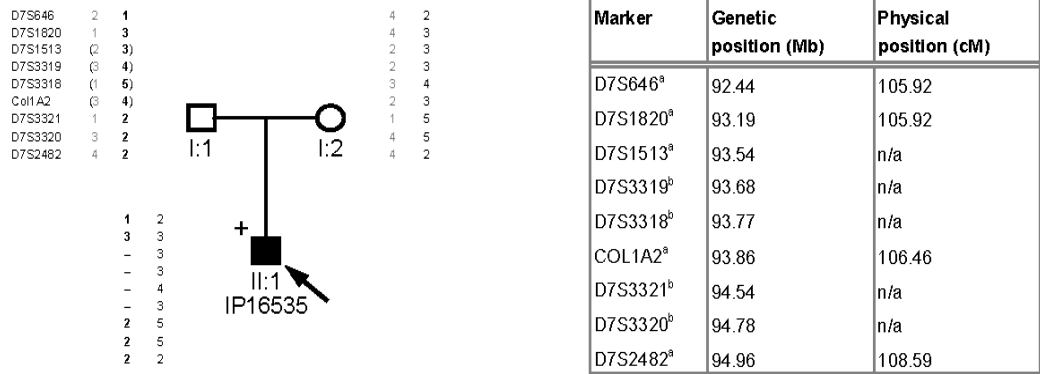
<sup>c</sup> Heterozygous deletion including at least *SGCE*, *COL1A2*, *CASD1*, *PEG10* and *ARF1P1*

<sup>d</sup> Heterozygous deletion including at least *SGCE*, *COL1A2* and *CASD1*

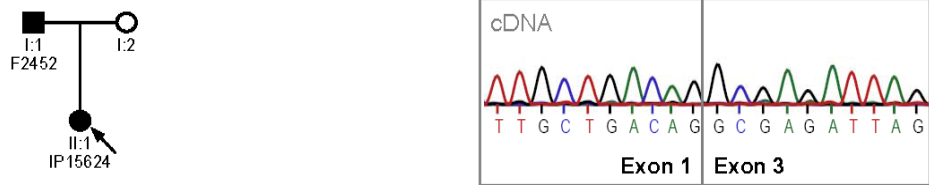
A



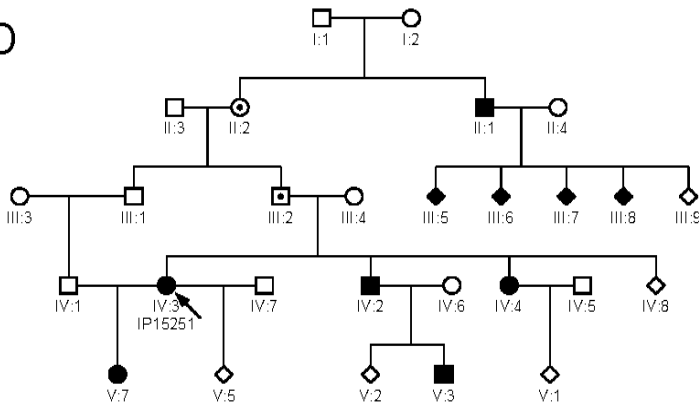
B



C



D



E

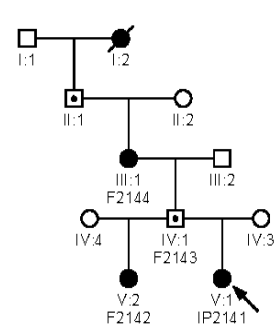


**Fig 8 (previous page)** Relevant pedigrees of families with M-D of index patients (A) IP15916; (B) IP16535; (C) IP15624; (D) IP15251 and (E) IP2141. For reasons of confidentiality, only select family members are included and shown as sex-unspecific diamonds unless relevant to demonstrate parent-of-origin dependent transmission of M-D. Numbers enclosed in diamonds indicate the number of individuals. Circles represent female subjects; squares represent male subjects; deceased individuals are slashed; the individual pedigree number is below each symbol. Black arrows point to index patients. Family members included in the clinical and molecular genetic studies are denoted by their code number. The clinical status of the remaining family members is obtained by history. Filled symbols indicate definitely M-D affected members. Predicted or confirmed unaffected mutation carriers are marked by a dot. Patients with painful joints are highlighted by an asterisk. A patient with hip and knee replacement due to severe generalized osteoporosis is indicated by a plus sign.

(A) Inset: *Genotyping for estimation of the deletion size in IP15916.* Part of pedigree A displaying the index patient IP15916 and her parents, along with the results of a haplotype analysis at the indicated markers. The heterozygous deletion of D7S3319, D7S3318, COL1A2 and D7S3321 is visualized by a hyphen in the paternal allele of IP15916.

(B) *Genotyping for estimation of the deletion size in IP16535.* Haplotype analysis of the index patient and his parents showed hemizygoty for the markers D7S1513, D7S3319, D7S3318 and COL1A2 at the parental allele of IP16535. Phase of genotypes in parentheses could not be established. At the markers COL1A2, D7S3319, D7S1513 and D7S1820 heterozygosity or hemizygoty was confirmed by qPCR in IP16535.

(B) Inset: *Physical and genetic positions of markers used in the study.*

<sup>a</sup> <http://research.marshfieldclinic.org/genetics/GeneticResearch/compMaps.asp>

<sup>b</sup> Markers generated at relevant genomic positions to define the size of the heterozygous *SGCE* deletion.

(C) Inset: *cDNA sequence of IP15624.* The deletion of *SGCE* exon 2 is visualized, since exon 1 is directly followed by exon 3.

### 3.1.2 Quantitative mutational screening

In three of the patients (8.6%) a novel large heterozygous deletion of one or more exons was identified. Using MLPA (cp. 2.3.2.5), a heterozygous deletion for all tested exons in two index patients (IP15916 and IP16535) was detected. For the definitely affected patient IP15916, the deletion is indicated by normalized value ratios between 0.42 and 0.70 (Fig 9). Further gene dosage analysis demonstrated the *SGCE* exon 1-12 deletion also in the father and two additional relatives.

For the probably affected index case IP16535, ratios resulting from MLPA varied between 0.37 and 0.71 (Fig 9). The *SGCE* gene dosage was also investigated in his parents. These tests revealed normal ratios of about 1.0 for all of the exons.

An additional definitely affected index case (IP15624) showed a heterozygous deletion of exon 2, indicated by a normalized value ratio of 0.58 after evaluation of the MLPA assay (Fig 9). The exon rearrangement was also present in the father of IP15624 (F2454) and was proven

on the cDNA level (Fig 8C inset). Due to the imprinting mechanism, only one parental, in this case the mutated, transcript was detectable.

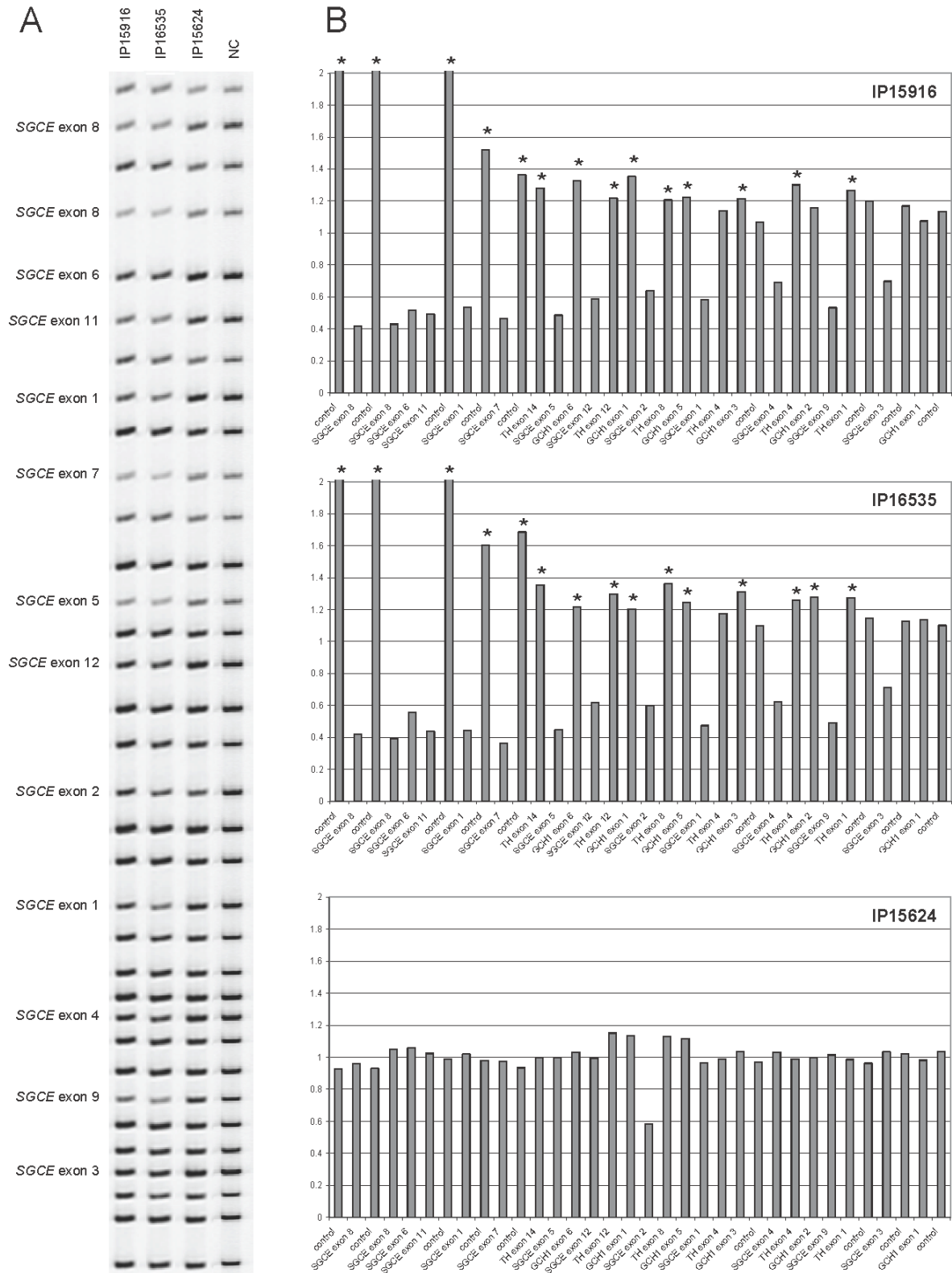


**Fig 9 (previous page)** *Screening for exon rearrangements.* MLPA band pattern comparing patient IP15916, IP16535, IP15624 and a negative control (NC). (B) Histograms of normalized probe-specific band volumes resulting from MLPA for IP15916, IP16535, and IP15624. Heterozygous deletions of the *SGCE* exons are indicated by relative intensities of approximately 0.5. Bars representing non-*SGCE*-exons (internal reference genes) show relative values around 1.0, indicative for the presence of both wildtype alleles. Increased/decreased ratios of “nearest-neighbour” probes (highlighted by an asterisk) to those indicating deletions/multiplications, were regarded as an artefact caused by the normalization process (e.g. a normal value gets higher when divided by a value lower than the average). Differentiation between aberrant values and true results were made after visual inspection of intensity of bands on the gel.

### 3.1.3 Determination of the extent of the large deletions

In the family of index patient IP15916, the extent of the identified genomic deletion including *SGCE* was investigated by haplotype analysis (cp. 2.3.2.2). This deletion is located on chromosome 7q21.3-q22.1 and flanked by the markers D7S1513 and D7S3320 (Fig 8A inset and Fig 10). Hemizygoty was found at the markers D7S3319, D7S3318, COL1A2, and D7S3321. To further narrow the deletion breakpoints, two qPCRs were performed, one between the markers D7S1513 and D7S3319 and a second one between D7S3321 and D7S3320. The *SGCE*/ $\beta$ -globin ratios at both positions amounted to approximately 1.0, referring to a maximum size of the deletion of ~1.09 Mb (Fig 10). In addition to *SGCE*, the genes *COL1A2*, *CAS1 domain containing 1 (CASD1)*, *paternally expressed 10 (PEG10)* and *ADP-ribosylation factor 1 pseudogene 1 (ARF1P1)* are also localized within the definitely deleted region.

For the index case IP16535, a combination of haplotype analysis and qPCR (qPCR1: *SGCE*/ $\beta$ -globin ratio ~0.5; qPCR2: *SGCE*/ $\beta$ -globin ratio ~1.0) revealed a deletion on 7q21.3-q22.1 with a maximal extent of 1.35 Mb (cp. 2.3.2.3 for methodical background). At the markers D7S1513, D7S3319, D7S3318 and COL1A2 hemizygoty was detected (Fig 8B and Fig 10). This suggests that in this case, in addition to *SGCE*, the genes *CASD1* and *COL1A2* are also deleted. Since a deletion of *SGCE* and the adjacent chromosomal region was excluded for the mother as well as for the father of IP16535 this mutation must have arisen *de novo* in the patient in whom paternity was confirmed.

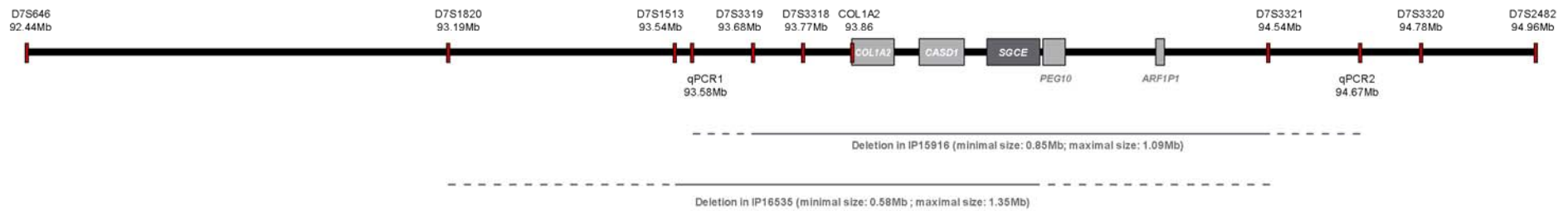


**Fig 10** Scheme of the genomic region, surrounding *SGCE*, with relevant markers and *qPCRs*. The position (in Mb) of the previously established microsatellite markers *D7S646*, *D7S1820*, *D7S1513*, *COL1A2* and *D7S2482* on chromosome 7 is given according to the reference sequence genomic assembly NC\_000007.12. The markers *D7S3319*, *D7S3318*, *D7S3321* and *D7S3320* were generated to narrow the deletion breakpoints in *IP15916* and *IP16535*. At position 93.58Mb (*qPCR1*) and 94.67Mb (*qPCR2*) the gene dosage of a suitable DNA fragment was quantified by *qPCR* for *IP15916* and *IP16535*. The minimal size of the heterozygous deletions is indicated by a solid line. The areas highlighted by a dashed line are undefined.

### 3.1.4 Qualitative mutational screening

Six out of 35 (17.1%) index patients had either a point mutation (5 cases) or a small deletion (1 case) in the *SGCE* gene (four of these mutation-positive cases showed definite signs of M-D). One of the identified mutations was novel. This two base pair deletion in exon 6 induced a premature stop at codon 258 (c.771\_772delAT, p.C258X).

The remaining mutations had been previously described and are also predicted to prevent the synthesis of a full-length protein: Three index patients (IP1601, IP15251 and IP2625) carried disease-causing sequence changes in exon 3 (c.289C>T, p.R97X and twice c.304C>T; p.R102X). A one base pair substitution was detected in exon 6 (c.709C>T; p.R237X in IP15039). In the last patient (IP2141), a nonsense mutation in exon 9 (c.1114C>T, p.R372X) was found.

### 3.1.5 Review of mutations in *SGCE*

Out of 51 publications, available on PubMed, 28 are reviewed here (see also 2.3.14). Taken together, 107 mutation-positive M-D cases have been described. For these patients, 64 sequence changes in *SGCE* were identified, including 15 recurrent mutations (Fig 11). In 37% (40/107) of the above-mentioned individuals a single nucleotide change led to a truncation of *SGCE*. With 33% (35/107), deletions were the second most frequent mutational cause of M-D. Among the 35 known deletions, ten are gene dosage alterations encompassing whole exons. Those account for 9% (10/107) of all cases with known mutations in *SGCE*. In addition to that, 12 (out of 107) patients with missense mutations (11%), 17 with splice site alterations (16%) and three individuals with insertions (3%) have been identified yet. The mutation detected with the highest frequency is a cytosine to thymine change at cDNA position 304 which leads to a premature stopcodon at AA position 102.

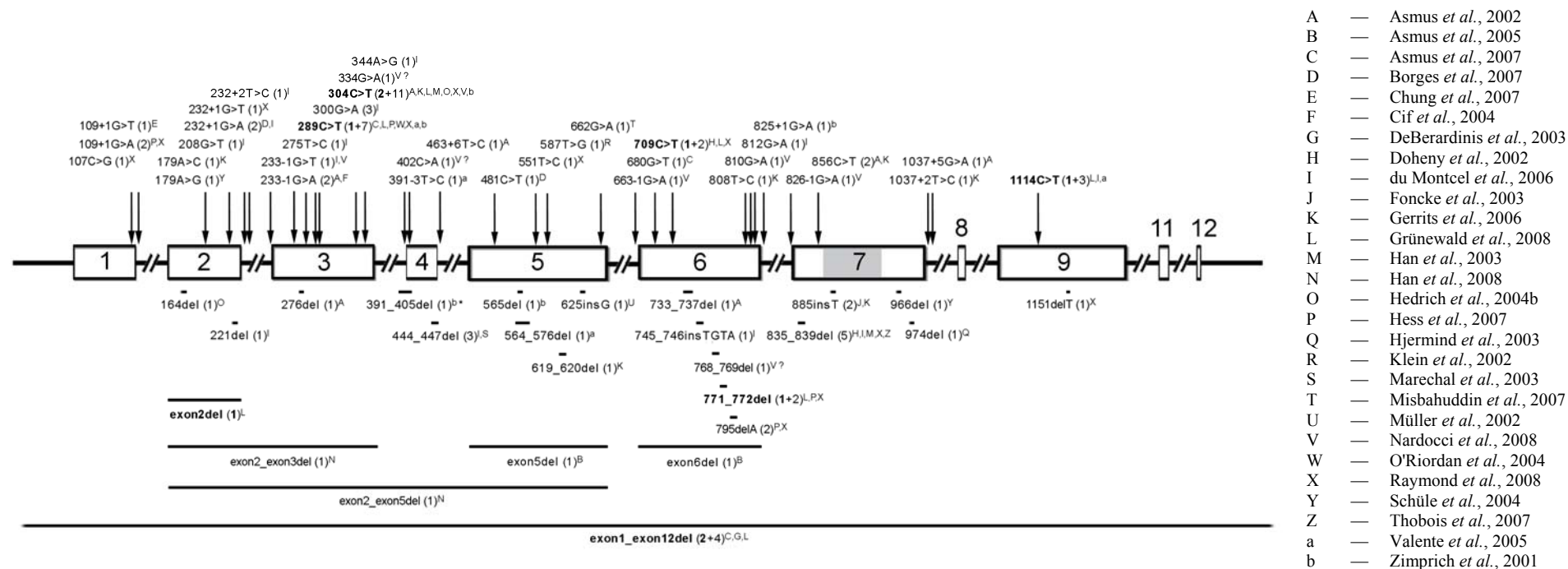


**Fig 11** Schematic representation of the *SGCE* gene and identified mutations. Point mutations are indicated above the gene, and small deletions and exon rearrangements are shown below the gene. Mutations detected in the current study are emphasized by bold characters. The number of published reports of each mutation is given in parentheses, and the respective references are given in the legend. The sequence encoding the transmembrane domain of *SGCE* is highlighted in gray. A deletion which also includes 82bp of the adjacent intron is highlighted by an asterisk. Mutations with a designation not explicitly given in the literature are distinguished by a question mark. Numbering of the mutation according to the translation start as +1; GenBank reference sequence: NM\_001099401.1.

### 3.2 Parkinson's disease: Gene expression in patients with *PINK1* mutations

This section deals with the consequences of *PINK1* mutations on the expression of the gene (see Fig 12, Project B). Genomic and cDNA sequencing was performed to confirm previously detected mutations and to compare for variations among both results (3.2.1). All families with the *PINK1* c.1366C>T mutation were tested for a common haplotype (3.2.2). The *PINK1* gene expression was determined for the members of Family W and Family MI-002 (3.2.3). Finally, an overview about currently known mutations in *PINK1* is given (3.2.4).

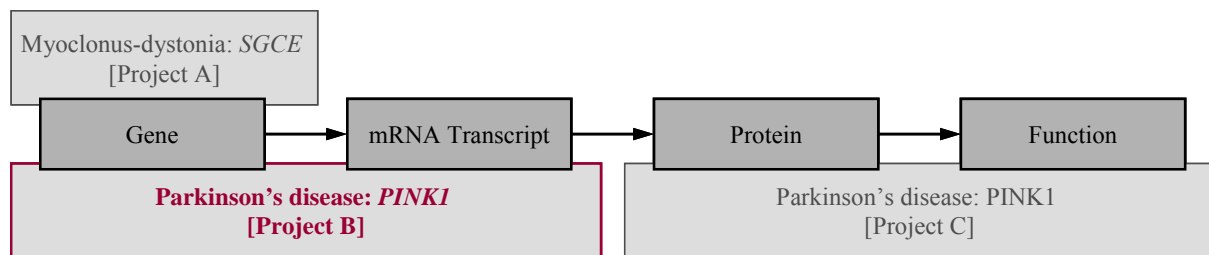


**Fig 12** Projects and levels of investigation in the present thesis [Project B]. The scheme shows the three research projects (A, B and C) included in this thesis according to their level of investigation: Gene, mRNA transcript, protein and function. The part of the thesis described in the current section is highlighted in red.

#### 3.2.1 *PINK1* genomic and cDNA sequencing analysis

Genomic sequencing (cp. 2.3.2.2) of the entire *PINK1* coding region confirmed in each individual the presence, nature and zygosity of *PINK1* mutations reported previously (Bonifati *et al.*, 2005; Hedrich *et al.*, 2006; Ibanez *et al.*, 2006). In the German Family W (n=20), the Italian family MI-002 (n=4) and the Italian individuals Roma-360 and NE-166 the *PINK1* c.1366C>T mutation was detected. In the French Family FPD (n=2) the compound heterozygous *PINK1* mutations c.373T>C/c.1366C>T were determined in one individual and a homozygous c.1366C>T mutation in the other (cp. 2.1.2).

In all investigated individuals (n=28), expression of the *PINK1* gene was documented. cDNA sequencing (cp. 2.3.2.2) in heterozygous carriers of the c.1366C>T mutation in the families W, MI-002 and individual Roma-360 showed a strong 1366C wildtype signal and a much weaker or almost absent 1366T signal (Fig 13 and data not shown). In the available homozygous patients (four from Family W and one from FPD), only the mutant 1366T allele was detected. In one French patient known to be a compound heterozygous carrier of the c.373T>C and c.1366C>T mutations, a much weaker or almost absent 373T (wildtype) and 1366T (mutant) signal was documented, in keeping with only minimal amounts of the

transcript containing the c.1366C>T mutation being present in the cDNA pool (Fig 13). Cycloheximide treatment of fibroblasts from one German heterozygous c.1366C>T mutation carrier markedly increased the mutant transcript signal (Fig 13).

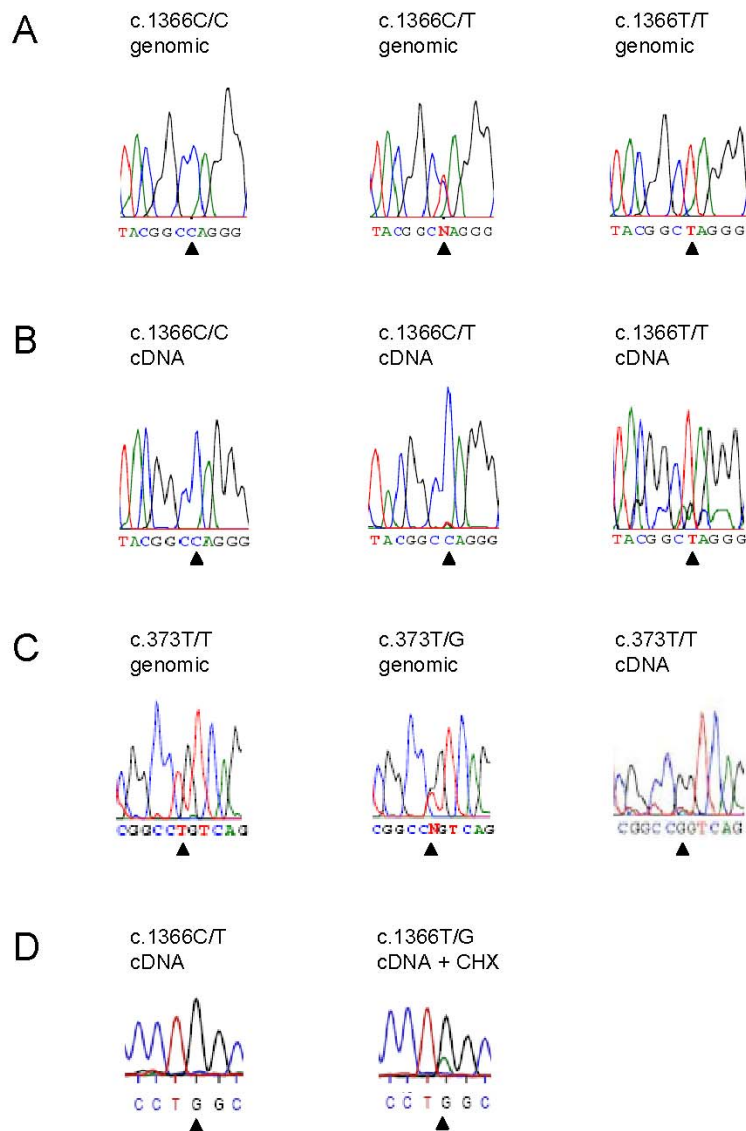


**Fig 13** Electropherograms of genomic DNA and cDNA. Representative examples of wildtype, heterozygous and homozygous *PINK1* mutants. CHX – cycloheximide.

A – Family W, c.1366C>T mutation, genomic DNA

B – Family W, c.1366C>T mutation, cDNA

C – Family FPD, c.373T>G mutation, genomic DNA and cDNA

D – Family W, cDNA without and with cycloheximide treatment

### 3.2.2 Haplotype analysis

All carriers of the c.1366C>T mutation shared at least one allele at three SNPs within the coding region of *PINK1* (see 2.3.2.2 for methodical background). Further, mutation-positive members of Family W and the Family MI-002 had at least one allele at all tested microsatellite markers in common. In addition to the *PINK1* coding SNPs, the patients Roma-360 and NE-166, and the family members of FPD share a 383bp-allele at the flanking marker D1S3720 (Fig 14).

NCBI build 36.1 position	Marker	MAF	Family W F2126 (homozygous)		MI-002-03 (homozygous)		Roma-360 (heterozygous)		NE-166 (homozygous)		FPD (homozygous)	
19139553-19139802 (bp)	D1S552		262	271	262	262	266	266	266	266	266	266
20508935-20509198 (bp)	D1S2732		194	194	196	194	186	196	196	196	190	190
20784515-20784652 (bp)	D1S3720		377	377	383	377	383	383	383	383	383	383
20832821 (bp) <i>PINK1</i> exon 1	C189T	0.218	C	C	T	C	C	C	C	C	C	C
20844721 (bp) <i>PINK1</i> exon 5	G1018A	0.024	G	G	G	G	G	G	G	G	G	G
20848190 (bp) <b>mutation <i>PINK1</i> exon 7</b>	<b>C1366T</b>		<b>T</b>	<b>T</b>	C	<b>T</b>	C	<b>T</b>	<b>T</b>	<b>T</b>	<b>T</b>	<b>T</b>
20849585 (bp) <i>PINK1</i> exon 8	A1562C	0.209	A	A	A	A	A	A	A	A	A	A
21472314-21472484 (bp)	D1S478		307	307	303	307	303	307	301	301	301	301
21815058-21815329 (bp)	D1S2828		230	215	238	215	219	240	228	228	215	215
22745615-22745773 (bp)	D1S2864		190	172	172	172	190	172	192	192	192	192

**Fig 14** *PINK1* haplotype analysis. Haplotype at six flanking microsatellite markers and three *PINK1* intragenic single nucleotide polymorphism (SNP) are shown for individuals belonging to five unrelated European families. The main intragenic haplotype shared by all patients is highlighted in light gray. More extended regions of sharing between some families are marked in dark gray. Data are compatible with either a very old, common founder, or with two independent origins of the mutation. MAF = minor allele frequency (for details regarding frequencies see Bonifati *et al.*, 2005).

### 3.2.3 *PINK1* gene expression

Among the ten reference genes tested, *SDHA* and *YWHAZ* showed the most reliable expression pattern in blood and therefore served as internal standards for the real-time approach (see 2.3.2.4).

All four assays (*PINK1* exon 5-6 or exon 7-8 relative to *SDHA* or *YWHAZ*) revealed comparable *PINK1* mRNA levels for the group of mutation-negative ( $x_{\text{median}}(\text{wt/wt}) \approx 0.9-1.0$ ), heterozygous ( $x_{\text{median}}(\text{wt/mut}) \approx 0.5-0.6$ ) and homozygous individuals ( $x_{\text{median}}(\text{mut/mut}) \approx 0.1-0.2$ ) in families W and MI-002 (see Fig 15 and Fig 16 for details).

When all heterozygous members of Family W were stratified into clinically unaffected vs. affected cases ( $x_{\text{median}}(\text{wt/mut}_{\text{unaffected}}) \approx 0.4-0.6$ ;  $x_{\text{median}}(\text{wt/mut}_{\text{affected}}) \approx 0.5-0.7$ ) (Hedrich *et al.*, 2006), no correlation between phenotypes and expression levels of *PINK1* was found.



sequence alterations were discovered in a homozygous and compound heterozygous expression.

The majority of investigated cases harboured a missense mutation accounting for 72% (57/79). Nonsense mutations cause the disease in 17% (13/79) of all *PINK1*-related PD patients. Up to date, only four cases with small (5%) and three with large deletions (4%) were characterized. Insertion mutations were only found in two cases so far (3%). The most common mutation occurred in five cases and results in a change of glycine to serine at AA position 411. For 80% (63/79) of the mutation-positive cases, the mutation was identified within the kinase domain of *PINK1* possibly influencing the activity of the enzyme.

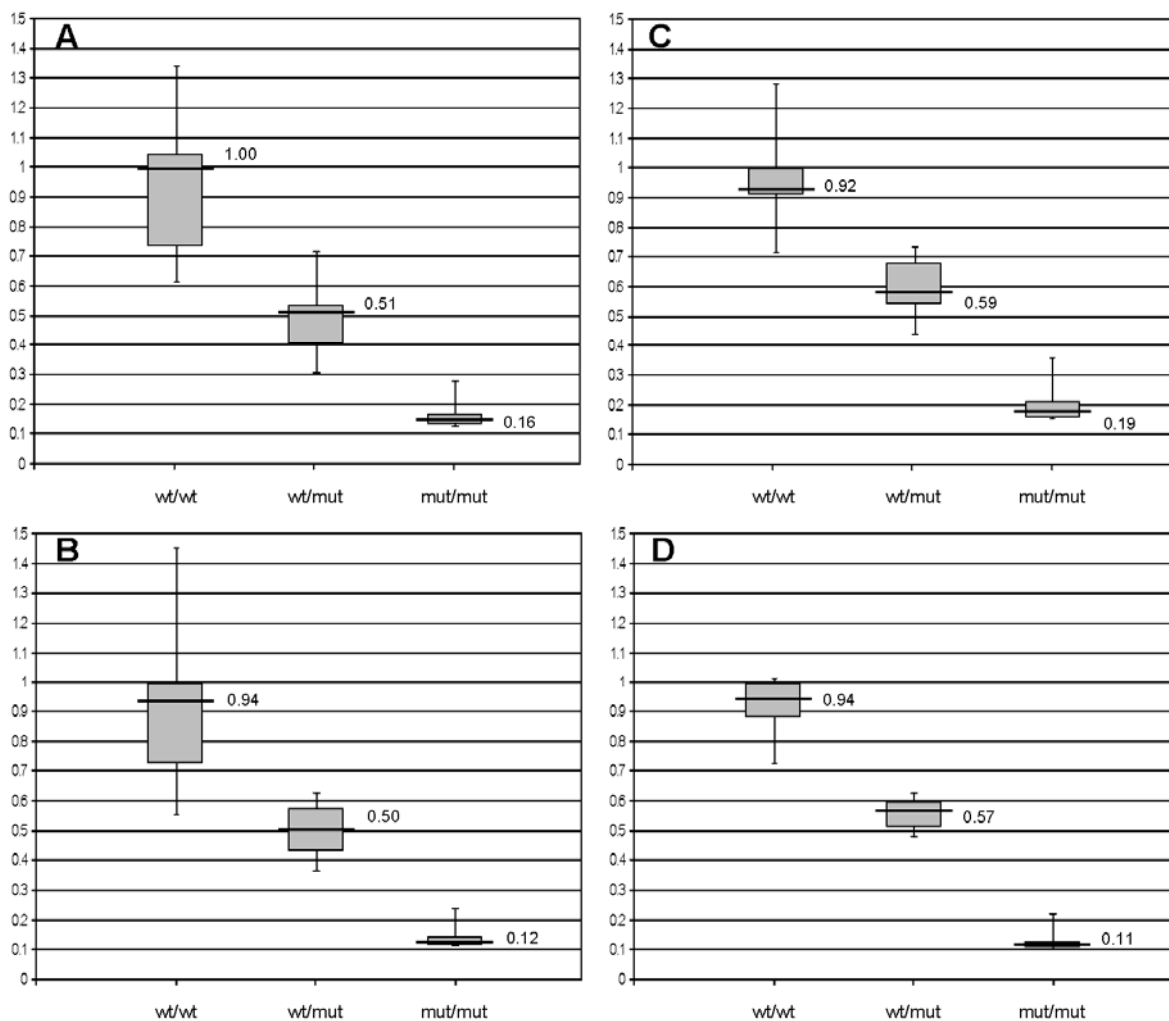


**Fig 16** Box-and-Whisker Plot showing clustered results of the mRNA expression analysis for each mutational status in Family W. Combined data from the real-time PCR assays: (A) *PINK1* exon 5-6/*SDHA*; (B) *PINK1* exon 7-8/*SDHA*; (C) *PINK1* exon 5-6/*YWHAZ*; (D) *PINK1* exon 7-8/*YWHAZ*. Data are medians.

wt/wt – control

wt/mut – heterozygous

mut/mut – homozygous

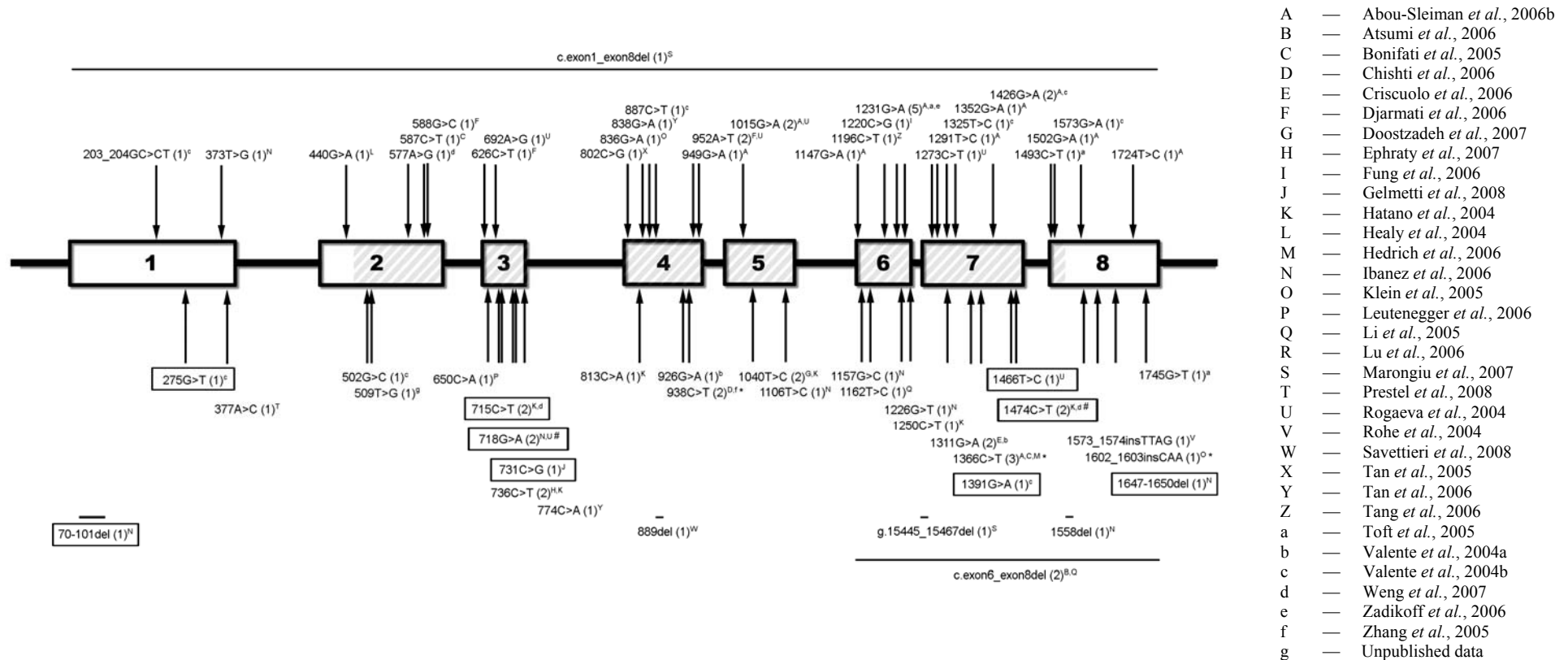


**Fig 17** The human PINK1 gene and identified mutations. Scheme representing the genomic structure of PINK1. The gene consists of eight exons shown as quadrants. Introns are symbolized by the lines in between the exons. The protein kinase domain is highlighted by a grey pattern. Mutations above the scheme indicate a heterozygous genetic status. Mutations below stand for homozygous mutations. Compound heterozygous mutations are marked with an asterisk. Mutations identified in heterozygous as well as homozygous state are highlighted by a numeration mark. Point mutations, insertion and transition mutation are shown by an arrow. Deletions are represented by lines. The total detection number of each mutation according to the literature is given in brackets with the respective publication shown in the index. Numbering of the mutation according to the translation start as +1; GenBank reference sequence: NM\_032409.

### 3.3 Parkinson's disease: Mitochondrial function and morphology in patients with PINK1 mutations

Project C was concentrated on the link between PD and mitochondria. Experiments were performed in fibroblast samples gained from the homozygous PINK1 p.Q456X mutant members of Family W, and a number of related and unrelated control individuals. One case with the PINK1 p.V170G mutation was also included. First, the effects of these mutations on the respiratory chain enzyme function were investigated (3.3.1). In the following section, the cellular mitochondria content and mtDNA levels were investigated (3.3.2). Chapter 3.3.3 is concerned with the assembly of complexes I to V. Furthermore,  $\Delta\psi_m$  (3.3.4) and the cellular ATP concentration (3.3.5) were determined in all available fibroblast samples. The next section deals with the assessment of oxidative stress levels in mutant PINK1 cells (3.3.6). Finally, the mitochondrial network (3.3.7) and structure (3.3.8) was microscopically studied.

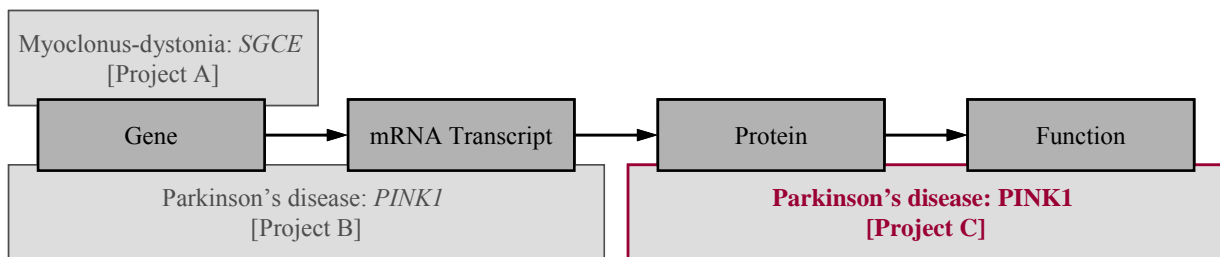


**Fig 18** Projects and levels of investigation in the present thesis [Project C]. The scheme shows the three research projects (A, B and C) included in this thesis according to their level of investigation: Gene, mRNA transcript, protein and function. The part of the thesis described in the current section is highlighted in red.

#### 3.3.1 Mitochondrial respiratory chain enzyme complexes

To test for the effects of PINK1 mutations on mitochondrial function the activities of respiratory chain enzyme complexes were investigated (cp. 2.3.8).

No difference in complex I activity was found when comparing four homozygous p.Q456X (c.1366C>T) PINK1 nonsense mutants with one wildtype family member and five unrelated controls. The culture of the patient with a p.V170G (c.509T>G) PINK1 missense mutation showed a complex I activity at the lower limit of the control range. A positive control with a known complex I deficiency had a marked decrease in complex I activity (33% of the average control activity; see Fig 19A).

For the activity of complexes II and III there was no apparent difference between the nonsense mutants (n=4) and the control samples (n=6). However, in the missense mutant

complex II and III activity was markedly higher than in the controls. It amounted to 212% of the average control activity (Fig 19B). The activity of the missense sample can be considered as an outlier of the control group as it falls outside of the fourfold range of the control standard deviation (Chebyshev's Theorem).

The activity of complex IV in the sample with the missense mutation was decreased to 57% of the average control activity (n=6). Therewith, the value lies outside of the twofold range of the control standard deviation. Again, the average activity in the nonsense mutants was indistinguishable from the respective value for controls (compare Fig 19C).

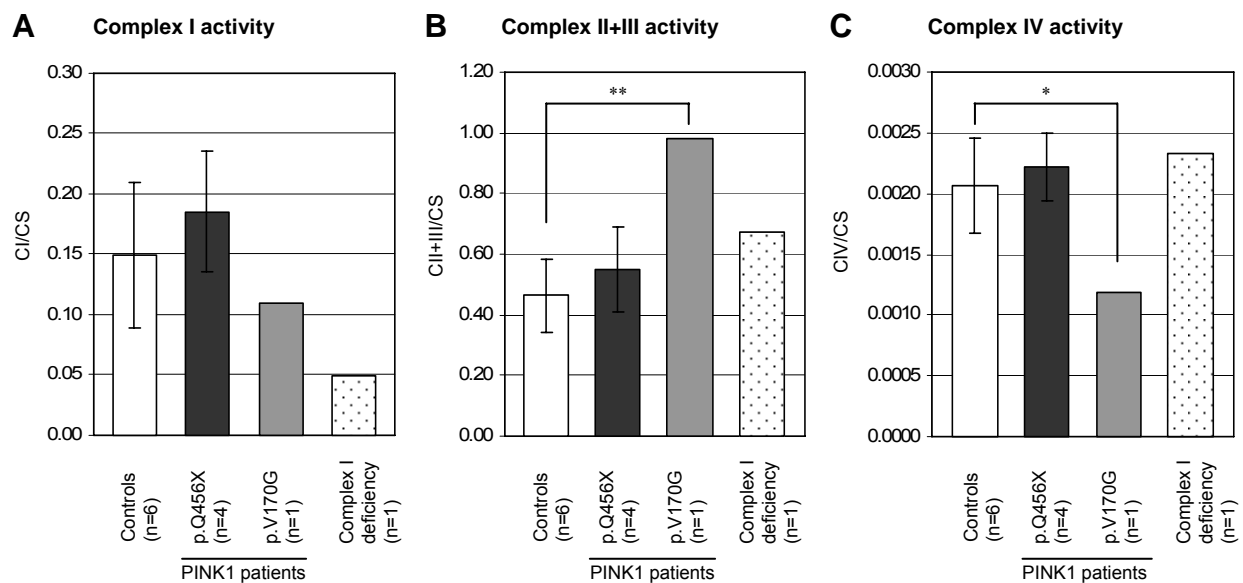


**Fig 19** Respiratory chain enzyme complexes I-IV. (A) Controls and patients with a nonsense mutation showed comparable CI. The activity in the missense mutation sample was at the lower limit of the control range. Low CI was confirmed in the positive control with a known complex I defect. (B) In the p.V170G mutant elevated CII-III was detected. The activity of the missense amounted 212% of the average control activity. (C) CIV of the missense mutant was 57% of the average control activity. CI-IV were normalized to CS (representing the amount of mitochondria in the cells). C – Complex, \*\* – increase > fourfold standard deviation of the control group, \* – decrease > twofold standard deviation of the control group, n – number of individuals.

### 3.3.2 Mitochondria content and mtDNA levels

The differences in the activities of complexes I-IV may be caused by variations in the amount of mitochondria in the samples. To test for this possibility, citrate synthase activity and malate dehydrogenase activity as markers of mitochondrial integrity and content were measured in the mitochondrial preparations (cp. 2.3.8.1) or cell lysates. For malate dehydrogenase the enzyme activities in cell lysates was comparable for controls (n=6), nonsense mutants (n=4) and the missense mutant (n=1) (cp. Fig 20A). The citrate synthase assay revealed higher

activity in the nonsense mutants (n=4) and the missense mutant (n=1) when compared with controls (n=6). However, both values lay within the control range (cp. Fig 20B).

A number of subunits of the respiratory chain enzyme complexes are encoded by mtDNA. To see whether the changes in the respiratory chain enzyme activities are due to altered mtDNA levels a real-time PCR quantification assay was applied (for details see 2.3.2.3). This approach did not reveal any differences across the three groups (Fig 20C). These data further support the idea that the mitochondrial content is similar in all fibroblast cultures.

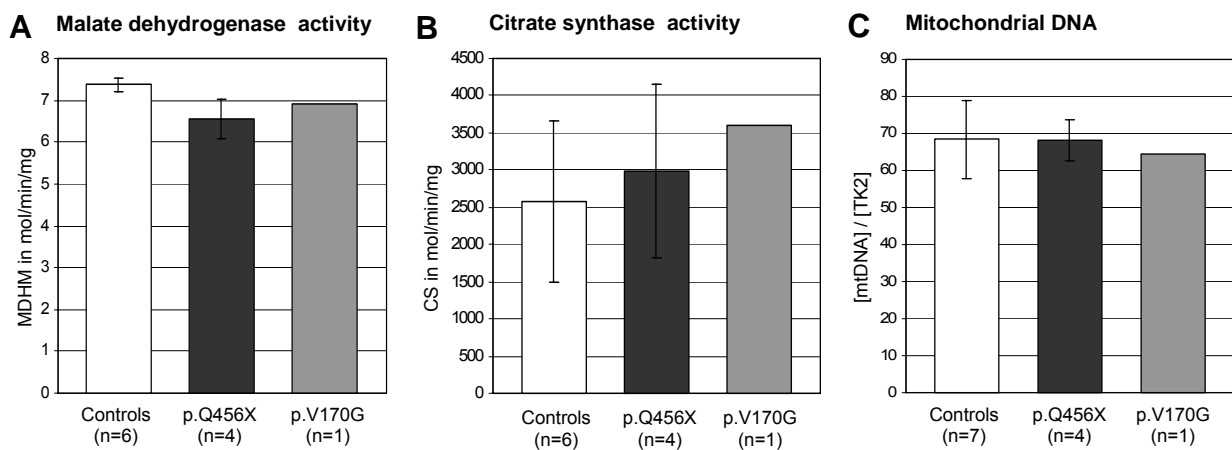


**Fig 20** *Mitochondria content and mtDNA levels.* (A) MDHM was measured as a marker of mitochondrial content in the cell lysates. The assay revealed comparable activities in controls, nonsense and missense mutants. (B) CS was determined as a mitochondrial marker in the mitochondria preparations. The average CS in nonsense mutants and the missense mutant was higher than in the controls, but within the control range. (C) Mitochondrial DNA levels. No significant differences were determined for any of the three investigated groups. n –number of individuals.

### 3.3.3 Assembly of respiratory chain enzyme complexes

As a next step, blue-native PAGE was performed to investigate the assembly of the respiratory chain enzyme complexes (see also 2.3.11).

A Western blot incubated with antibodies against complexes I to V displayed bands of expected molecular weight. No additional bands indicative of complex subassemblies were detected (Fig 21A).

Densitometry did not reveal any differences in the cellular expression level of the complexes between control and nonsense mutant samples (Fig 21B). For the p.V170G mutant, however, a decreased complex I concentration (33%) and complex II concentration (72%) along with a trend towards a reduced complex IV concentration (69%) was detected when compared with the control average.

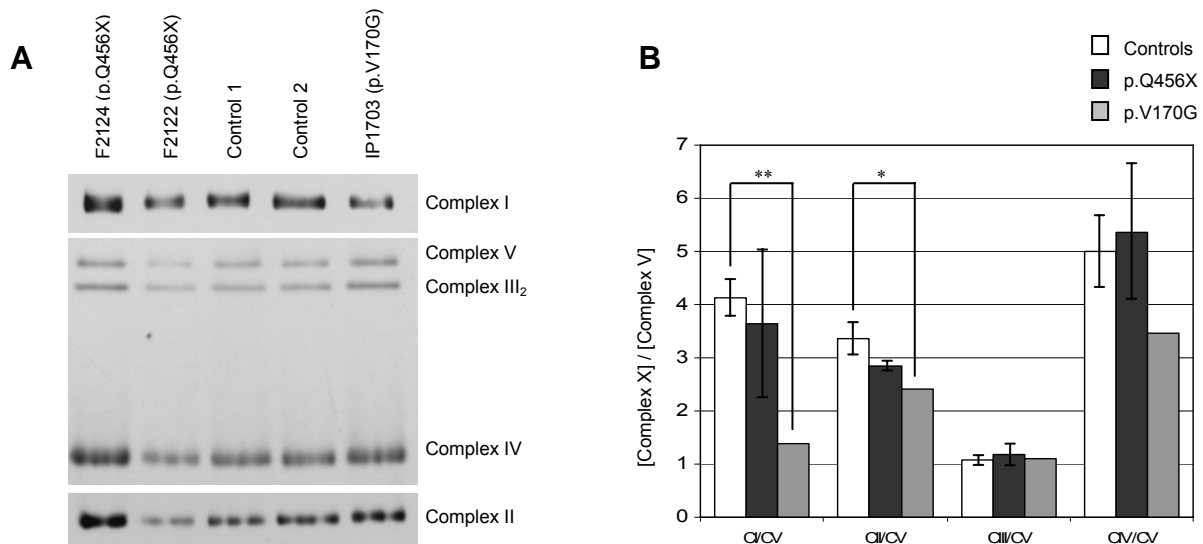


**Fig 21** Protein expression of the respiratory chain enzyme complexes. (A) Western blot showing complex I to V for two controls, two homozygous PINK1 p.Q456X mutants and the p.V170G mutant. (B) Densitometric quantification of the expression of the complexes relative to complex V ([complex X]/ [complex V]). Loading of the samples (whole cell homogenates) was corrected for the protein concentration. In the missense mutant the cellular concentration of complex I amounted to 33%, complex II to 72% and complex IV to 69% of the control level. \*\* – reduction > fourfold standard deviation of the control group, \* – reduction > twofold standard deviation of the control group.

### 3.3.4 Mitochondrial membrane potential

The mitochondrial membrane potential plays a central role in the mitochondrial biology. It provides the force that drives the influx of protons into the mitochondria.  $\Delta\psi_m$  is upheld through oxidation-reduction reactions catalyzed by the respiratory chain enzymes. Vice versa, it indicates dysfunction of the complexes I to V (Abou-Sleiman *et al.*, 2006b).

In this thesis, the influence of mutant PINK1 on  $\Delta\psi_m$  was investigated by means of a cytofluorimetric assay (see also 2.3.10). Under normal culturing conditions, the test showed no difference for any of the investigated groups (Fig 22, open bars).

There is increasing evidence that free-radical damage and oxidative stress play a role in the pathogenesis of PD. PINK1 was previously reported to function in the response to cellular stress (Pridgeon *et al.*, 2007; Wang *et al.*, 2006). Thus, the functional consequences of cellular treatment with the free radical generator paraquat were determined. Following incubation with this stressor  $\Delta\psi_m$  was unaffected in the controls and nonsense mutant cultures. However, in the missense culture,  $\Delta\psi_m$  was decreased by 31% reaching the lower limit of the control range (Fig 22, slashed bars).

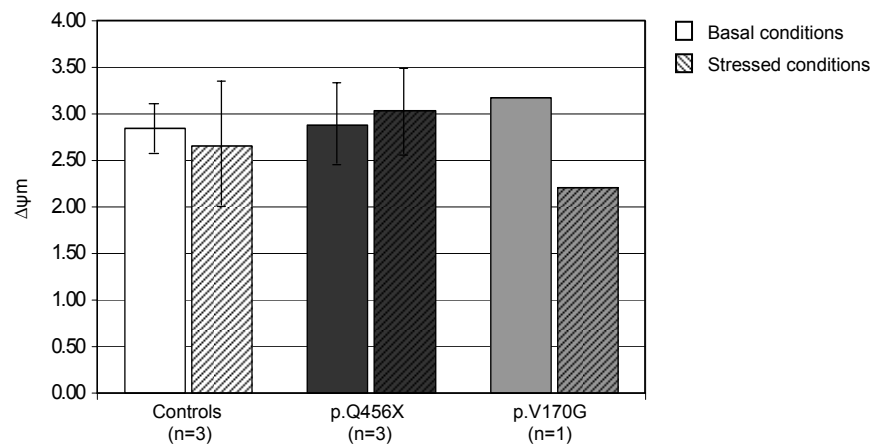


**Fig 22** Membrane potential under basal and stress conditions. For controls, patients with the p.Q456X mutation as well as for the p.V170G mutant sample, a similar  $\Delta\psi_m$  was detected when measured under basal conditions. After treatment with paraquat, controls showed an average decrease, whereas for the homozygous mutants an increase in  $\Delta\psi_m$  was determined. In the p.V170G missense mutant a decrease in membrane potential of 32% was determined under conditions of oxidative stress. Therewith the potential reached the lower limit of the control range. n – number of individuals.

### 3.3.5 Cellular ATP content

Maintenance of  $\Delta\psi_m$  is essential for the generation of ATP by the electron transport chain (Duchen *et al.*, 2003). Here, the total cellular ATP concentration was quantified in all available patient fibroblast cultures and eight control cultures (cp. 2.3.9). The experiment revealed a significant decrease of 25% ( $p < 0.01$ ) in the nonsense mutants when compared with the average of the control individuals (Fig 23). Three of the controls were relatives of the PINK1 p.Q456X PD patients who did not carry the nonsense mutation. ATP concentration in cells of the missense mutant patient did not differ from the average control level.

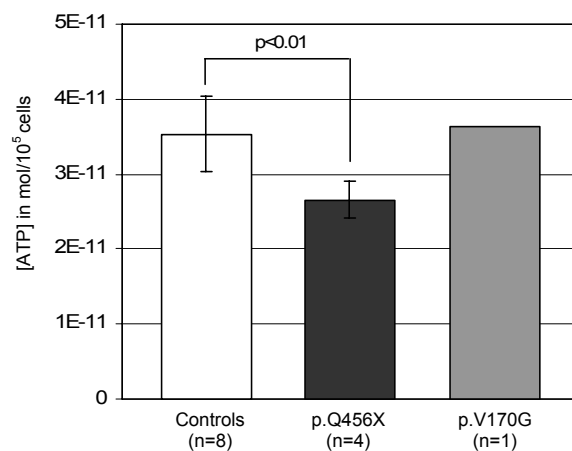


**Fig 23** ATP levels under normal conditions. Controls and the missense mutation sample showed comparable cellular ATP concentrations. In patients with a nonsense mutation a significantly reduced ATP level (75% of the average wildtype activity) was detected ( $p < 0.01$ ).

### 3.3.6 Oxidative stress in PINK1 mutant fibroblasts

Superoxide dismutase 2 (SOD2) and GSH are important antioxidants, which function in the cellular stress defence. Whereas SOD2 can only be found in mitochondria, GSH is additionally detectable in the cytosol.

The cellular SOD2 level was determined relative to the complex II expression by densitometric analysis of three western blots (cp. 2.3.11) prepared with cell lysates of all available mutant samples and six controls. In comparison to the average control level the nonsense mutants expressed 36% less SOD2 ( $p < 0.05$ ) whereas the missense sample presented a 45% higher average expression (increase > fourfold standard deviation of the control group) (see Fig 24A).

When GSH levels were chromatographically measured (cp. 2.3.4) in the cell lysates of control, nonsense or missense PINK1 fibroblast cultures, GSH levels were similar. However, upon treatment with exogenous oxidizing species generated by paraquat, GSH levels were elevated in control and nonsense cultures by 66% and 65%, respectively. GSH levels were elevated to a greater extent (148%) in missense cultures, despite the cells having impaired mitochondrial function (cp. Fig 24B).

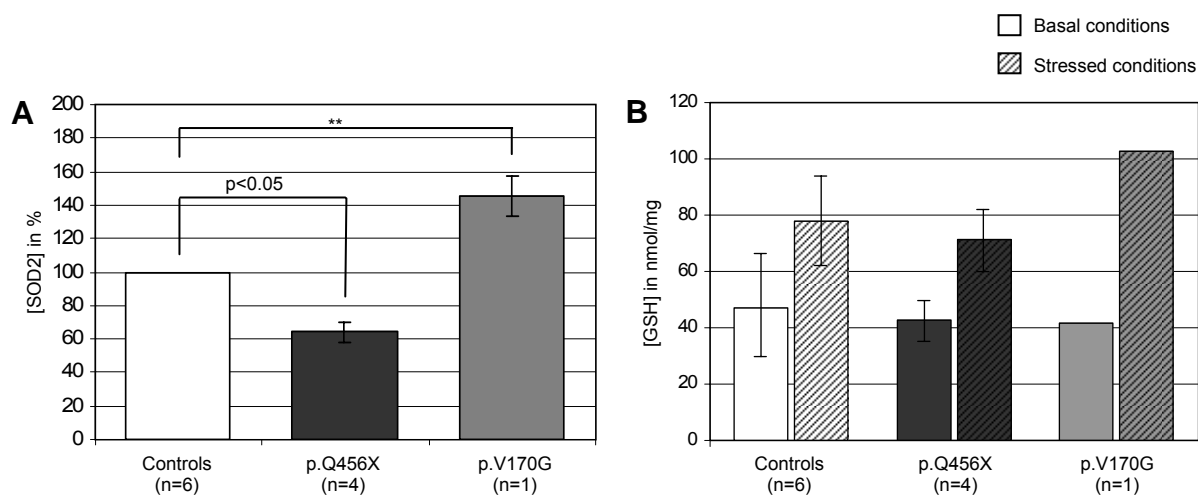


**Fig 24** Indicators of oxidative stress. (A) SOD2 protein expression under basal conditions (normalized to complex II expression and the mean value in the control group). The missense mutant showed a markedly higher SOD2 expression level (145%) than seen in controls (100%). The average expression in the nonsense mutants was significantly lower (64%). (B) GSH levels under basal and stressed conditions. For controls, patients with the p.Q456X mutation as well as the sample with the p.V170G mutation comparable GSH levels were detected when measured under normal conditions. After treatment with paraquat, all samples showed an increase in the cellular glutathione concentration. However, the sample with the p.V170G mutation tended to show a greater increase ( $\Delta[\text{GSH}]_{\text{p.V170G}}=148\%$ ) than the other groups ( $\Delta[\text{GSH}]_{\text{controls}}=66\%$ ,  $\Delta[\text{GSH}]_{\text{p.Q456X}}=65\%$ ). \*\* – increase > fourfold standard deviation of the control group, n – number of individuals.

### 3.3.7 Mitochondrial network

When the mitochondrial network was studied by use of MitoTracker Green FM controls, missense mutants and nonsense mutants showed a similar pattern.

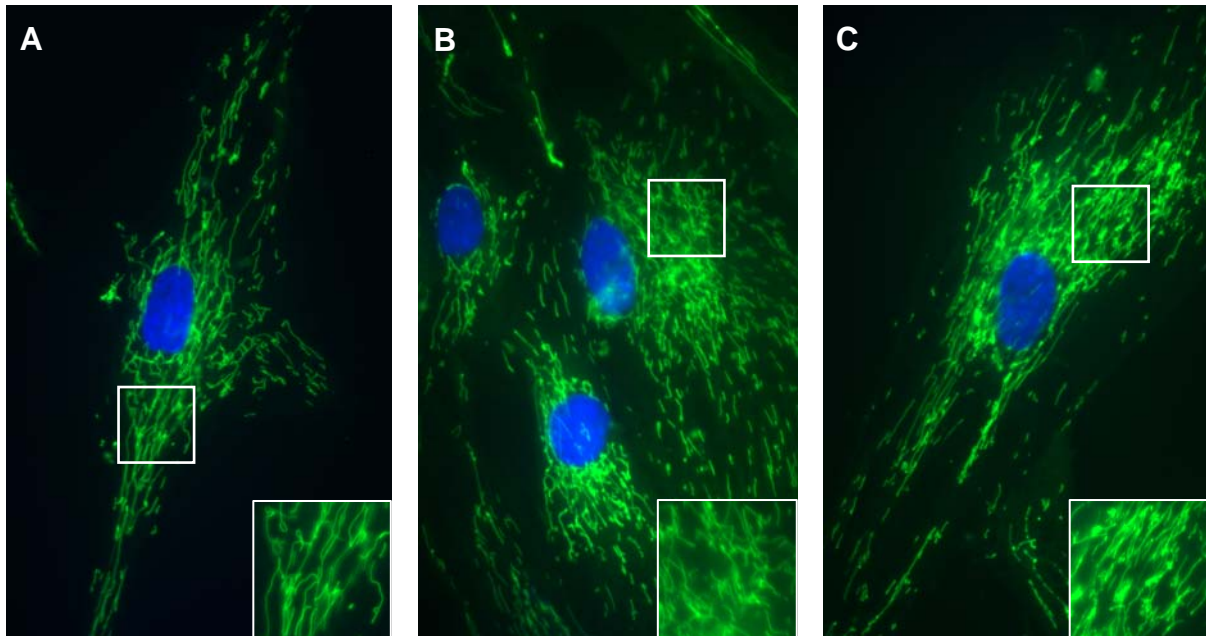


**Fig 25** *Mitochondrial network in primary fibroblasts.* MitoTracker Green FM was used to visualize the mitochondrial network. The cell nucleus is stained with DAPI. (A) Control, (B) nonsense mutant and (C) missense mutant fibroblasts with comparable mitochondrial structure.

### 3.3.8 Electron microscopy studies

To study the mitochondrial morphology in the cells, pellets of four controls, the four nonsense mutant samples and the missense mutant sample were prepared (procedure described in 2.3.13.1). The latter sample was repeated once. Transverse sections of the pellets were cut and microscopically examined by a specialist, who was blinded to the mutational status of the samples. In a subset of the PINK1 p.V170G mutant fibroblasts the EM analysis revealed a mitochondrial pattern clearly different from the structures seen in controls. The respective mitochondria in the missense sample were swollen and markedly enlarged (see mitochondrial shape in Fig 26).

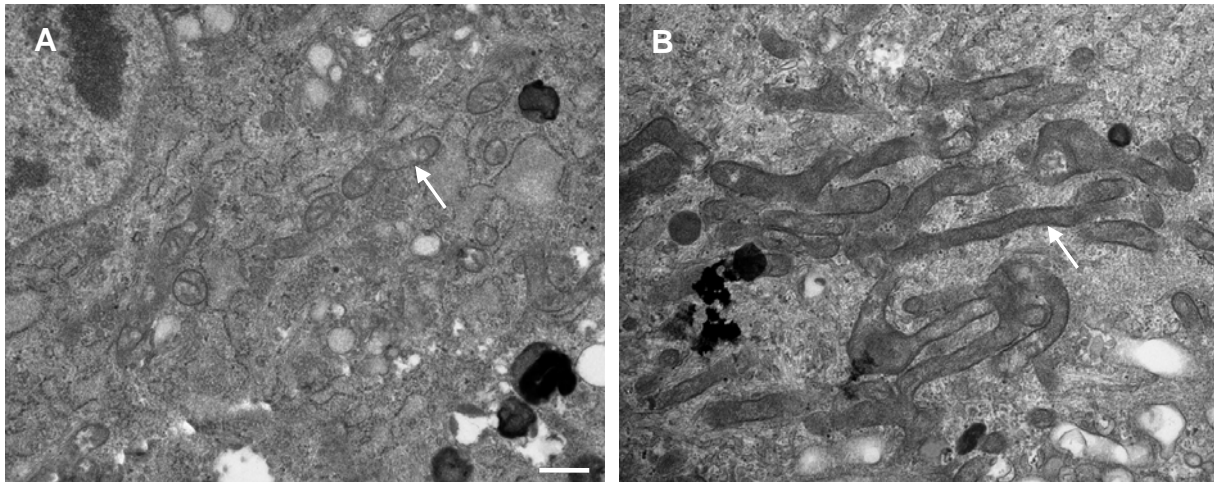


**Fig 26 Mitochondrial morphology in fibroblasts.** Transverse sections of control and missense mutant fibroblast pellets were examined using electron microscopy. (A) The picture shows mitochondria of normal size and structure in a control. (B) In the p.V170G missense sample mitochondria fusion was detected. Mitochondria are exemplarily marked by an arrow. Scale bar 2 $\mu$ m.

The results of all mitochondrial function experiments performed are summarized in Table 6.

**Table 6 Summary of the mitochondrial function and morphology data**

Experiment	Controls	p.Q456X (c.1366C>T)	p.V170G (c.509T>G)
<b>Respiratory chain enzyme activities</b>			
Complex I	0	0	(-)
Complex II/III	0	0	++
Complex IV	0	0	-
<b>Mitochondrial content</b>			
Malate dehydrogenase activity (cell lysates)	0	0	0
Citrate synthase activity (mitochondrial preparations)	0	0	(+)
<b>mtDNA levels</b>			
	0	0	0
<b>Protein expression</b>			
Complex I	0	0	--
Complex II	0	0	-
Complex III	0	0	0
Complex IV	0	0	(-)
<b>Membrane potential</b>			
Basal conditions	0	0	0
Stressed conditions	0	0	(-)
<b>ATP level</b>			
	0	-	0
<b>Marker of oxidative stress</b>			
SOD2 (basal conditions)	0	-	++
GSH (basal conditions)	0	0	0
GSH (stressed conditions)	(+)	+	++
<b>Mitochondrial morphology</b>			
Mitochondrial network	0	0	0
Mitochondrial fusion	0	0	+

Note: 0 – no change, (+) – slight increase, (-) – slight decrease, +- increase, -- decrease, ++ – marked increase, --- marked decrease

## 4 DISCUSSION

The outcome of the projects (A-C, cp. Fig 1) performed as a part of this thesis is discussed in the following: first, the significance of large deletions in *SGCE* (4.1); second, the results of the *PINK1* gene expression study (4.2); and finally, the findings from the mitochondrial function approach in *PINK1* mutant fibroblasts (4.3).

### 4.1 Myoclonus-dystonia: Significance of large *SGCE* deletions

In this project, the *SGCE* gene was screened in 35 index patients with an M-D syndrome ranging from definite to possible phenotypes according to the applied classification. In these three groups there were no significant differences in age of onset. However, when comparing mutation carriers versus non-mutation carriers, the latter group had a significantly later onset of the condition.

#### 4.1.1 Frequency and type of *SGCE* mutations

Mutations were detected in 36% (9/25) of the definite and probable M-D patients. When compared with previous studies from the literature on *SGCE* screening in M-D cases, not including other dystonia or movement disorder phenotypes, mutations were detected in only 23% (see Table 1B in Grünewald *et al.*, 2008). There are two possible explanations for the higher mutation frequency in our study:

First, a rigorous selection of patients for clinical features and family structure was performed. In the present study, all but three mutations were discovered in definitely affected patients. Concentrating on cases with a diagnosis of definite M-D, the mutation rate further increased to 60% (6/10). The mutation carriers IP16535, IP2625 and IP15039 had a negative family history and were therefore characterized as probable M-D candidates. In concordance with previous studies, no mutations in patients with sole symptoms of dystonia or signs of other movement disorders were identified.

A second explanation for the lower mutation detection rate in M-D patients in the past is that exonic deletions in *SGCE* may have been missed. Gene dosage alterations were only recently discovered as a type of mutation in M-D (Asmus *et al.*, 2005; DeBerardinis *et al.*, 2003).

Homozygous deletions are easily detectable by a lacking PCR product in the respective region. For the detection of heterozygous mutations three different techniques are used nowadays: (i) Southern-blot analysis (Furukawa *et al.*, 2000; Lee *et al.*, 1989), (ii) cytogenetic

methods – FISH (Macville *et al.*, 1997; Wallis *et al.*, 1999), comparative genomic hybridization (Bentz *et al.*, 1998) and (iii) different PCR amplification techniques – competitive PCR (Lee *et al.*, 1997), differential PCR (Neubauer *et al.*, 1990), PCR at polymorphic DNA strands (Brice *et al.*, 1992; Ruiz-Ponte *et al.*, 2000), real-time PCR (Hedrich *et al.*, 2001) and MLPA (Schouten *et al.*, 2002). While Southern-blot analysis and cytogenetic methods are very complex, expensive and not sensitive to small deletions PCR-based techniques gain more and more importance in the genetic research.

Here, gene dosage analysis of all coding exons was performed in the set of samples. Due to its high reliability and easy applicability in large screens (Djarmati *et al.*, 2007), MLPA was our method of choice. Nine percent of our cases had a large deletion which can explain the difference between the published and our observed *SGCE* mutation frequency. In our sample, gene dosage alterations accounted for 33% of the detected mutations, emphasizing the importance of qPCR as previously shown for other genes, such as *GTP cyclohydrolase 1* (*GCHI*), *Parkin* (*PARK2*) or *alpha-synuclein* (*SNCA*; *PARK1*) (Hagenah *et al.*, 2005; Hedrich *et al.*, 2004c; Singleton *et al.*, 2003).

However, even when applying a strict clinical selection procedure and performing an extensive genetic screen, a considerable number of our definite M-D patients (4/10) and of cases reported in the literature did not show mutations in the *SGCE* gene. Possible reasons are undetected nucleotide changes in *SGCE*, for example, in regulatory or intronic regions. Alternatively, M-D may be due to mutations in one or more additional, as yet unknown M-D genes.

#### 4.1.2 Comparison of phenotype and genotype

Similar to the results from the literature (40/107; Fig 11), the majority of identified *SGCE* mutations from this thesis are causing a nonsense codon (6/9). The respective patients did not show any clinical features which would make it possible to distinguish them from other M-D patients. Since a premature stop in the sequence of a gene can lead to nonsense-mediated mRNA decay and to subsequent haploinsufficiency an indifferent phenotype is not surprising for such mutations.

Missense mutations were not found in our sample of patients. According to other studies this type of mutation accounts for only a tenth of all sequence alterations known in *SGCE* (12/107). Exemplarily, it has recently been shown for three of these missense mutations that *SGCE* trafficking in the plasma membrane is impaired and that mutated proteins are rapidly degraded by the proteasome (Esapa *et al.*, 2007). This result might further explain the lack of

reports about genotype-phenotype correlations in M-D patients in the literature (Bressman, 2004).

Nevertheless, particular clinical features occurring in two mutation-positive cases from this study gave rise to the assumption of a genotypic link:

First, the phenotype of the family of IP15916 is especially interesting since several members reported painful joints in addition to typical signs of M-D. All relatives with joint problems were also confirmed or predicted mutation carriers. Intriguingly, apart from *SGCE*, at least the genes *COL1A2*, *CASD1*, *PEG10* and *ARFIP1* are affected by the deletion on chromosome 7q21.3-q22.1 that runs in this family. However, only the non-imprinted *COL1A2* gene has been linked to genetic diseases resulting in common disorders such as osteoporosis, and osteoarthritis (De Paepe, 1998; Kuivaniemi *et al.*, 1991). Consequently, the unusual, non-motor clinical features occurring in this family are likely linked to the chromosome 7q21.3-q22.1 deletion that should result in haploinsufficiency of the *COL1A2* gene product.

A similar genotype-phenotype correlation was observed in a second case (IP16535) who presented with delayed skeletal development and severe osteoporosis requiring hip and knee replacement in his early twenties. A heterozygous deletion on the parental allele of the patient includes at least the genes *SGCE*, *COL1A2* and *CASD1*. This is the second report of a *de novo* deletion containing *SGCE*. A different multiplex phenotype comprising M-D and other features has been reported in another case (DeBerardinis *et al.*, 2003): Due to a large *de novo* deletion on chromosome 7 (q21.2-q21.3), the described patient is additionally affected with microcephaly, short stature, dysmorphic face and language delay. This deletion did not include the *COL1A2* gene and the patient was not reported to have joint problems.

After this screen for mutations in *SGCE* was completed and evaluated at the beginning of 2007 two studies concerned with large deletions in *SGCE* were published.

Asmus *et al.* presented three M-D patients with heterozygous large deletions in the 7q21.13-21.3 region (2007). The deletion size was determined to range from 1.63 to 8.78 Mb in those three cases. In case of the largest deletion 43 genes were affected in addition to *SGCE*. This included also the genes *split-hand/splitfoot malformation 1 (SHFM1)*, *distal-less homeobox 6 (DLX6)* and *distal-less homeobox 5 (DLX5)*. Due to the deletion of *SHFM1* the respective case suffered not only from the movement disorder but also from split-hand/split-foot malformation and sensorineural hearing loss. All three deletions contained the *COL1A2* gene. Similar to our case IP15916, haploinsufficiency of *COL1A2* resulted in subtle symptoms like recurrent joint subluxation or hypodontia.

At the beginning of this year *Han et al.* reported two families with a heterozygous deletion of several exons in *SGCE* (2008). Both index patients had clinical features in keeping with a diagnosis of M-D and no additional non-motor symptoms.

Taken together, these data indicate that there is no correlation between the location of a mutation within *SGCE* and the phenotype of a patient. Only for the M-D cases with additional non-motor signs vague conclusions about the genotype may be possible.

#### **4.1.3 Clinical relevance of deletion mutations in *SGCE***

The discovery of deletion mutations comprising single exons or even the whole *SGCE* gene plus the surrounding genomic region allows for a better definition of the clinical spectrum of M-D. The combination of the M-D phenotype with seemingly unrelated clinical signs (like in the two mentioned cases) helps facilitate the identification of genetic causes for both the movement disorder and the additional non-motor syndrome. Furthermore, this finding has important implications on clinical care of the patients including specific genetic counselling and treatment.

#### **4.1.4 Deviation from paternal transmission**

The *SGCE* gene is known to be maternally imprinted (*Grabowski et al.*, 2003; *Müller et al.*, 2002). In the families of our identified mutation carriers, only one member might have deviated from paternal transmission, supporting the predominance of this inheritance pattern. Importantly, the vast majority of M-D patients have not been examined at the cDNA level to determine the expression status of both parental alleles. Similarly, in this study, there was only a single cDNA sample available to test for the expression pattern. The father (F2454) of an index patient expressed only the mutated allele. However, due to a lack of samples from his parents the parental origin of this allele could not be confirmed. Further analysis will be necessary to completely clarify how the maternal allele can escape imprinting in some cases.

## 4.2 Parkinson's disease: Gene expression in patients with *PINK1* mutation

This part of the thesis is concerned with the effect of *PINK1* mutations on the expression of the gene. The data, which was mainly collected in a three-generation-family with the *PINK1* c.1366C>T mutation, is discussed in the following. Thereby, the heterozygous mutation state is of particular interest. Furthermore, the question of whether the mutant *PINK1* mRNA level may be correlated with the disease status in heterozygous carriers was addressed.

### 4.2.1 Frequency and significance of heterozygous *PINK1* mutations

The pathogenic significance of heterozygous *PINK1* mutations has been a matter of debate since the identification of the *PARK6* gene (Bonifati *et al.*, 2005; Hedrich *et al.*, 2006; Klein *et al.*, 2006; Valente *et al.*, 2004a; Valente *et al.*, 2004b; Zadikoff *et al.*, 2006). According to the review of *PINK1* mutations which was performed in this thesis, about 50% of all sequence alterations detected are heterozygous (see Fig 17).

The clinical signs in the heterozygous mutation carriers of Family W ranged from slight slowness of fine finger movement to full-blown PD (Hedrich *et al.*, 2006). This phenotypic variability is likely caused by genetic, epigenetic, or environmental factors, or a combination of them that either promotes the development of PD signs or compensate for a latent motor deficit (Bonifati *et al.*, 2005; Hedrich *et al.*, 2006).

An other study performed on a large series of 768 PD cases and the same number of controls found an enrichment of *PINK1* single heterozygous mutations among the cases, supporting further the view that these single mutations are a risk factor for the development of PD (Abou-Sleiman *et al.*, 2006b).

### 4.2.2 Genetic origin of the *PINK1* c.1366C>T mutation

With the exception of the French patient (compound heterozygous carrier of c.373T>C and c.1366C>T) mentioned earlier (3.2), no evidence of an additional mutation was found, in all investigated individuals with a single heterozygous c.1366C>T transition, neither at the genomic DNA nor at the cDNA level.

The haplotype analysis in patients from five unrelated families (Family W, MI-002, FPD and individuals Roma-360, NE-166) revealed different potential scenarios. The allele sharing at the three intragenic SNPs is compatible with a common, but ancient founder; however, the shared alleles are also the most commonly observed in the population (Bonifati *et al.*, 2005),

and the observed sharing could also be a chance finding. The results from the microsatellite marker analysis alternatively suggest that the c.1366C>T mutation has arisen at least twice independently.

#### **4.2.3 Influence of the c.1366C>T mutation on the *PINK1* gene expression**

Although the genomic sequences of the heterozygotes in families W, MI-002, FPD and of the patient Roma-360 showed an equivalent signal for the wildtype 1366C and the mutant 1366T allele, the cDNA sequences indicated differences in intensity. A much weaker or almost absent 1366T signal suggests that the mutant transcript is less expressed or less stable than the wildtype transcript. Consequently, a real-time PCR assay was performed to establish whether the frequent c.1366C>T mutation affects *PINK1* mRNA levels.

The real-time data confirmed our assumptions from the sequencing analysis. As expected, *PINK1* expression reached approximately 100% in all wildtype individuals. However, it was reduced to 50 to 60% in the heterozygous mutation carriers and to 10 to 20% in the homozygous mutation carriers.

Real-time PCR is a sensitive and accurate method for monitoring gene expression. Potential variability that may be caused during the processing of samples can be controlled for by the use of internal standard genes. Ideally, these housekeeping genes should be expressed at a constant level, independent of experimental conditions (Vandesompele *et al.*, 2002). In keeping with this notion, *SDHA* and *YWHAZ* were chosen as control genes as they showed the lowest variability and greatest reproducibility in our experimental setup.

Consistent findings in both heterozygotes and homozygotes indicate that the mutant 1366T allele is expressed at a very low level, or that the mRNA is partially degraded, for instance, by NMD, a cellular mechanism that reduces the abundance of transcripts containing a premature termination codon (Holbrook *et al.*, 2004). In this study, the treatment with cycloheximide, a known NMD inhibitor (Holbrook *et al.*, 2004), markedly increased the signal of the mutant 1366T allele in cDNA sequencing experiments, suggesting that NMD is indeed the mechanism leading to the reduced mutant 1366T signal observed in our mutation carriers.

Although it is tempting to speculate that the 1366T allele exerts its pathogenic effect as a functional null allele, the degradation of the mutated allele does not appear to be 100% complete as indicated by our detected mRNA ratios of 0.1–0.2 in the homozygous and of 0.5–0.6 in the heterozygous mutation carriers. Therefore, it cannot be fully excluded that low amounts of truncated proteins lead to a dominant-negative or gain-of-function mechanism.

#### **4.2.4 Genotype-phenotype correlation in Family W**

The different clinical status of the heterozygous mutation carriers of Family W was not explained by correlation with *PINK1* mRNA levels, suggesting that other genetic or environmental factors play a role in determining the phenotypic variability associated with the c.1366C>T mutation. However, more subtle effects of reduced *PINK1* mRNA levels might be appreciated in future studies if larger numbers of c.1366C>T mutation carriers become available for quantitative cDNA study and more clinical parameters are taken into account.

### **4.3 Parkinson's disease: Mitochondrial function and morphology in patients with PINK1 mutations**

To date, studies investigating functional consequences of mutations in PINK1 were mostly performed in expression cell models, animal models or for very small groups of PD patients. Here, four siblings (from Family W, see 2.1.2.1 and Fig 4 for details) with the homozygous PINK1 p.Q456X nonsense mutation were examined and compared to a group of eight controls, three of whom were relatives of the affected cases. A PINK1 p.V170G missense sample was also included in the approach.

#### **4.3.1 Mutations in PINK1 alter respiratory chain enzyme activities**

Several research groups have recently demonstrated a link between the electron transport chain and PD (Hoepken *et al.*, 2007; Parker *et al.*, 1989; Piccoli *et al.*, 2008). In *Drosophila melanogaster* a PINK1 knock-down was reported to cause mitochondrial dysfunction (Park *et al.*, 2006). The NMD initiating mutation p.Q456X in PINK1 may also lead to loss of function in the homozygous members of Family W. However, the activities of the respiratory chain enzymes in fibroblasts of such nonsense mutants were not different from those in controls. This finding is analogous to results from Piccoli *et al.* (2008). The authors showed that fibroblasts with the homozygous p.W347X nonsense mutation have unaltered activities of complex I, III and IV when measured spectrophotometrically. Why PINK1 haploinsufficiency does not result in a detectable impairment of the respiratory chain function in PD patients remains elusive.

In contrast, for the p.V170G missense mutant fibroblasts complex I activity was low, although not significantly reduced. Decreased complex I activity is a common feature of several different forms of parkinsonism. NADH dehydrogenase deficiency has been discovered in the substantia nigra, platelets and fibroblasts of PD patients (Haas *et al.*, 1995; Hoepken *et al.*, 2007; Janetzky *et al.*, 1994; Krige *et al.*, 1992; Mann *et al.*, 1994; Schapira *et al.*, 1990b). Lacking significance of the complex I data presented here might be due to variations in the control values, a phenomenon which was observed earlier (Williams *et al.*, 2001). However, reduced complex I activity was not present in all patients with PD in a study investigating lymphocyte mitochondria (Martin *et al.*, 1996).

For the combined measurement of complexes II and III, the missense mutant showed elevated activity. If there was indeed an inhibition of complex I in the p.V170G mutant, hyperactivity of complexes II and III could be interpreted as a compensatory mechanism to maintain

cellular ATP levels (which were unaffected in the sample). In the literature, activity changes of complexes II and III in PD patients are discussed controversially. Haas *et al.* claim complex II/III activity to be significantly decreased in platelets from affected (Haas *et al.*, 1995). Thus, the data from Hanagasi and colleagues indicate no differences for complex III in a group of cases with a familial history of PD (2005).

For complex IV, the missense sample revealed reduced activity. Similar results were obtained for parkin in mammalian models. Deletion of exon 3 of parkin in mice resulted in decreased mitochondrial respiratory capacity due to low protein levels of complex IV (Palacino *et al.*, 2004).

Next, implications of the mitochondrial content on the identified activity changes were addressed in cell lysates and in the mitochondrial preparations. The malate dehydrogenase activities in the cell lysates of all samples were comparable. Although the citrate synthase activity in the mitochondrial pellet of the missense mutant was higher than the average activity in the nonsense mutant pellets or control pellets, it was still within the range of the two groups. It is therefore unlikely, that the observed hyperactivity of complexes II and III in the PINK1 p.V170G mutant is caused by elevated mitochondria concentration. This assumption is further supported by equal mtDNA levels in all investigated fibroblast cultures. In addition, faulty respiratory complex assembly was excluded by blue-native PAGE. Hence, misassembly of the subunits does most probably not account for the functional changes. The protein expression analysis for the complexes performed in whole cell homogenates revealed reduced complex I and complex IV levels in the missense fibroblasts, possibly explaining the reduced NADH dehydrogenase and cytochrome c oxidase activity in this individual.

PINK1 has been shown to protect cells from oxidative stress (Pridgeon *et al.*, 2007). Therefore, it cannot be discounted that loss of PINK1 activity is decreasing a phosphorylation pathway that protects the cells from reactive oxygen species (ROS) and that the ETC inhibition seen in the investigated missense mutant is caused by a subsequent increase in ROS. Alternatively, disabled phosphorylation due to PINK1 haploinsufficiency could affect the mitochondrial morphology (cp. 4.3.4), which in turn could significantly disrupt the function of the ETC.

#### **4.3.2 Reductions in membrane potential and ATP level**

Proper function of the respiratory chain enzyme complexes is crucial for the maintenance of  $\Delta\psi_m$  (Abou-Sleiman *et al.*, 2006b). Under basal conditions  $\Delta\psi_m$  was similar in control, nonsense and missense mutant fibroblasts. When stressed with the superoxide generator

paraquat, only cells harbouring the p.V170G mutation showed a loss of potential, consistent with the abnormal mitochondrial function in the sample. This might suggest that mechanisms compensating for the dysfunction of complex I and IV can no longer be perpetuated under influence of additional oxidative stress. Valente and colleagues reported similar results. When they stressed SH-SY5Y cells, which were transfected with p.G309D mutant PINK1,  $\Delta\psi_m$  decreased significantly (2004a). In the future, it would be interesting to see whether paraquat treatment reduces the observed complex II and III hyperactivity in the missense mutant fibroblasts. Such an experiment would investigate the relevance of the up-regulation for the maintenance of  $\Delta\psi_m$  under basal conditions in the PINK1 p.V170G mutant.

In this thesis, the results gained from the ATP quantification approach appear to be in conflict with the outcome from the enzyme activity assays. The cellular ATP concentration in the missense mutant was comparable with the control level. Apparently, the functional deficits of complex I and IV in the p.V170G mutant did not result in a detectable cellular ATP variation. By contrast, a significant reduction in the level of ATP was determined in the nonsense mutant cultures. Since the mitochondrial function was “normal” in these samples this result can only be explained by increased cellular ATP consumption. Piccoli and colleagues report reduced cellular ATP levels in a PD patient harbouring the p.W437X mutation when the respective fibroblasts were cultured in a galactose medium. In a glucose cultivation medium the ATP level was, on the contrary, higher than in control cells (2008).

As a further step it would be interesting to examine the consequences of overexpressed p.V170G and p.Q456X PINK1 on the cellular ATP concentration in fibroblasts and to compare these results with the findings in patient cells.

### 4.3.3 Elevated oxidative stress in PINK1 mutant cells

Signs of oxidative stress are a common finding in the substantia nigra of patients with PD. Post-mortem studies of PD patient brains revealed increased damage of lipids and proteins by ROS (Bowling and Beal, 1995).

SOD2 scavenges superoxide radicals in the mitochondrial matrix. In the missense fibroblasts, where inhibition of the respiratory chain was observed, levels of SOD2 were elevated. Assuming that respiratory chain dysfunction increases the production of ROS the enhanced antioxidant release could be a protective mechanism to prevent the mitochondria from further damage. Alternatively, the cellular SOD2 levels may be increased to compensate for the loss of a PINK1-dependent antioxidant pathways. High superoxide production in PINK1 missense-mutant fibroblasts was also seen by Hoepken *et al* (2007).

However, the protein amount for SOD2 in the nonsense mutant samples was lower than in controls. Similar findings were reported by Piccoli and colleagues (2008). They detected a small decrease of the mitochondrial manganese superoxide dismutase activity in fibroblasts of a patient with homozygous p.W437X nonsense mutation.

The observed differences are most likely not age-related as the average age of the control group equals the age of the missense sample (70 years, cp. 2.1.2).

In addition, the cellular concentration of the antioxidant GSH was determined. The GSH levels in all samples were unaffected under basal conditions. Only following treatment with the stressor paraquat an overall elevation of the GSH concentration occurred. The cellular up-regulation of GSH was even more pronounced for the missense mutant than for the nonsense mutants or controls. An enhancement of the GSH metabolism pathways in the response to oxidative stress was described earlier (Gegg *et al.*, 2003). The results by Gegg and colleagues suggested that astrocytes up-regulate GSH synthesis as a defence mechanism when exposed to free radicals. This mechanism enables the cells to resist acute stress. However, in case of persistent exposure to stress and mitochondrial dysfunction (as found in the substantia nigra in PD brains) the protection is unlikely to be maintained.

#### 4.3.4 Mitochondrial fusion in PINK1 mutant cells

When the mitochondrial network was studied by means of MitoTracker Green FM in control, nonsense mutant and missense mutant fibroblasts no structural differences were detected. However, the investigation of the mitochondrial shape with electron microscopy in two controls, two p.Q456X nonsense mutants and the p.V170G missense mutant revealed histological differences in the last sample. Mitochondria with normal morphology were also found in fibroblasts from a patient with the p.W437X nonsense mutation in PINK1 (Piccoli *et al.*, 2008). In the missense mutant cells, on the contrary, elongated mitochondria imply mitochondrial fusion. This finding is in keeping with results by Poole *et al.* (2008). The authors found that loss-of-function mutations in PINK1 result in enlarged or swollen mitochondria in *Drosophila* tissues and cell lines. As an explanation for this phenomenon, Yang *et al.* (2008) could show that PINK1 interacts with the mitochondrial fission/fusion machinery and modulates mitochondrial dynamics. According to their data, overexpression of PINK1 in mammalian cells promotes mitochondrial fission, whereas inhibition of PINK1 leads to excessive fusion. Apparently, PINK1 acts through *Fission 1 (mitochondrial outer membrane) homolog (S. cerevisiae) (Fis1)* and *Dynamin-related protein 1 (Drp1)* to regulate mitochondrial fission. Contradicting these results from animal models, Exner *et al.* reported

that the mitochondrial network was fragmented in PINK1 mutant patient fibroblasts (2007). Here, no fragmentation of the mitochondrial network was observed in any of the available fibroblast cultures when treated under basal conditions. Thus, the findings from this thesis further support the reports by Poole *et al.* (2008) and Yang *et al.* (2006).

## 4.4 Conclusions

### Project A:

*Deletions in the SGCE gene are an underestimated cause of M-D.*

According to the literature deletions in *SGCE* are a rare cause of M-D (cp. Fig 11, p. 55). In the current study, however, 9% of the included cases showed a deletion in *SGCE* (cp. Table 5, p. 48). Therewith, gene dosage alterations accounted for a third of the mutations detected here, emphasizing the importance of quantitative screening methods.

Deletions were only recently discovered as a type of mutation in M-D. Though, recent developments of reliable and easily applicable qPCR techniques, such as MLPA, allow standard screenings for gene dosage alterations nowadays.

The result of this thesis suggests a much higher identification quote of deletions in *SGCE* in future screens.

*There is a link between genotype and phenotype in M-D patients.*

The investigated M-D patients were classified according to their phenotype into definite, probable and possibly affected (see Table 3, p. 19). This preselection led to a mutational detection rate of 36% in *SGCE* for the first two groups. When compared with previous studies from the literature on *SGCE* screening in M-D cases mutations were detected in only 23%. Concentrating on patients with a diagnosis of definite M-D, the mutation rate in the screen, processed here, further increased to 60% (cp. 4.1.1, p. 70). Apparently, the risk for M-D patients to harbour a mutation in *SGCE* increases with certain clinical characteristics.

However, no explicit correlation between the type or location of the mutations and the phenotype could be observed for cases with small sequence alterations in *SGCE* (cp. 3.1.1., p. 46 and 4.1.1, p. 70). Only in two M-D cases who presented with additional non-motor signs a specific genetic link was identified. In those patients, the particular features could be explained by large deletions involving several genes surrounding *SGCE* on chromosome 7q. Consequently, a comprehensive clinical examination, including a careful accounting for non-motor signs, should precede molecular investigations.

### Project B:

*The c.1366C>T mutation in PINK1 influences the expression of the gene.*

In the current thesis the expression of the PD-associated gene *PINK1* was determined in two families with the c.1366C>T mutation coding for a premature stop codon. Taken together, samples of four homozygous mutants, 13 heterozygous mutants and seven mutation-negative individuals participated were included in the study (see 2.1.2, p. 20). The gene expression analysis revealed that the nonsense mutation leads to partial degradation of the *PINK1* mRNA, caused by NMD (cp. Fig 13, p. 57 and Fig 15, p. 59). Therefore, c.1366T exerts its pathogenic effect most likely as a functional null allele.

*The variable phenotype of patients with heterozygous mutations in PINK1 is explained by the expression level of the gene.*

Eleven heterozygous members of Family W were previously classified according to their PD status. In this thesis the phenotype of the heterozygous c.1366C>T mutants was correlated with the *PINK1* gene expression in their blood samples. No link between the clinical and genetic mRNA data was found (cp. 3.2.3, p. 58).

### Project C:

*Mutant PINK1 exerts its pathogenic effect by inhibition of the respiratory chain function.*

As a part of this thesis the mitochondrial function in *PINK1* p.Q456X nonsense mutant, *PINK1* p.V170G missense mutant and control fibroblasts was compared. In homozygous nonsense mutant cells, which are supposed to express very low levels of *PINK1*, no alterations for the respiratory chain enzyme activities were determined. The missense mutant showed low activities of complexes I and IV, whereas the activities of complexes II and III were high (see Fig 19, p. 63). *PINK1* haploinsufficiency did also not effect the mitochondrial membrane potential. The missense mutation, however, led to a decrease in potential, pointing further towards defective respiratory chain function in the respective fibroblasts (cp. Fig 22, p. 66).

*Loss of PINK1 function leads to oxidative stress in the cell.*

To question this hypothesis, the concentration of the antioxidants SOD2 and GSH was determined in available fibroblasts. Under basal conditions only the p.V170G mutant showed elevated levels of cellular stress, which were detected by increased SOD2 expression (cp. Fig 24A, p. 67). In addition, cell treatment with the superoxide generator paraquat led to an

overall increase of the GSH concentration, which was particularly strong in the missense mutant (cp. Fig 24B, p. 67).

On one hand, the higher antioxidant levels could indicate a cellular response mechanism to increased ROS production caused by mitochondrial dysfunction in the missense mutant sample. This finding is supported by unaltered SOD2 concentrations in the nonsense mutants for which no respiratory chain inhibition was detected.

On the other hand, if PINK1's primary function was to protect cells from oxidative stress, loss of PINK1 activity would lead to the induction of independent antioxidant pathways in order to protect cells. The elevated SOD2 levels might then be due to such alternative mechanisms.

*PINK1 plays a role in the process of mitochondrial fission.*

The investigation of the mitochondrial network in controls, nonsense and missense mutant fibroblasts revealed no differences among the three groups (cp. Fig 25, p. 68).

To further assess the influence of PINK1 on mitochondrial fission electron microscopic pictures were taken from cellular sections. Here, only the missense sample showed histological alterations when compared to controls (cp. Fig 26, p. 69). Enlarged and swollen mitochondria might indicate a malfunction of the mitochondrial fission/fusion pathway in the PINK1 p.V107G mutant.

## 5 PERSPECTIVES

A critical selection of M-D patients, preceding an *SGCE* mutational screen markedly increased the detection rate of the study. Further optimization of the applied criteria might contribute to even more successful mutation analyses.

The result of the performed screen pointed to the significance of deletions in the *SGCE* gene. Especially large deletions including several genes were an interesting finding as they allowed an explanation of additional non-motor signs in the respective patients. Knowing about this background might facilitate the diagnosis for special M-D cases in the future.

The great number of deletions among the investigated M-D patients implies a high probability of this mutation type overall. Hence, quantitative mutational studies might improve the quality of routine diagnostic tests.

*PINK1* gene expression was determined in a large family with a segregating c.1366C>T mutation. The results led to the assumption that about 90% of the *PINK1* mRNA is degraded in homozygous mutation carrier, referring to haploinsufficiency as the disease causing mechanism for those cases. Due to the lack of a working PINK1 antibody the protein level, however, was not quantified. Further investigations will be needed to completely exclude a gain-of-function effect of the c.1366C>T mutation in the affected.

When investigating the phenotype of the heterozygous *PINK1* mutation carriers from Family W the responsible neurologists were confronted with a wide spectrum of features. The clinical signs of the 11 heterozygotes varied from unaffected to full blown PD. The cause of these differences was searched for in the genotype. However, their phenotype could not be correlated with the expression of *PINK1* on mRNA level. Additional studies, possibly considering the influence of environmental factors on the occurrence of the disease, are necessary to clarify this question.

In this thesis the involvement of PINK1 in mitochondrial function was addressed. Structural changes in the protein caused by a missense mutation seem to affect the function of the respiratory enzyme complexes. To further characterize this effect, the *PINK1* c.509T>G sequence alteration could be silenced in the patient cells by means of siRNA, which should recover basal respiratory chain enzyme activities, as seen in the nonsense mutants. Another strategy to define the results of this thesis would be to overexpress *PINK1* constructs with both mutations in wildtype fibroblasts.

In addition, mutant PINK1 appears to inhibit mitochondrial fission. The mitochondrial morphology in fibroblasts of PD patient with an identified missense mutation differed from the shape in control cells. Molecular-biological investigations to explain this phenomenon were not part of this thesis. A stepwise discovering of the pathways involving PINK1 in the control of respiratory chain function and mitochondrial fission will help to better understand the molecular background of PD in the future.

## 6 SUMMARY

This thesis investigates phenotype-genotype correlations on the genomic, cDNA, protein and functional level of two different movement disorders: *SGCE*-associated myoclonus dystonia (M-D – Project A) and *PINK1*-associated Parkinson's disease (PD – Project B and C).

M-D is inherited in an autosomal-dominant fashion and caused by mutations in *SGCE*. In Project A two specific hypotheses were addressed: (i) *Deletions in the SGCE gene are an underestimated cause of M-D.* (ii) *There is a link between genotype and phenotype in M-D patients.* To this end, 35 M-D index patients were tested by multiplex ligation-dependent probe amplification and genomic sequencing. Mutations were found in 26% (9/35) of the cases, all but three with definite M-D. Two heterozygous deletions of the entire *SGCE* gene and flanking DNA and a heterozygous deletion of exon 2 only were detected, accounting for 33% (3/9) of the mutations found. Both large deletions contained *COL1A2* and were additionally associated with joint problems. Further, one novel small deletion and four recurrent point mutations were discovered. A Medline search identified 22 articles on *SGCE* mutational screening. Sixty-four unrelated M-D patients were described with 41 different mutations. No genotype-phenotype association was found, except in patients with deletions encompassing additional genes. In conclusion, a rigorous clinical preselection of patients and careful accounting for non-motor signs should precede mutational tests. Gene dosage studies should be included in routine *SGCE* genetic testing.

Recessively inherited PD can be caused by mutations in the *PINK1* gene. Despite extensive mutation screening, only a single heterozygous mutation has been found in some patients, including the recurrent c.1366C>T transition. Related to this aspect the following hypotheses were raised in Project B: (i) *The c.1366C>T mutation in PINK1 influences the expression of the gene.* (ii) *The variable phenotype of patients with heterozygous mutations in PINK1 is explained by the expression level of the gene.* Consequently, the genomic DNA and cDNA were investigated from 21 individuals carrying the c.1366C>T mutation in the homozygous (n=6), heterozygous (n=14) or compound heterozygous (n=1) state. In 17 mutants, mRNA was quantified by real-time PCR using four different assays. Genomic sequencing confirmed the presence and zygosity of the *PINK1* mutations. Sequencing at the cDNA level in heterozygous mutation carriers revealed a strong wild-type and a much weaker or almost absent mutant signal, whereas in the homozygous patients, only the mutant signal was detected. Homozygous and heterozygous mutants showed *PINK1* mRNA levels relative to a reference gene in the range of 0.1–0.2 and 0.5–0.6, respectively, compared with values of 0.9–

1.0 in mutation-negative individuals. Treatment of fibroblasts from a heterozygous mutation carrier with cycloheximide markedly increased the mutant transcript signal. Apparently, the recurrent *PINK1* c.1366C>T mutation exerts its major effect at the mRNA level, most likely via nonsense-mediated mRNA decay. The absence of a correlation between *PINK1* mRNA levels and clinical status in heterozygous mutation carriers suggests that other genetic or environmental factors play a role in determining the phenotypic variability associated with the c.1366C>T mutation.

*PINK1* encodes a mitochondrial kinase and may function in the protection of cells against stress conditions. Regarding the molecular role of PINK1, the following hypotheses were formulated in Project C: (i) *Mutant PINK1 exerts its pathogenic effect by inhibition of the respiratory chain function.* (ii) *Loss of PINK1 function leads to oxidative stress in the cell.* (iii) *PINK1 plays a role in the process of mitochondrial fission.* Functional assays were performed in fibroblast cultures gained from four members of Family W harbouring the c.1366C>T (p.Q456X) nonsense mutation in homozygous state and three of their wildtype relatives, one individual with the homozygous missense mutation c.509T>G (p.V170G) in *PINK1* and five independent controls. Investigations of the respiratory chain enzymes in the fibroblast samples showed decreased activity of complexes I and IV and increased activity of complex II+III for the missense. By contrast, in the nonsense mutants the enzyme activities were normal. Correlating with lower complex I and IV activity, the expression level of NADH dehydrogenase and cytochrome c oxidase was reduced in the missense sample. Altered respiratory chain activities caused no alterations of the mitochondrial membrane potential under basal conditions, however, when the missense mutant cells were stressed, the potential decreased. Similarly, the electron transport chain malfunction did not affect the cellular ATP level in the missense sample. However, the ATP concentration in the nonsense mutant fibroblasts was significantly lower than in control cells. In the fibroblasts with the p.V170G mutation, the concentration of the antioxidant SOD2 was elevated. In the nonsense mutant cells SOD2 was decreased. Additionally, elongated and swollen mitochondria were found in fibroblasts from the missense mutant. These data indicate that mutant PINK1 impairs respiratory chain function and increases the cellular vulnerability to oxidative stress. In the nonsense mutant cells with a supposedly low PINK1 level, the respiratory chain enzyme complexes were normal. Therefore, PINK1 haploinsufficiency does not seem to directly influence the function of the electron transport chain but enhances the cellular ATP consumption. Furthermore, PINK1 appears to be involved in the mitochondrial fission/fusion machinery.

## 7 ZUSAMMENFASSUNG

In dieser Promotionsarbeit wurden Genotyp-Phänotyp-Beziehungen zweier Bewegungsstörungen auf Gen-, cDNA-, Protein- und funktioneller Ebene untersucht. Dabei standen die *SGCE*-assoziierte Myoklonus-Dystonie (M-D – Projekt A) und das *PINK1*-assoziiertes Parkinson-Syndrom (PS – Projekt B und C) im Mittelpunkt.

Die M-D ist autosomal-dominant vererbt und wird durch Mutationen in *SGCE* verursacht. Projekt A befasste sich mit folgenden Hypothesen: (i) *Deletionen im SGCE-Gen sind eine unterschätzte Krankheitsursache.* (ii) *Es besteht ein Zusammenhang zwischen Genotyp und Phänotyp bei M-D-Patienten.* Zu diesem Zweck wurden 35 M-D-Indexpatienten mittels *multiplex ligation-dependent probe amplification* und genomischer Sequenzierung untersucht. In 26 % aller getesteten Fälle (9/35) wurden Mutationen identifiziert (6/9 Patienten mit definitiver M-D-Diagnose). Darunter waren zwei heterozygote Deletionsmutationen, die das komplette *SGCE*-Gen sowie flankierende DNA-Bereiche beinhalteten, und eine heterozygote Exon 2-Deletion. Damit stellten sie ein Drittel aller identifizierten Mutationen (3/9). Die beiden komplexen Deletionen beinhalteten *COL1A2* und waren zusätzlich mit einer schweren Gelenkerkrankung assoziiert. Darüber hinaus wurden eine neue kleine Deletion und vier bereits bekannte Punktmutationen entdeckt. Bei einer Literaturrecherche in der *Medline*-Datenbank wurden 22 Veröffentlichungen zur *SGCE*-Mutationsanalyse gefunden. Diese beschrieben 64 nicht verwandte M-D-Patienten mit 41 verschiedenen Mutationen. Außer bei Patienten mit Deletionen mehrerer Gene bestand keine Verbindung zwischen Genotyp und Phänotyp. Anhand der Ergebnisse von Projekt A lässt sich schlussfolgern, dass jeder genetischen Analyse eine sorgfältige klinische Untersuchung der Patienten mit besonderem Schwerpunkt auf nicht-motorischen Symptomen vorausgehen sollte. Außerdem wäre es sinnvoll, Genedosisuntersuchungen in die *SGCE*-Routinediagnostik aufzunehmen.

Die durch Mutationen in *PINK1*-Gen verursachte Form von PS wird rezessiv vererbt. Trotz umfangreicher Analysen konnte bei manchen PS-Patienten allerdings nur eine einzelne heterozygote Mutation gefunden werden. So auch im Fall des häufige auftretenden Basenaustausches c.1366C>T. Zu dieser Thematik wurden im Projekt B zwei Hypothesen aufgestellt: (i) *Die c.1366C>T-Mutation in PINK1 beeinflusst die Expression des Gens.* (ii) *Die Phänotypvarianz bei PS-Patienten mit heterozygoten Mutationen in PINK1 hängt vom Expressionsniveau des Gens ab.* Um diese Annahmen zu hinterfragen, wurden DNA- und cDNA-Proben von 21 Trägern der c.1366C>T Mutation mit homozygoter (n = 6), heterozygoter (n = 14) oder *compound*-heterozygoter (n = 1) Ausprägung untersucht. Bei 17

mutationspositiven Proben wurde die mRNA-Konzentration mittels Echtzeit-PCR gemessen. Bei den heterozygoten Mutationsträgern zeigte die Sequenzierung auf cDNA-Ebene ein deutlich stärkeres Signal für das Wildtyp-Allel als für das mutierte Allel. Bei den homozygoten Mutationsträgern war nur das mutierte Signal sichtbar. Die heterozygoten bzw. homozygoten Mutanten wiesen ein *PINK1*-mRNA-Niveau zwischen 50 - 60 % bzw. 10 - 20 % auf. Im Vergleich dazu betrug das Niveau in den Wildtypfällen 90 - 100 %. Die Behandlung einer heterozygoten c.1366C>T-Fibroblastenkultur mit Cycloheximid bewirkte eine deutliche Zunahme des c.1366T-Signals. Offenbar löst die c.1366C>T-Mutation *nonsense-mediated mRNA decay* aus. Da bei den heterozygoten c.1366C>T-Mutationsträgern kein Zusammenhang zwischen *PINK1*-Expressionsniveau und klinischem Status bestand, ist anzunehmen, dass andere genetische Ursachen oder Umweltfaktoren zur Phänotypvarianz beitragen.

*PINK1* kodiert für eine mitochondriale Kinase und schützt die Zelle möglicherweise vor den Einflüssen von oxidativem Stress. Bezüglich der molekularen Rolle von *PINK1* wurden in Projekt C drei Hypothesen aufgestellt: (i) *Die pathogene Wirkung von mutiertem PINK1 basiert auf der Hemmung der Atmungskette.* (ii) *Ein Funktionsverlust des PINK1-Proteins führt zu erhöhtem oxidativen Stress in der Zelle.* (iii) *PINK1 spielt eine Rolle im mitochondrialen Fissionsprozess.* In Fibroblastenkulturen von vier homozygoten c.1366C>T-Mutationsträgern (p.Q456X) der Familie W und drei ihrer mutations-negativen Verwandten bzw. einer Patientin mit c.509T>G-*missense*-Mutation (p.V170G) und fünf unabhängigen Kontrollen wurden funktionelle Analysen durchgeführt. Die Untersuchung der Enzyme der Atmungskette in der *missense*-Mutationsprobe deuteten auf eine verminderte Aktivität der Komplexe I und IV und eine erhöhte Aktivität der Komplexe II und III hin. Die Enzymaktivitäten der *nonsense*-Mutationsproben waren hingegen normal. Die verringerte Aktivität der Komplexe I und IV in der *missense*-Probe stand im Einklang mit verminderter Proteinexpression. Die veränderten Enzymaktivitäten hatten unter Standardkultivierungsbedingungen keinen Effekt auf das mitochondriale Membranpotential. Unter Einfluss des Superoxidgenerators Paraquat fiel das Potential in der *missense*-Probe allerdings deutlich ab. Die Dysfunktion der Atmungskette wirkte sich in den Zellen mit p.V170G-Mutation nicht auf die zelluläre ATP-Konzentration aus. In den *nonsense*-Proben war die ATP-Konzentration jedoch signifikant geringer als in Kontrollen. Während die Konzentration des Antioxidans SOD2 in der Probe mit p.V170G-Mutation erhöht war, zeigten die p.Q456X-Kulturen hier eine Konzentrationserhöhung. Des Weiteren wurden in der *missense*-Probe einige Zellen mit auffälliger Mitochondrienmorphologie identifiziert. Die in Projekt C ermittelten Daten legen

nahe, dass die p.V170G mutierte Form von PINK1 die Funktionalität der Atmungskette beeinträchtigt und die Empfindlichkeit der Fibroblasten gegenüber oxidativem Stress erhöht. In den *nonsense*-Mutationskulturen mit (vermutlich) verminderter PINK1-Konzentration wurden keine Aktivitätsveränderungen der Komplexe I-IV festgestellt. Demnach scheint die PINK1-Haploinsuffizienz die Atmungskette nicht unmittelbar zu beeinflussen, jedoch führt sie zu erhöhtem zellulären ATP-Verbrauch. Außerdem scheint PINK1 in die mitochondriale Fissions-/Fusionsmaschinerie einzugreifen.

## 8 REFERENCES

- Abou-Sleiman PM, Muqit MM, McDonald NQ, Yang YX, Gandhi S, Healy DG, et al. A heterozygous effect for PINK1 mutations in Parkinson's disease? *Ann Neurol* 2006a.
- Abou-Sleiman PM, Muqit MM, Wood NW. Expanding insights of mitochondrial dysfunction in Parkinson's disease. *Nat Rev Neurosci* 2006b; 7: 207-19.
- Abrahams JP, Leslie AG, Lutter R, Walker JE. Structure at 2.8 Å resolution of F1-ATPase from bovine heart mitochondria. *Nature* 1994; 370: 621-8.
- Ackrell BA. Progress in understanding structure-function relationships in respiratory chain complex II. *FEBS Lett* 2000; 466: 1-5.
- Almeida A, Medina JM. Isolation and characterization of tightly coupled mitochondria from neurons and astrocytes in primary culture. *Brain Res* 1997; 764: 167-72.
- Asmus F, Hjermand LE, Dupont E, Wagenstaller J, Haberlandt E, Munz M, et al. Genomic deletion size at the epsilon-sarcoglycan locus determines the clinical phenotype. *Brain* 2007; 130: 2736-45.
- Asmus F, Salih F, Hjermand LE, Ostergaard K, Munz M, Kuhn AA, et al. Myoclonus-dystonia due to genomic deletions in the epsilon-sarcoglycan gene. *Ann Neurol* 2005; 58: 792-7.
- Asmus F, Zimprich A, Tezenas Du Montcel S, Kabus C, Deuschl G, Kupsch A, et al. Myoclonus-dystonia syndrome: epsilon-sarcoglycan mutations and phenotype. *Ann Neurol* 2002; 52: 489-92.
- Atsumi M, Li Y, Tomiyama H, Sato K, Hattori N. [A 62-year-old woman with early-onset Parkinson's disease associated with the PINK1 gene deletion]. *Rinsho Shinkeigaku* 2006; 46: 199-202.
- Bai RK, Wong LJ. Simultaneous detection and quantification of mitochondrial DNA deletion(s), depletion, and over-replication in patients with mitochondrial disease. *J Mol Diagn* 2005; 7: 613-22.
- Barraquer-Roviralta L. Contribución al estudio de la atetosis. *Gac Med Catalana* 1897; 20: 385-91.
- Bauman JG, Wiegant J, Borst P, van Duijn P. A new method for fluorescence microscopical localization of specific DNA sequences by in situ hybridization of fluorochromelabelled RNA. *Exp Cell Res* 1980; 128: 485-90.

- Beal MF. Bioenergetic approaches for neuroprotection in Parkinson's disease. *Ann Neurol* 2003; 53 Suppl 3: S39-47; discussion S47-8.
- Benecke R, Strumper P, Weiss H. Electron transfer complexes I and IV of platelets are abnormal in Parkinson's disease but normal in Parkinson-plus syndromes. *Brain* 1993; 116 ( Pt 6): 1451-63.
- Bentz M, Plesch A, Stilgenbauer S, Dohner H, Lichter P. Minimal sizes of deletions detected by comparative genomic hybridization. *Genes Chromosomes Cancer* 1998; 21: 172-5.
- Betarbet R, Sherer TB, MacKenzie G, Garcia-Osuna M, Panov AV, Greenamyre JT. Chronic systemic pesticide exposure reproduces features of Parkinson's disease. *Nat Neurosci* 2000; 3: 1301-6.
- Birch-Machin MA, Briggs HL, Saborido AA, Bindoff LA, Turnbull DM. An evaluation of the measurement of the activities of complexes I-IV in the respiratory chain of human skeletal muscle mitochondria. *Biochem Med Metab Biol* 1994; 51: 35-42.
- Bonifati V, Oostra BA, Heutink P. Linking DJ-1 to neurodegeneration offers novel insights for understanding the pathogenesis of Parkinson's disease. *J Mol Med* 2004; 82: 163-74.
- Bonifati V, Rizzu P, van Baren MJ, Schaap O, Breedveld GJ, Krieger E, et al. Mutations in the DJ-1 gene associated with autosomal recessive early-onset parkinsonism. *Science* 2003; 299: 256-9.
- Bonifati V, Rohe CF, Breedveld GJ, Fabrizio E, De Mari M, Tassorelli C, et al. Early-onset parkinsonism associated with PINK1 mutations: frequency, genotypes, and phenotypes. *Neurology* 2005; 65: 87-95.
- Borges V, Aguiar Pde C, Ferraz HB, Ozelius LJ. Novel and de novo mutations of the SGCE gene in Brazilian patients with myoclonus-dystonia. *Mov Disord* 2007; 22: 1208-9.
- Bowling AC, Beal MF. Bioenergetic and oxidative stress in neurodegenerative diseases. *Life Sci* 1995; 56: 1151-71.
- Boyer PD. New insights into one of nature's remarkable catalysts, the ATP synthase. *Mol Cell* 2001; 8: 246-7.
- Bressman SB. Dystonia genotypes, phenotypes, and classification. *Adv Neurol* 2004; 94: 101-7.
- Brice A, Ravise N, Stevanin G, Gugenheim M, Bouche P, Penet C, et al. Duplication within chromosome 17p11.2 in 12 families of French ancestry with Charcot-Marie-Tooth disease type 1a. The French CMT Research Group. *J Med Genet* 1992; 29: 807-12.

- Butler AG, Duffey PO, Hawthorne MR, Barnes MP. An epidemiologic survey of dystonia within the entire population of northeast England over the past nine years. *Adv Neurol* 2004; 94: 95-9.
- Camargos S, Scholz S, Simon-Sanchez J, Paisan-Ruiz C, Lewis P, Hernandez D, et al. DYT16, a novel young-onset dystonia-parkinsonism disorder: identification of a segregating mutation in the stress-response protein PRKRA. *Lancet Neurol* 2008; 7: 207-15.
- Caviness JN, Alving LI, Maraganore DM, Black RA, McDonnell SK, Rocca WA. The incidence and prevalence of myoclonus in Olmsted County, Minnesota. *Mayo Clin Proc* 1999; 74: 565-9.
- Chishti MA, Bohlega S, Ahmed M, Loualich A, Carroll P, Sato C, et al. T313M PINK1 mutation in an extended highly consanguineous Saudi family with early-onset Parkinson disease. *Arch Neurol* 2006; 63: 1483-5.
- Chung EJ, Lee WY, Kim JY, Kim JH, Kim GM, Ki CS, et al. Novel SGCE gene mutation in a Korean patient with myoclonus-dystonia with unique phenotype mimicking Moya-Moya disease. *Mov Disord* 2007; 22: 1206-7.
- Cif L, Valente EM, Hemm S, Coubes C, Vayssiere N, Serrat S, et al. Deep brain stimulation in myoclonus-dystonia syndrome. *Mov Disord* 2004; 19: 724-7.
- Clark IE, Dodson MW, Jiang C, Cao JH, Huh JR, Seol JH, et al. Drosophila pink1 is required for mitochondrial function and interacts genetically with parkin. *Nature* 2006.
- Coore HG, Denton RM, Martin BR, Randle PJ. Regulation of adipose tissue pyruvate dehydrogenase by insulin and other hormones. *Biochem J* 1971; 125: 115-27.
- Criscuolo C, Volpe G, De Rosa A, Varrone A, Marongiu R, Mancini P, et al. PINK1 homozygous W437X mutation in a patient with apparent dominant transmission of parkinsonism. *Mov Disord* 2006.
- Crofts AR, Hong S, Ugulava N, Barquera B, Gennis R, Guergova-Kuras M, et al. Pathways for proton release during ubihydroquinone oxidation by the bc(1) complex. *Proc Natl Acad Sci U S A* 1999; 96: 10021-6.
- Daube JR, Peters HA. Hereditary essential myoclonus. *Arch Neurol* 1966; 15: 587-94.
- Davidson RG, Cortner JA. Mitochondrial malate dehydrogenase: a new genetic polymorphism in man. *Science* 1967; 157: 1569-71.
- de Carvalho Aguiar P, Sweadner KJ, Penniston JT, Zaremba J, Liu L, Caton M, et al. Mutations in the Na<sup>+</sup>/K<sup>+</sup> -ATPase alpha3 gene ATP1A3 are associated with rapid-onset dystonia parkinsonism. *Neuron* 2004; 43: 169-75.

- De Paepe A. Heritable collagen disorders: from phenotype to genotype. *Verh K Acad Geneeskd Belg* 1998; 60: 463-82; discussion 482-4.
- DeBerardinis RJ, Conforto D, Russell K, Kaplan J, Kollros PR, Zackai EH, et al. Myoclonus in a patient with a deletion of the epsilon-sarcoglycan locus on chromosome 7q21. *Am J Med Genet A* 2003; 121: 31-6.
- Djarmati A, Guzvic M, Grünewald A, Lang AE, Pramstaller PP, Simon DK, et al. Rapid and reliable detection of exon rearrangements in various movement disorders genes by multiplex ligation-dependent probe amplification. *Mov Disord* 2007; 22: 1708-14.
- Djarmati A, Hedrich K, Svetel M, Lohnau T, Schwinger E, Romac S, et al. Heterozygous PINK1 mutations: A susceptibility factor for Parkinson disease? *Mov Disord* 2006.
- Doheny D, Danisi F, Smith C, Morrison C, Velickovic M, De Leon D, et al. Clinical findings of a myoclonus-dystonia family with two distinct mutations. *Neurology* 2002; 59: 1244-6.
- Doostzadeh J, Tetrud JW, Allen-Auerbach M, Langston JW, Schüle B. Novel features in a patient homozygous for the L347P mutation in the PINK1 gene. *Parkinsonism Relat Disord* 2007; 13: 359-61.
- du Montcel, Clot F, Vidailhet M, Roze E, Damier C, Jedynek P, et al. Epsilon sarcoglycan mutations and phenotype in French patients with myclonic syndromes. *J Med Genet* 2006; 43: 394-400.
- Duchen MR, Surin A, Jacobson J. Imaging mitochondrial function in intact cells. *Methods Enzymol* 2003; 361: 353-89.
- Ephraty L, Porat O, Israeli D, Cohen OS, Tunkel O, Yael S, et al. Neuropsychiatric and cognitive features in autosomal-recessive early parkinsonism due to PINK1 mutations. *Mov Disord* 2007; 22: 566-9.
- Esapa CT, Waite A, Locke M, Benson MA, Krauss M, McIlhinney RA, et al. SGCE missense mutations that cause myoclonus-dystonia syndrome impair {epsilon}-sarcoglycan trafficking to the plasma membrane: modulation by ubiquitination and torsinA. *Hum Mol Genet* 2007.
- Ettinger AJ, Feng G, Sanes JR. epsilon-Sarcoglycan, a broadly expressed homologue of the gene mutated in limb-girdle muscular dystrophy 2D. *J Biol Chem* 1997; 272: 32534-8.
- Evidente VG, Nolte D, Niemann S, Advincula J, Mayo MC, Natividad FF, et al. Phenotypic and molecular analyses of X-linked dystonia-parkinsonism ("lubag") in women. *Arch Neurol* 2004; 61: 1956-9.

- Exner N, Treske B, Paquet D, Holmstrom K, Schiesling C, Gispert S, et al. Loss-of-function of human PINK1 results in mitochondrial pathology and can be rescued by parkin. *J Neurosci* 2007; 27: 12413-8.
- Fahn S, Elton RL, Committee UD. Unified Parkinson's Disease Rating Scale. In: Fahn S, Marsden C, Calne D and Goldstein M, editors. *Recent Developments in Parkinson's Disease*. Florham Park: NJ: Macmillan, 1987: 153-163.
- Foncke EM, Klein C, Koelman JH, Kramer PL, Schilling K, Muller B, et al. Hereditary myoclonus-dystonia associated with epilepsy. *Neurology* 2003; 60: 1988-90.
- Fung HC, Chen CM, Hardy J, Singleton AB, Lee-Chen GJ, Wu YR. Analysis of the PINK1 gene in a cohort of patients with sporadic early-onset parkinsonism in Taiwan. *Neurosci Lett* 2006; 394: 33-6.
- Furukawa Y, Graf WD, Wong H, Shimadzu M, Kish SJ. Dopa-responsive dystonia simulating spastic paraplegia due to tyrosine hydroxylase (TH) gene mutations. *Neurology* 2001; 56: 260-3.
- Furukawa Y, Guttman M, Sparagana SP, Trugman JM, Hyland K, Wyatt P, et al. Dopa-responsive dystonia due to a large deletion in the GTP cyclohydrolase I gene. *Ann Neurol* 2000; 47: 517-20.
- Gegg ME, Beltran B, Salas-Pino S, Bolanos JP, Clark JB, Moncada S, et al. Differential effect of nitric oxide on glutathione metabolism and mitochondrial function in astrocytes and neurones: implications for neuroprotection/neurodegeneration? *J Neurochem* 2003; 86: 228-37.
- Gelmetti V, Ferraris A, Brusa L, Romano F, Lombardi F, Barzaghi C, et al. Late onset sporadic Parkinson's disease caused by PINK1 mutations: Clinical and functional study. *Mov Disord* 2008.
- Genova ML, Pich MM, Bernacchia A, Bianchi C, Biondi A, Bovina C, et al. The mitochondrial production of reactive oxygen species in relation to aging and pathology. *Ann N Y Acad Sci* 2004; 1011: 86-100.
- Gerrits MC, Foncke EM, de Haan R, Hedrich K, van de Leemput YL, Baas F, et al. Phenotype-genotype correlation in Dutch patients with myoclonus-dystonia. *Neurology* 2006; 66: 759-61.
- Gibb WR, Lees AJ. The relevance of the Lewy body to the pathogenesis of idiopathic Parkinson's disease. *J Neurol Neurosurg Psychiatry* 1988; 51: 745-52.

- Grabowski M, Zimprich A, Lorenz-Depiereux B, Kalscheuer V, Asmus F, Gasser T, et al. The epsilon-sarcoglycan gene (SGCE), mutated in myoclonus-dystonia syndrome, is maternally imprinted. *Eur J Hum Genet* 2003; 11: 138-44.
- Greene JC, Whitworth AJ, Kuo I, Andrews LA, Feany MB, Pallanck LJ. Mitochondrial pathology and apoptotic muscle degeneration in *Drosophila parkin* mutants. *Proc Natl Acad Sci U S A* 2003; 100: 4078-83.
- Grigorieff N. Structure of the respiratory NADH:ubiquinone oxidoreductase (complex I). *Curr Opin Struct Biol* 1999; 9: 476-83.
- Grünewald A, Djarmati A, Lohmann-Hedrich K, Farrell K, Zeller JA, Allert N, et al. Myoclonus-dystonia: significance of large SGCE deletions. *Hum Mutat* 2008; 29: 331-2.
- Gu M, Gash MT, Mann VM, Javoy-Agid F, Cooper JM, Schapira AH. Mitochondrial defect in Huntington's disease caudate nucleus. *Ann Neurol* 1996; 39: 385-9.
- Haas RH, Nasirian F, Nakano K, Ward D, Pay M, Hill R, et al. Low platelet mitochondrial complex I and complex II/III activity in early untreated Parkinson's disease. *Ann Neurol* 1995; 37: 714-22.
- Hagenah J, Saunders-Pullman R, Hedrich K, Kabakci K, Habermann K, Wiegers K, et al. High mutation rate in dopa-responsive dystonia: detection with comprehensive GCHI screening. *Neurology* 2005; 64: 908-11.
- Hammond WA. *Treatise on diseases of the nervous system*. New York, 1871: 654-662.
- Han F, Lang AE, Racacho L, Bulman DE, Grimes DA. Mutations in the epsilon-sarcoglycan gene found to be uncommon in seven myoclonus-dystonia families. *Neurology* 2003; 61: 244-6.
- Han F, Racacho L, Yang H, Read T, Suchowersky O, Lang AE, et al. Large deletions account for an increasing number of mutations in SGCE. *Mov Disord* 2008; 23: 456-60.
- Hanagasi HA, Ayribas D, Baysal K, Emre M. Mitochondrial complex I, II/III, and IV activities in familial and sporadic Parkinson's disease. *Int J Neurosci* 2005; 115: 479-93.
- Hatano Y, Li Y, Sato K, Asakawa S, Yamamura Y, Tomiyama H, et al. Novel PINK1 mutations in early-onset parkinsonism. *Ann Neurol* 2004; 56: 424-7.
- Healy DG, Abou-Sleiman PM, Gibson JM, Ross OA, Jain S, Gandhi S, et al. PINK1 (PARK6) associated Parkinson disease in Ireland. *Neurology* 2004; 63: 1486-8.
- Hedrich K, Eskelson C, Wilmot B, Marder K, Harris J, Garrels J, et al. Distribution, type, and origin of Parkin mutations: review and case studies. *Mov Disord* 2004a; 19: 1146-57.

- Hedrich K, Hagenah J, Djarmati A, Hiller A, Lohnau T, Lasek K, et al. Clinical spectrum of homozygous and heterozygous PINK1 mutations in a large German family with Parkinson disease: role of a single hit? *Arch Neurol* 2006; 63: 833-8.
- Hedrich K, Kann M, Lanthaler AJ, Dalski A, Eskelson C, Landt O, et al. The importance of gene dosage studies: mutational analysis of the parkin gene in early-onset parkinsonism. *Hum Mol Genet* 2001; 10: 1649-56.
- Hedrich K, Meyer EM, Schüle B, Kock N, de Carvalho Aguiar P, Wiegers K, et al. Myoclonus-dystonia: detection of novel, recurrent, and de novo SGCE mutations. *Neurology* 2004b; 62: 1229-31.
- Hedrich K, Saunders-Pullman R, Wiegers K, Hinrichs F, Hellenbroich Y, Kabakci K, et al. An expanding deletion on chromosome 14 in a family with dopa-responsive dystonia and ptosis. *Am J Hum Genet* 2004c; Suppl: 440.
- Herrero MT, Barcia C, Navarro JM. Functional anatomy of thalamus and basal ganglia. *Childs Nerv Syst* 2002; 18: 386-404.
- Hess CW, Raymond D, Aguiar Pde C, Frucht S, Shriberg J, Heiman GA, et al. Myoclonus-dystonia, obsessive-compulsive disorder, and alcohol dependence in SGCE mutation carriers. *Neurology* 2007; 68: 522-4.
- Hirawake H, Taniwaki M, Tamura A, Amino H, Tomitsuka E, Kita K. Characterization of the human SDHD gene encoding the small subunit of cytochrome b (cybS) in mitochondrial succinate-ubiquinone oxidoreductase. *Biochim Biophys Acta* 1999; 1412: 295-300.
- Hjermind LE, Werdelin LM, Eiberg H, Krag-Olsen B, Dupont E, Sorensen SA. A novel mutation in the epsilon-sarcoglycan gene causing myoclonus-dystonia syndrome. *Neurology* 2003; 60: 1536-9.
- Hoepken HH, Gispert S, Morales B, Wingerter O, Del Turco D, Mulsch A, et al. Mitochondrial dysfunction, peroxidation damage and changes in glutathione metabolism in PARK6. *Neurobiol Dis* 2007; 25: 401-11.
- Hoglinger GU, Carrard G, Michel PP, Medja F, Lombes A, Ruberg M, et al. Dysfunction of mitochondrial complex I and the proteasome: interactions between two biochemical deficits in a cellular model of Parkinson's disease. *J Neurochem* 2003; 86: 1297-307.
- Holbrook JA, Neu-Yilik G, Hentze MW, Kulozik AE. Nonsense-mediated decay approaches the clinic. *Nat Genet* 2004; 36: 801-8.
- Hsu LJ, Sagara Y, Arroyo A, Rockenstein E, Sisk A, Mallory M, et al. alpha-synuclein promotes mitochondrial deficit and oxidative stress. *Am J Pathol* 2000; 157: 401-10.

- Ibanez P, Lesage S, Lohmann E, Thobois S, De Michele G, Borg M, et al. Mutational analysis of the PINK1 gene in early-onset parkinsonism in Europe and North Africa. *Brain* 2006; 129: 686-94.
- Ichinose H, Ohye T, Takahashi E, Seki N, Hori T, Segawa M, et al. Hereditary progressive dystonia with marked diurnal fluctuation caused by mutations in the GTP cyclohydrolase I gene. *Nat Genet* 1994; 8: 236-42.
- Janetzky B, Hauck S, Youdim MB, Riederer P, Jellinger K, Pantucek F, et al. Unaltered aconitase activity, but decreased complex I activity in substantia nigra pars compacta of patients with Parkinson's disease. *Neurosci Lett* 1994; 169: 126-8.
- Karrasch S, Walker JE. Novel features in the structure of bovine ATP synthase. *J Mol Biol* 1999; 290: 379-84.
- Khan NL, Horta W, Eunson L, Graham E, Johnson JO, Chang S, et al. Parkin disease in a Brazilian kindred: Manifesting heterozygotes and clinical follow-up over 10 years. *Mov Disord* 2005; 20: 479-84.
- King TS. Preparation of succinate cytochrome c reductase, and the cytochrome b-c1 particle, and reconstitution of succinate cytochrome c reductase. *Methods Enzymol* 1967; 10: 217-235.
- Kitada T, Asakawa S, Hattori N, Matsumine H, Yamamura Y, Minoshima S, et al. Mutations in the parkin gene cause autosomal recessive juvenile parkinsonism. *Nature* 1998; 392: 605-8.
- Klein C. Myoclonus and Myoclonus Dystonia. *Genetics of Movement Disorders* 2003a.
- Klein C. Myoclonus and myoclonus-dystonias. In: *Genetics of Movement Disorders*. Academic Press 2003b.
- Klein C. Movement disorders: classifications. *J Inherit Metab Dis* 2005; 28: 425-39.
- Klein C, Djarmati A, Hedrich K, Schafer N, Scaglione C, Marchese R, et al. PINK1, Parkin, and DJ-1 mutations in Italian patients with early-onset parkinsonism. *Eur J Hum Genet* 2005; 13: 1086-93.
- Klein C, Grünewald A, Hedrich K. Early-onset parkinsonism associated with PINK1 mutations: frequency, genotypes, and phenotypes. *Neurology* 2006; 66: 1129-30; author reply 1129-30.
- Klein C, Liu L, Doheny D, Kock N, Müller B, de Carvalho Aguiar P, et al. Epsilon-sarcoglycan mutations found in combination with other dystonia gene mutations. *Ann Neurol* 2002; 52: 675-9.

- Klein C, Lohmann-Hedrich K, Rogaeva E, Schlossmacher MG, Lang AE. Deciphering the role of heterozygous mutations in genes associated with parkinsonism. *Lancet Neurol* 2007; 6: 652-62.
- Kock N, Kasten M, Schüle B, Hedrich K, Wiegers K, Kabakci K, et al. Clinical and genetic features of myoclonus-dystonia in 3 cases: a video presentation. *Mov Disord* 2004; 19: 231-4.
- Kopp JH. *Denkwürdigkeiten in der ärztlichen Praxis*. Frankfurt, 1830-45.
- Krige D, Carroll MT, Cooper JM, Marsden CD, Schapira AH. Platelet mitochondrial function in Parkinson's disease. The Royal Kings and Queens Parkinson Disease Research Group. *Ann Neurol* 1992; 32: 782-8.
- Kruger R, Kuhn W, Müller T, Woitalla D, Graeber M, Kosel S, et al. Ala30Pro mutation in the gene encoding alpha-synuclein in Parkinson's disease. *Nat Genet* 1998; 18: 106-8.
- Kuivaniemi H, Tromp G, Prockop DJ. Mutations in collagen genes: causes of rare and some common diseases in humans. *Faseb J* 1991; 5: 2052-60.
- Laemmli UK. Cleavage of structural proteins during the assembly of the head of bacteriophage T4. *Nature* 1970; 227: 680-5.
- Lai JC, Clark JB. Preparation and properties of mitochondria derived from synaptosomes. *Biochem J* 1976; 154: 423-32.
- Langston JW, Ballard P, Tetrud JW, Irwin I. Chronic Parkinsonism in humans due to a product of meperidine-analog synthesis. *Science* 1983; 219: 979-80.
- Lee B, Vissing H, Ramirez F, Rogers D, Rimoin D. Identification of the molecular defect in a family with spondyloepiphyseal dysplasia. *Science* 1989; 244: 978-80.
- Lee HH, Chang JG, Lin SP, Chao HT, Yang ML, Ng HT. Rapid detection of trisomy 21 by homologous gene quantitative PCR (HGQ-PCR). *Hum Genet* 1997; 99: 364-7.
- Lee HY, Xu Y, Huang Y, Ahn AH, Auburger GW, Pandolfo M, et al. The gene for paroxysmal non-kinesigenic dyskinesia encodes an enzyme in a stress response pathway. *Hum Mol Genet* 2004; 13: 3161-70.
- Lee SJ. alpha-synuclein aggregation: a link between mitochondrial defects and Parkinson's disease? *Antioxid Redox Signal* 2003; 5: 337-48.
- Lengauer C, Speicher MR, Popp S, Jauch A, Taniwaki M, Nagaraja R, et al. Chromosomal bar codes produced by multicolor fluorescence in situ hybridization with multiple YAC clones and whole chromosome painting probes. *Hum Mol Genet* 1993; 2: 505-12.
- Leroux PD. *Contribution à l'étude des causes de la paralysie agitante*. Paris, 1880.

- Leroy E, Boyer R, Auburger G, Leube B, Ulm G, Mezey E, et al. The ubiquitin pathway in Parkinson's disease. *Nature* 1998; 395: 451-2.
- Leung JC, Klein C, Friedman J, Vieregge P, Jacobs H, Doheny D, et al. Novel mutation in the TOR1A (DYT1) gene in atypical early onset dystonia and polymorphisms in dystonia and early onset parkinsonism. *Neurogenetics* 2001; 3: 133-43.
- Leutenecker AL, Salih MA, Ibanez P, Mukhtar MM, Lesage S, Arabi A, et al. Juvenile-onset Parkinsonism as a result of the first mutation in the adenosine triphosphate orientation domain of PINK1. *Arch Neurol* 2006; 63: 1257-61.
- Li Y, Tomiyama H, Sato K, Hatano Y, Yoshino H, Atsumi M, et al. Clinicogenetic study of PINK1 mutations in autosomal recessive early-onset parkinsonism. *Neurology* 2005; 64: 1955-7.
- Lowerson SA, Taylor L, Briggs HL, Turnbull DM. Measurement of the activity of individual respiratory chain complexes in isolated fibroblast mitochondria. *Anal Biochem* 1992; 205: 372-4.
- Lu CS, Chou YH, Weng YH, Chen RS. Genetic and DAT imaging studies of familial parkinsonism in a Taiwanese cohort. *J Neural Transm Suppl* 2006: 235-40.
- Macville M, Veldman T, Padilla-Nash H, Wangsa D, O'Brien P, Schrock E, et al. Spectral karyotyping, a 24-colour FISH technique for the identification of chromosomal rearrangements. *Histochem Cell Biol* 1997; 108: 299-305.
- Makino S, Kaji R, Ando S, Tomizawa M, Yasuno K, Goto S, et al. Reduced neuron-specific expression of the TAF1 gene is associated with X-linked dystonia-parkinsonism. *Am J Hum Genet* 2007; 80: 393-406.
- Mann VM, Cooper JM, Daniel SE, Srai K, Jenner P, Marsden CD, et al. Complex I, iron, and ferritin in Parkinson's disease substantia nigra. *Ann Neurol* 1994; 36: 876-81.
- Marechal L, Raux G, Dumanchin C, Lefebvre G, Deslandre E, Girard C, et al. Severe myoclonus-dystonia syndrome associated with a novel epsilon-sarcoglycan gene truncating mutation. *Am J Med Genet B Neuropsychiatr Genet* 2003; 119: 114-7.
- Marongiu R, Brancati F, Antonini A, Ialongo T, Ceccarini C, Scarciolla O, et al. Whole gene deletion and splicing mutations expand the PINK1 genotypic spectrum. *Hum Mutat* 2007; 28: 98.
- Marongiu R, Ghezzi D, Ialongo T, Soleti F, Elia A, Cavone S, et al. Frequency and phenotypes of LRRK2 G2019S mutation in Italian patients with Parkinson's disease. *Mov Disord* 2006.

- Martin MA, Molina JA, Jimenez-Jimenez FJ, Benito-Leon J, Orti-Pareja M, Campos Y, et al. Respiratory-chain enzyme activities in isolated mitochondria of lymphocytes from untreated Parkinson's disease patients. *Grupo-Centro de Trastornos del Movimiento. Neurology* 1996; 46: 1343-6.
- Matsumoto S, Nishimura M, Shibasaki H, Kaji R. Epidemiology of primary dystonias in Japan: comparison with Western countries. *Mov Disord* 2003; 18: 1196-8.
- McNally EM, Ly CT. Human epsilon-sarcoglycan is highly related to alpha-sarcoglycan (adhalin), the limb girdle muscular dystrophy 2d gene. *FEBS Lett* 1998; 422: 27-32.
- Michel H, Behr J, Harrenga A, Kannt A. Cytochrome c oxidase: structure and spectroscopy. *Annu Rev Biophys Biomol Struct* 1998; 27: 329-56.
- Miller SA, Dykes DD, Polesky HF. A simple salting out procedure for extracting DNA from human nucleated cells. *Nucleic Acids Res* 1988; 16: 1215.
- Misbahuddin A, Placzek M, Lennox G, Taanman JW, Warner TT. Myoclonus-dystonia syndrome with severe depression is caused by an exon-skipping mutation in the epsilon-sarcoglycan gene. *Mov Disord* 2007; 22: 1173-5.
- Mitchell P. Coupling of phosphorylation to electron and hydrogen transfer by a chemi-osmotic type of mechanism. *Nature* 1961; 191: 144-8.
- Moro E, Volkmann J, Konig IR, Winkler S, Hiller A, Hassin-Baer S, et al. Bilateral subthalamic stimulation in Parkin and PINK1 parkinsonism. *Neurology* 2008; 70: 1186-91.
- Müller B, Hedrich K, Kock N, Dragasevic N, Svetel M, Garrels J, et al. Evidence that paternal expression of the epsilon-sarcoglycan gene accounts for reduced penetrance in myoclonus-dystonia. *Am J Hum Genet* 2002; 71: 1303-11.
- Nakajima A, Kataoka K, Hong M, Sakaguchi M, Huh NH. BRPK, a novel protein kinase showing increased expression in mouse cancer cell lines with higher metastatic potential. *Cancer Lett* 2003; 201: 195-201.
- Nardocci N, Zorzi G, Barzaghi C, Zibordi F, Ciano C, Ghezzi D, et al. Myoclonus-dystonia syndrome: clinical presentation, disease course, and genetic features in 11 families. *Mov Disord* 2008; 23: 28-34.
- Neubauer A, Neubauer B, Liu E. Polymerase chain reaction based assay to detect allelic loss in human DNA: loss of beta-interferon gene in chronic myelogenous leukemia. *Nucleic Acids Res* 1990; 18: 993-8.

- Nicklas WJ, Vyas I, Heikkila RE. Inhibition of NADH-linked oxidation in brain mitochondria by 1-methyl-4-phenyl-pyridine, a metabolite of the neurotoxin, 1-methyl-4-phenyl-1,2,5,6-tetrahydropyridine. *Life Sci* 1985; 36: 2503-8.
- Nishioka K, Hayashi S, Farrer MJ, Singleton AB, Yoshino H, Imai H, et al. Clinical heterogeneity of alpha-synuclein gene duplication in Parkinson's disease. *Ann Neurol* 2006; 59: 298-309.
- Noensie EN, Dietz HC. A strategy for disease gene identification through nonsense-mediated mRNA decay inhibition. *Nat Biotechnol* 2001; 19: 434-9.
- Olanow CW, Watts RL, Koller WC. An algorithm (decision tree) for the management of Parkinson's disease (2001): treatment guidelines. *Neurology* 2001; 56: S1-S88.
- Oppenheim H. Über eine eigenartige Krampfkrankheit des kindlichen und jugendlichen Alters (Dysbasia lordotica progressiva, Dystonia musculorum deformans). *Neurologisches Zentralblatt* 1911; 30: 1090-1107.
- O'Riordan S, Ozelius LJ, de Carvalho Aguiar P, Hutchinson M, King M, Lynch T. Inherited myoclonus-dystonia and epilepsy: further evidence of an association? *Mov Disord* 2004; 19: 1456-9.
- Ozelius LJ, Hewett JW, Page CE, Bressman SB, Kramer PL, Shalish C, et al. The early-onset torsion dystonia gene (DYT1) encodes an ATP-binding protein. *Nat Genet* 1997; 17: 40-8.
- Paisan-Ruiz C, Jain S, Evans EW, Gilks WP, Simon J, van der Brug M, et al. Cloning of the gene containing mutations that cause PARK8-linked Parkinson's disease. *Neuron* 2004; 44: 595-600.
- Palacino JJ, Sagi D, Goldberg MS, Krauss S, Motz C, Wacker M, et al. Mitochondrial dysfunction and oxidative damage in parkin-deficient mice. *J Biol Chem* 2004; 279: 18614-22.
- Park J, Lee SB, Lee S, Kim Y, Song S, Kim S, et al. Mitochondrial dysfunction in *Drosophila* PINK1 mutants is complemented by parkin. *Nature* 2006.
- Parker WD, Jr., Boyson SJ, Parks JK. Abnormalities of the electron transport chain in idiopathic Parkinson's disease. *Ann Neurol* 1989; 26: 719-23.
- Pfeiffer RA. Langer-Giedion syndrome and additional congenital malformations with interstitial deletion of the long arm of chromosome 8 46, XY, del 8 (q 13-22). *Clin Genet* 1980; 18: 142-6.

- Piccoli C, Sardanelli A, Scrima R, Ripoli M, Quarato G, D'Aprile A, et al. Mitochondrial Respiratory Dysfunction in Familial Parkinsonism Associated with PINK1 Mutation. *Neurochem Res* 2008.
- Piras G, El Kharroubi A, Kozlov S, Escalante-Alcalde D, Hernandez L, Copeland NG, et al. Zac1 (Lot1), a potential tumor suppressor gene, and the gene for epsilon-sarcoglycan are maternally imprinted genes: identification by a subtractive screen of novel uniparental fibroblast lines. *Mol Cell Biol* 2000; 20: 3308-15.
- Plun-Favreau H, Klupsch K, Moiso N, Gandhi S, Kjaer S, Frith D, et al. The mitochondrial protease HtrA2 is regulated by Parkinson's disease-associated kinase PINK1. *Nat Cell Biol* 2007; 9: 1243-52.
- Polymeropoulos MH, Lavedan C, Leroy E, Ide SE, Dehejia A, Dutra A, et al. Mutation in the alpha-synuclein gene identified in families with Parkinson's disease. *Science* 1997; 276: 2045-7.
- Poole AC, Thomas RE, Andrews LA, McBride HM, Whitworth AJ, Pallanck LJ. The PINK1/Parkin pathway regulates mitochondrial morphology. *Proc Natl Acad Sci U S A* 2008; 105: 1638-43.
- Prestel J, Gempel K, Hauser TK, Schweitzer K, Prokisch H, Ahting U, et al. Clinical and molecular characterisation of a Parkinson family with a novel PINK1 mutation. *J Neurol* 2008.
- Pridgeon JW, Olzmann JA, Chin LS, Li L. PINK1 Protects against Oxidative Stress by Phosphorylating Mitochondrial Chaperone TRAP1. *PLoS Biol* 2007; 5: e172.
- Quinn NP. Essential myoclonus and myoclonic dystonia. *Mov Disord* 1996; 11: 119-24.
- Ragan CI, Wilson MT, Darley-Usmar VM, Lowe PN. Subfractionation of mitochondria and isolation of the proteins of oxidative phosphorylation. In: Darley-Usmar VM, Rickwood D and Wilson MT, editors. *Mitochondria: a practical approach*. London: IRL Press, 1987: 79-112.
- Rainier S, Thomas D, Tokarz D, Ming L, Bui M, Plein E, et al. Myofibrillogenesis regulator 1 gene mutations cause paroxysmal dystonic choreoathetosis. *Arch Neurol* 2004; 61: 1025-9.
- Ramirez A, Heimbach A, Grundemann J, Stiller B, Hampshire D, Cid LP, et al. Hereditary parkinsonism with dementia is caused by mutations in ATP13A2, encoding a lysosomal type 5 P-type ATPase. *Nat Genet* 2006; 38: 1184-1191.

- Raymond D, Saunders-Pullman R, de Carvalho Aguiar P, Schüle B, Kock N, Friedman J, et al. Phenotypic spectrum and sex effects in eleven myoclonus-dystonia families with epsilon-sarcoglycan mutations. *Mov Disord* 2008; 23: 588-92.
- Riederer P, Konradi C, Hebenstreit G, Youdim MB. Neurochemical perspectives to the function of monoamine oxidase. *Acta Neurol Scand Suppl* 1989; 126: 41-5.
- Rogaeva E, Johnson J, Lang AE, Gulick C, Gwinn-Hardy K, Kawarai T, et al. Analysis of the PINK1 gene in a large cohort of cases with Parkinson disease. *Arch Neurol* 2004; 61: 1898-904.
- Rohe CF, Montagna P, Breedveld G, Cortelli P, Oostra BA, Bonifati V. Homozygous PINK1 C-terminus mutation causing early-onset parkinsonism. *Ann Neurol* 2004; 56: 427-31.
- Ruiz-Ponte C, Loidi L, Vega A, Carracedo A, Barros F. Rapid real-time fluorescent PCR gene dosage test for the diagnosis of DNA duplications and deletions. *Clin Chem* 2000; 46: 1574-82.
- Saiki RK, Scharf S, Faloona F, Mullis KB, Horn GT, Erlich HA, et al. Enzymatic amplification of beta-globin genomic sequences and restriction site analysis for diagnosis of sickle cell anemia. *Science* 1985; 230: 1350-4.
- Savettieri G, Annesi G, Civitelli D, Ciro Candiano IC, Salemi G, Ragonese P, et al. Identification of the novel D297fsX318 PINK1 mutation and phenotype variation in a family with early-onset Parkinson's disease. *Parkinsonism Relat Disord* 2008.
- Sazanov LA, Peak-Chew SY, Fearnley IM, Walker JE. Resolution of the membrane domain of bovine complex I into subcomplexes: implications for the structural organization of the enzyme. *Biochemistry* 2000; 39: 7229-35.
- Schapira AH. Mitochondrial disease. *Lancet* 2006; 368: 70-82.
- Schapira AH, Cooper JM, Dexter D, Clark JB, Jenner P, Marsden CD. Mitochondrial complex I deficiency in Parkinson's disease. *J Neurochem* 1990a; 54: 823-7.
- Schapira AH, Cooper JM, Dexter D, Jenner P, Clark JB, Marsden CD. Mitochondrial complex I deficiency in Parkinson's disease. *Lancet* 1989; 1: 1269.
- Schapira AH, Mann VM, Cooper JM, Dexter D, Daniel SE, Jenner P, et al. Anatomic and disease specificity of NADH CoQ1 reductase (complex I) deficiency in Parkinson's disease. *J Neurochem* 1990b; 55: 2142-5.
- Scheffler IE. Mitochondria make a come back. *Adv Drug Deliv Rev* 2001; 49: 3-26.
- Schouten JP, McElgunn CJ, Waaijer R, Zwijnenburg D, Diepvens F, Pals G. Relative quantification of 40 nucleic acid sequences by multiplex ligation-dependent probe amplification. *Nucleic Acids Res* 2002; 30: e57.

- Schüle B, Kock N, Svetel M, Dragasevic N, Hedrich K, De Carvalho Aguiar P, et al. Genetic heterogeneity in ten families with myoclonus-dystonia. *J Neurol Neurosurg Psychiatry* 2004; 75: 1181-5.
- Schwalbe MW. Eine eigentümliche tonische Krampfform mit hysterischen Symptomen. Berlin, 1908: 36.
- Shimura H, Schlossmacher MG, Hattori N, Frosch MP, Trockenbacher A, Schneider R, et al. Ubiquitination of a new form of alpha-synuclein by parkin from human brain: implications for Parkinson's disease. *Science* 2001; 293: 263-9.
- Singleton AB, Farrer M, Johnson J, Singleton A, Hague S, Kachergus J, et al. alpha-Synuclein locus triplication causes Parkinson's disease. *Science* 2003; 302: 841.
- Steinlechner S, Stahlberg J, Volkel B, Djarmati A, Hagenah J, Hiller A, et al. Co-occurrence of affective and schizophrenia spectrum disorders with PINK1 mutations. *J Neurol Neurosurg Psychiatry* 2007; 78: 532-5.
- Strauss KM, Martins LM, Plun-Favreau H, Marx FP, Kautzmann S, Berg D, et al. Loss of function mutations in the gene encoding Omi/HtrA2 in Parkinson's disease. *Hum Mol Genet* 2005; 14: 2099-111.
- Swaans RJ, Rondot P, Renier WO, Van Den Heuvel LP, Steenbergen-Spanjers GC, Wevers RA. Four novel mutations in the tyrosine hydroxylase gene in patients with infantile parkinsonism. *Ann Hum Genet* 2000; 64: 25-31.
- Taanman JW. The mitochondrial genome: structure, transcription, translation and replication. *Biochim Biophys Acta* 1999; 1410: 103-23.
- Tan EK, Yew K, Chua E, Puvan K, Shen H, Lee E, et al. PINK1 mutations in sporadic early-onset Parkinson's disease. *Mov Disord* 2006; 21: 789-93.
- Tan EK, Yew K, Chua E, Shen H, Jamora RD, Lee E, et al. Analysis of PINK1 in Asian patients with familial parkinsonism. *Clin Genet* 2005; 68: 468-70.
- Tang B, Xiong H, Sun P, Zhang Y, Wang D, Hu Z, et al. Association of PINK1 and DJ-1 confers digenic inheritance of early-onset Parkinson's disease. *Hum Mol Genet* 2006; 15: 1816-25.
- Thobois S, Gervais-Bernard H, Xie-Brustolin J, Zyss J, Ostrowsky K, Broussolle E. Evidence for progressive changes in clinical presentation of myoclonus-dystonia. *Mov Disord* 2007; 22: 1516-7.
- Todd RD, Perlmutter JS. Mutational and biochemical analysis of dopamine in dystonia: evidence for decreased dopamine D2 receptor inhibition. *Mol Neurobiol* 1998; 16: 135-47.

- Toft M, Sando SB, Melquist S, Ross OA, White LR, Aasly JO, et al. LRRK2 mutations are not common in Alzheimer's disease. *Mech Ageing Dev* 2005; 126: 1201-5.
- Tormo JR, Estornell E. New evidence for the multiplicity of ubiquinone- and inhibitor-binding sites in the mitochondrial complex I. *Arch Biochem Biophys* 2000; 381: 241-6.
- Tsukihara T, Aoyama H, Yamashita E, Tomizaki T, Yamaguchi H, Shinzawa-Itoh K, et al. The whole structure of the 13-subunit oxidized cytochrome c oxidase at 2.8 Å. *Science* 1996; 272: 1136-44.
- Tsunoda SP, Aggeler R, Noji H, Kinosita K, Jr., Yoshida M, Capaldi RA. Observations of rotation within the F<sub>o</sub>F<sub>1</sub>-ATP synthase: deciding between rotation of the F<sub>o</sub>c subunit ring and artifact. *FEBS Lett* 2000; 470: 244-8.
- Unoki M, Nakamura Y. Growth-suppressive effects of BPOZ and EGR2, two genes involved in the PTEN signaling pathway. *Oncogene* 2001; 20: 4457-65.
- Valente EM, Abou-Sleiman PM, Caputo V, Muqit MM, Harvey K, Gispert S, et al. Hereditary early-onset Parkinson's disease caused by mutations in PINK1. *Science* 2004a; 304: 1158-60.
- Valente EM, Brancati F, Ferraris A, Graham EA, Davis MB, Breteler MM, et al. PARK6-linked parkinsonism occurs in several European families. *Ann Neurol* 2002; 51: 14-8.
- Valente EM, Edwards MJ, Mir P, DiGiorgio A, Salvi S, Davis M, et al. The epsilon-sarcoglycan gene in myoclonic syndromes. *Neurology* 2005; 64: 737-9.
- Valente EM, Salvi S, Ialongo T, Marongiu R, Elia AE, Caputo V, et al. PINK1 mutations are associated with sporadic early-onset parkinsonism. *Ann Neurol* 2004b; 56: 336-41.
- Vandesompele J, De Preter K, Pattyn F, Poppe B, Van Roy N, De Paepe A, et al. Accurate normalization of real-time quantitative RT-PCR data by geometric averaging of multiple internal control genes. *Genome Biol* 2002; 3: RESEARCH0034.
- Wallis DE, Roessler E, Hehr U, Nanni L, Wiltshire T, Richieri-Costa A, et al. Mutations in the homeodomain of the human SIX3 gene cause holoprosencephaly. *Nat Genet* 1999; 22: 196-8.
- Wang D, Qian L, Xiong H, Liu J, Neckameyer WS, Oldham S, et al. Antioxidants protect PINK1-dependent dopaminergic neurons in *Drosophila*. *Proc Natl Acad Sci U S A* 2006; 103: 13520-5.
- Weng YH, Chou YH, Wu WS, Lin KJ, Chang HC, Yen TC, et al. PINK1 mutation in Taiwanese early-onset parkinsonism : clinical, genetic, and dopamine transporter studies. *J Neurol* 2007; 254: 1347-55.

- Wharton DC, Tzagoloff A. Cytochrome oxidase from beef heart mitochondria. *Methods Enzymol* 1967; 10: 245–250.
- Wiegand G, Remington SJ. Citrate synthase: structure, control, and mechanism. *Annu Rev Biophys Biophys Chem* 1986; 15: 97-117.
- Williams SL, Scholte HR, Gray RG, Leonard JV, Schapira AH, Taanman JW. Immunological phenotyping of fibroblast cultures from patients with a mitochondrial respiratory chain deficit. *Lab Invest* 2001; 81: 1069-77.
- Winkler-Stuck K, Wiedemann FR, Wallesch CW, Kunz WS. Effect of coenzyme Q10 on the mitochondrial function of skin fibroblasts from Parkinson patients. *J Neurol Sci* 2004; 220: 41-8.
- Yang Y, Gehrke S, Imai Y, Huang Z, Ouyang Y, Wang JW, et al. Mitochondrial pathology and muscle and dopaminergic neuron degeneration caused by inactivation of *Drosophila Pink1* is rescued by Parkin. *Proc Natl Acad Sci U S A* 2006; 103: 10793-8.
- Yang Y, Ouyang Y, Yang L, Beal MF, McQuibban A, Vogel H, et al. Pink1 regulates mitochondrial dynamics through interaction with the fission/fusion machinery. *Proc Natl Acad Sci U S A* 2008; 105: 7070-5.
- Zadikoff C, Rogaeva E, Djarmati A, Sato C, Salehi-Rad S, St George-Hyslop P, et al. Homozygous and heterozygous PINK1 mutations: Considerations for diagnosis and care of Parkinson's disease patients. *Mov Disord* 2006; 21: 875-9.
- Zarranz JJ, Alegre J, Gomez-Esteban JC, Lezcano E, Ros R, Ampuero I, et al. The new mutation, E46K, of alpha-synuclein causes Parkinson and Lewy body dementia. *Ann Neurol* 2004; 55: 164-73.
- Zhang YH, Tang BS, Guo JF, Xia K, Xu B, Cai F, et al. [Mutation analysis of PINK1 gene in Chinese patients with autosomal recessive early-onset parkinsonism type 6]. *Zhonghua Yi Xue Za Zhi* 2005; 85: 1538-41.
- Zhang Z, Huang L, Shulmeister VM, Chi YI, Kim KK, Hung LW, et al. Electron transfer by domain movement in cytochrome bc1. *Nature* 1998; 392: 677-84.
- Zimprich A, Biskup S, Leitner P, Lichtner P, Farrer M, Lincoln S, et al. Mutations in LRRK2 cause autosomal-dominant parkinsonism with pleomorphic pathology. *Neuron* 2004; 44: 601-7.
- Zimprich A, Grabowski M, Asmus F, Naumann M, Berg D, Bertram M, et al. Mutations in the gene encoding epsilon-sarcoglycan cause myoclonus-dystonia syndrome. *Nat Genet* 2001; 29: 66-9.

## 9 APPENDIX

### 9.1 List of abbreviations

ACTB	–	Actin, beta
AD	–	Autosomal dominant
AR	–	Autosomal recessive
ARF1P1	–	ADP-ribosylation factor 1 pseudogene 1
ATP	–	Adenosine triphosphate
ATP1A3	–	ATPase alpha 3
ATP13A2	–	ATPase type 13A2
B2M	–	Beta 2-microglobulin
CI-IV	–	Complex I-IV activity
CASD1	–	CAS1 domain containing 1
cDNA	–	Copy (complementary) DNA
COL1A2	–	Collagen type I alpha 2 gene
CoQ1	–	Ubiquinone
CoQH <sub>2</sub>	–	Ubiquinol
CS	–	Citrate synthase activity
DAT	–	Dopamine transporter
$\Delta\psi_m$	–	Membrane potential
DJ-1	–	Amyotrophic lateral sclerosis-parkinsonism/dementia complex 2
D-Loop	–	Displacement loop
DLX5	–	Distal-less homeobox 5
DLX6	–	Distal-less homeobox 6
DNA	–	Deoxyribonucleic acid
Drp1	–	Dynamin-related protein 1
DSC3	–	Disease-specific sequence changes
DYT	–	Dystonia
EJC	–	Exon-junction complex
EPS	–	Extrapyramidal system
ETC	–	Electron transport chain
F	–	Family member
Fis1	–	Fission 1 (mitochondrial outer membrane) homolog ( <i>S. cerevisiae</i> )
FISH	–	Fluorescent in situ hybridization

---

FL	–	Fluorescence emission
GCH1	–	GTP cyclohydrolase 1
GPi/e	–	Internal/external globus pallidus
GSH	–	Reduced glutathione
HMBS	–	Hydroxymethylbilane synthase
HPLC	–	High-performance liquid chromatography
HPRT1	–	Hypoxanthine phosphoribosyltransferase 1
IP	–	Index patient
IRD	–	Infrared dye
L-Dopa	–	Levo-dopa
LGS	–	Langer-Giedion syndrome
LOC644604	–	Similar to eukaryotic translation elongation factor 1 alpha 2
LRRK2	–	Leucine-rich repeat kinase 2
MAF	–	Minor allele frequency
M-D	–	Myoclonus dystonia
MDHM	–	Mitochondrial malate dehydrogenase
MLPA	–	Multiplex ligation-dependent probe amplification
MPTP	–	1-methyl 4-phenyl 1,2,3,6-tetrahydropyridine
MR-1	–	Myofibrillogenesis regulator 1
mRNA	–	Messenger ribonucleic acid
Mut	–	Mutant
NMD	–	Nonsense-mediated mRNA decay
Omi/HtrA2	–	HtrA serine peptidase 2
PAGE	–	Polyacrylamide gel electrophoresis
PCR	–	Polymerase chain reaction
PD	–	Parkinson's disease
PEG 10	–	Paternally expressed 10
PINK1	–	PTEN-induced putative kinase 1
PRKRA	–	Protein kinase, interferone-inducible double stranded RNA dependent activator
qPCR	–	Quantitative PCR
SDH	–	Succinate dehydrogenase
SDHA	–	Succinate dehydrogenase complex, subunit A
SGCE	–	Epsilon-sarcoglycane

---

SHFM1	–	Split-hand/splitfoot malformation 1
SN	–	Substantia nigra
SNCA	–	Alpha-synuclein
SNP	–	Single nucleotide polymorphism
SOD2	–	Superoxide dismutase 2
SVA	–	SINE-VNTR-Alu
SYBR	–	Synergy Brands, inc.
TAF1	–	TAF1 RNA polymerase II
TH	–	Tyrosine hydrolase
TK2	–	Thymidine kinase 2
TRAP1	–	TNF receptor-associated protein 1
UBE2D2	–	Ubiquitin-conjugating enzyme E2D 2
UCH-L1	–	Ubiquitin C-terminal hydrolase-L1
UCL	–	University College London
UPDRS	–	Unified Parkinson's Disease Rating Scale
UPS	–	Ubiquitin proteasomal system
Wt	–	Wildtype
X	–	X-chromosomal
XR	–	X-chromosomal recessive
YWHAZ	–	Tyrosine 3-monooxygenase/tryptophan 5-monooxygenase activation protein, zeta polipeptide

## 9.2 Supplementary material

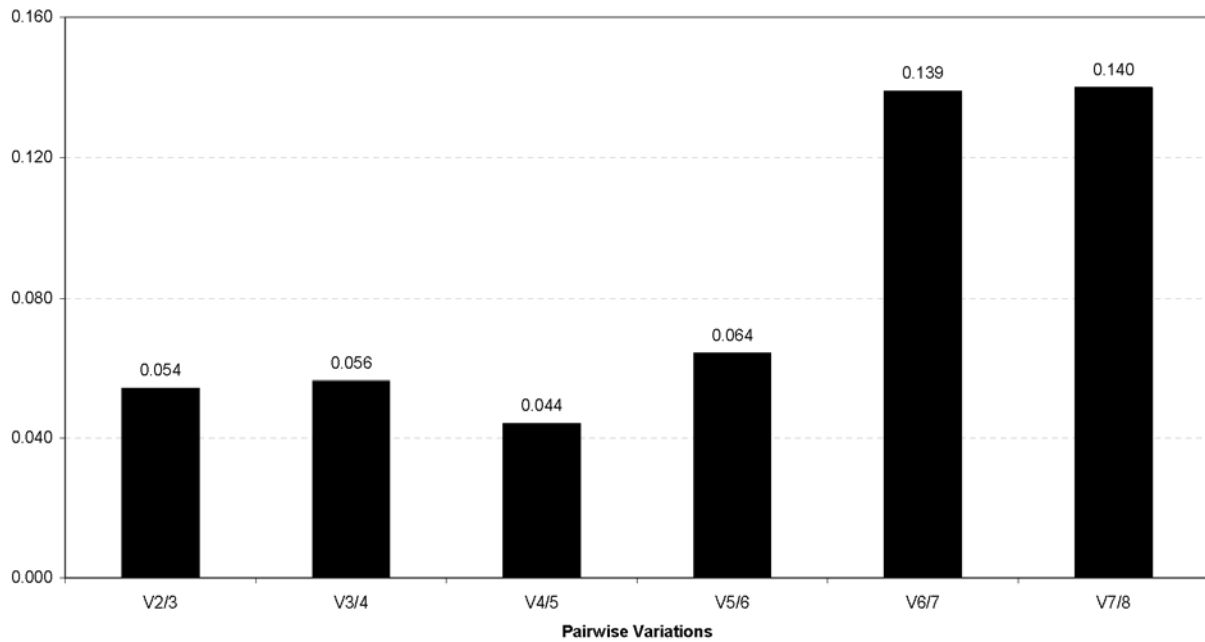


**Fig S1** Determination of the optimal number of control genes for normalization. By pairwise variation ( $V_n/n+1$ ) analysis, a total of two reference genes is shown to be sufficient for the real-time approach ( $V_{2/3} < \text{threshold of } 0.15$ ) (Vandesompele *et al.*, 2002).

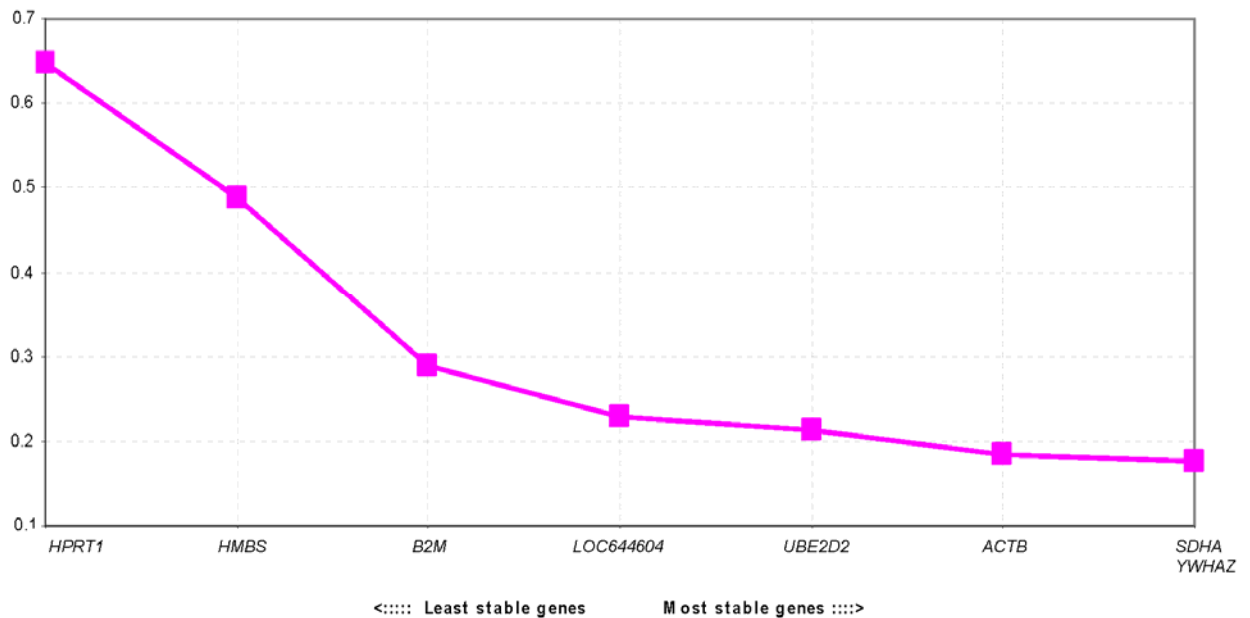


**Fig S2** Average expression stability values ( $M$ ) of reference genes calculated by the *geNorm VBA* applet. In the diagram, the eight reference genes with the highest PCR amplification efficiency are ranked according to their expression stability.

**Table S1** *Primer for PCR-amplification of SGCE genomic fragments*

Exon	Forward primer sequence	Reverse primer sequence	Amplicon size
1	CTGTAGCTGAACTGGCCAAG	AGAGAGGCTGGTGCCCAAAG	304 bp
2	CTGAATTATCAAGGGCGTATC	CCATTTGAAATAATGTTAATG	295 bp
3	AGACAGAATGTTTTGATTGAAAC	ACCACCATCAGGTAAGTTTAG	355 bp
4	TTCTCATTGCCAGAGAAGG	TCAGTTATATTAGGTATGTGGC	339 bp
5	CTTCATTAAGATATGCATGC	ATAAGTTTGATAAGATCACCG	306 bp
6	TAAATCCTGCTTTAAGGTGG	TTATTCCTAAAAGCAGTTCAG	335 bp
7	AAGAATGCTTTAGTGTATCCAG	TTGTTATCTTAGCAGGATCTC	348 bp
8	GACAATGTCAGCATTCCAC	GTTTTAGTTTCTACCCCTCT	309 bp
9	CAAATTGATGCCCATCAGGC	CATGCATATTAATAATTATGGCTC	295 bp
10	TAATGTAGCCTAGTGCCAC	AGCCAACCTCATGACTTCTAG	448 bp
11	CTGGGGTCATAGTTTACCCG	ATTTGGTGAAGATAAAGCTTC	249 bp
12	GATGGAACTTTCTCCTTGCC	CAACATGCATAACATATGCCAG	230 bp

**Table S2** *Primer for gene dosage quantification of SGCE exons*

SGCE Exon	Forward primer sequence	Reverse primer sequence	Amplicon size
3	GGCGAGATTAGTAATBATCCC	TTACCTCAATGATTGTTGGC	163 bp
4	GATAACTGCCTACAACAGGCG	CATACCTACCTTCTGCAGAC	83 bp
6	CTACCTCAGGGATGAGTCTAG	CTCAAGGGAAGTCAACTGCAG	418 bp
8	GACAATGTCAGCATTCCAC	GTTTTAGTTTCTACCCCTCT	291 bp
9	CCAACTGGTCCATCACAGTG	GTGTGTAAGGTATGATTTC	144 bp
11	CTGGGGTCATAGTTTACCCG	CCTCCATGGATGCTTTTGCTC	385 bp
12	GATGGAACTTTCTCCTTGCC	CAACATGCATAACATATGCCAG	230 bp
Beta-globin	ACACAACCTGTGTTCACTAGC	CAACTTCATCCACGTTCCACC	352 bp

**Table S3** *Primer for PCR-amplification of PINK1 genomic fragments*

Exon	Forward primer sequence	Reverse primer sequence	Amplicon size
1a	CCCCAAGTTTGTGTGACC	CGAAGGCCAGAAAGACTGC	394 bp
1b	CCGCTTCTTCGCCAGTCG	GATGAGCTTTAAGGACCCTCG	329 bp
2	GGCTGAGCAGTAGAACCTGG	CCACTAAGATGGCATTGAG	504 bp
3	CAGGTCATCTTATCTCGAAGG	GCATCATCATTTGGGGTCAG	432 bp
4	GAATGTCAGTGCCAGTGTTG	CCTGATCAAGGTGCACATGG	366 bp
5	CGTATTGGGAGTCGTCGATG	GACCTGAAGAGTCAGTCCTAAA	300 bp
6	TGACCTCCTGGGCCAACAC	TCACAAGGCATCGAGTCTCC	343 bp
7	GAGTTCAGATTAGCCCATGG	ATCTGTCACTGTGGCTCTGG	430 bp
8	AGACCCTCACTAACAAAGCAG	CCTTTTCCGGCTAACAGCCC	466 bp

**Table S4** *Primer for the quantification of the PINK1 expression level***PCR amplification of PINK1**

Variant	Forward primer sequence	Reverse primer sequence	Amplicon size
c.373T>G	TCCAGGCTGGGCCGAGGACC	GCCCTATCAGATACTCCTCC	344 bp
c.1366C>T	CCCTTCAGCAGCTGGTACGT	GGTCAGGCCCGGCTTGC	448 bp

**Real-time PCR assays***Target gene*

Gene name	Gene bank accession #	Forward primer sequence	Reverse primer sequence
<i>PINK1</i>	Ex2-3 NM_032409	TTCCCCTTGGCCATCAAGA	ACCAGCTCCTGGCTCATTGT
	Ex5-6	ATCGCGCACAGAGACCTGA	AGCAGCCAAAATCTGCGATC
	Ex7-8	GTCAGTGCCTCCAGACGTGA	CACATTTGCGGCTACTCGG

*Reference genes*

Gene name	Gene bank accession #	Forward primer sequence	Reverse primer sequence
<i>ACTB</i> –assay 1	NM_001101	CTGGAACGGTGAAGGTGACA	AAGGGACTTCCTGTAACAATGCA
<i>ACTB</i> –assay 2	NM_001101	AACCGCGAGAAGATGACCC	GCCAGAGGCGTACAGGGATAG
<i>HMBS</i>	NM_000190	GGCAATGCGGCTGCAA	GGGTACCCACGCGAATCAC
<i>HPRT1</i>	NM_000194	TGACACTGGCAAACAATGCA	GGTCCTTTTCACCAGCAAGCT
<i>LOC644604</i>	XM_934145	CAAGCCCATGTGTGTTGAGA	TCCACTGCTTTGATGACACC
<i>UBE2D2</i>	NM_181838	GATCACAGTGGTCTCCAGCA	CGAGCAATCTCAGGCACTAA
<i>YWHAZ</i>	NM_145690	CAGAGAGAAAATTGAGACGGAGCT	CTTTGCTCTCTGCTTGTGAAGC
<i>SDHA</i>	NM_004168	GTTGTCTTTGGTCGGGCATG	CCAGCGTTTGGTTAATTGGAG
<i>B2M</i>	NM_004048	ACCATGTGACTTTGTACAGCC	AAATGCGGCATCTTCAAACC

### 9.3 Curriculum vitae

#### BIOGRAPHICAL INFORMATION

Date of Birth: 27/02/1982  
Place of Birth: Chemnitz, Germany  
Marital Status: single

#### EDUCATION

1992 – 2000 Johann-Wolfgang-von-Goethe-Gymnasium in Chemnitz;  
Profile: Natural Sciences (advanced courses: Biology, German)  
“Abitur” certificate, mark: “good” (1.7)  
2000 – 2005 University of Applied Science Jena;  
Prediploma, mark: “good” (2.4)  
Graduate engineer degree (Dipl.-Ing., FH), mark: “very good” (1.5)  
2005 – 2008 Faculty of Neurology at the University of Lübeck; PhD studies

#### SCIENTIFIC TRAINING

06 – 09/2000 INNOVENT e.V., Department of Biochemistry, Jena. Practical training as an admission condition for studies at the University of Applied Sciences Jena. Surface coating of metals with biopolymers.  
07 – 09/2002 INNOVENT e.V., Department of Biochemistry, Jena. Student assistant. Optimization of an assay for phosphate detection. Creation of a practical course for trainees in Biology.  
04 – 08/2003 Centre National de la Recherche Scientifique, Institute of Functional Genomics (Laboratory of Professor P. Marin), Montpellier. Practical semester. Proteomics: Search for interaction partners of the metabotropic glutamate receptor 7b (mGluR7b).  
2004 – 2005 University of Göttingen, European Neuroscience Institute (Laboratory of Professor S. Sigrist), Göttingen. Diploma thesis, mark: “very good” (1.0). In vivo imaging of the neuromuscular junction in *Drosophila melanogaster*.  
2005 – 2008 University of Lübeck, Department of Neurology/Neurogenetics (Laboratory of Professor C. Klein), Lübeck. PhD studies (current position). Molecular characterization of neurological disorders (M-D and PD).

- 04 – 06/2006 Erasmus MC, Department of Clinical Genetics (Laboratory of Professor V. Bonifati), Rotterdam. Expression analysis of *PTEN-induced kinase 1* (*PINK1*).
- 07/07 – 02/08 University College London, Royal Free University and Medical School, London. Department of Clinical Neurosciences (Laboratory of Professor A. Schapira). Investigation of the mitochondrial function in fibroblast cultures from PD patients with mutations in *PINK1*.

### **LANGUAGE SKILLS**

- German Native speaker
- English Excellent knowledge
- French Good knowledge

### **FELLOWSHIPS**

- 04 – 08/2003 DAAD travel student fellowship (LEONARDO DA VINCI II program)
- 09 – 12/2007 DAAD graduate student short term fellowship, grant # D/07/44883

### **SUPERVISION AND TEACHING EXPERIENCE**

- 2005 – 2008 Supervision of practical work of two Bachelor of Sciences students at the University of Lübeck, Germany.
- 07/2008 Teaching and supervision in a genetics course for pupils (9th grade) of the Katherineum, Lübeck, Germany.

### **MISCELLANEOUS**

- 07/2007 Proposal:  
Participation in a successful application of the University of Lübeck for support of a “Graduate School for Computing in Medicine and Life Sciences” by the German Research Foundation (5 Million Euro funding).

## 9.4 Publications

### ORIGINAL ARTICLES

1. Klein C, **Grünwald A**, Hedrich K. Early-onset parkinsonism associated with PINK1 mutations: frequency, genotypes, and phenotypes. *Neurology* 2006; 66: 1129-30; author reply 1129-30. (IF: 5.690)
2. Hedrich K, Hagenah J, Djarmati A, Hiller A, Lohnau T, Lasek K, **Grünwald A**, *et al.* Clinical spectrum of homozygous and heterozygous PINK1 mutations in a large German family with Parkinson disease: role of a single hit? *Arch Neurol* 2006; 63: 833-8. (IF: 5.204)
3. **Grünwald A**, Breedveld GJ, Lohmann-Hedrich K, Rohe CF, König IR, Hagenah J, *et al.* Biological effects of the PINK1 c.1366C>T mutation: implications in Parkinson disease pathogenesis. *Neurogenetics* 2007;8:103-9. (IF: 4.250)
4. Djarmati A, Guzvic M (equally contributed), **Grünwald A**, Lang AE, Pramstaller PP, Simon DK, *et al.* Rapid and reliable detection of exon rearrangements in various movement disorders genes by multiplex ligation-dependent probe amplification. *Mov Disord* 2007; 22: 1708-14. (IF: 3.323)
5. **Grünwald A**, Djarmati A, Lohmann-Hedrich K, Farrell K, Zeller JA, Allert N, *et al.* Myoclonus-dystonia: significance of large SGCE deletions. *Hum Mutat* 2008; 29: 331-2. (IF: 6.894)
6. Orth M, Djarmati A, Baumer T, Winkler S, **Grünwald A**, Lohmann-Hedrich K, *et al.* Autosomal dominant myoclonus-dystonia and Tourette syndrome in a family without linkage to the SGCE gene. *Mov Disord* 2007; 22: 2090-6. (IF: 3.323)
7. Paus S, **Grünwald A**, Klein C, Knapp M, Zimprich A, Janetzky B, *et al.* The DRD2 TaqIA polymorphism and demand of dopaminergic medication in Parkinson's disease. *Mov Disord* 2008; 23: 599-602. (IF: 3.323)
8. Brüggemann N, Odin P, **Grünwald A**, Tadic V, Hagenah J, Seidel G, Lohmann K, Klein C, Djarmati A. De novo  $\alpha$ -Synuclein duplication as cause of sporadic early onset parkinsonism. *Neurology*; in press. (IF: 5.690)
9. **Grünwald A**, Gegg ME, Taanman JW, Klein C, Schapira AHV. Differential effects of PINK1 nonsense and missense mutations on mitochondrial function and morphology. *Neurobiol Dis*; in preparation.

Up to now eight original articles were published, among these two are first author papers. The publications have a cumulative impact factor (IF) of 37.697 and an average of 4.712.

**ABSTRACTS**

1. **Grünwald A**, Djarmati A, Lohmann-Hedrich K, Farrell K, Klein C. Phenotypes and genotypes in myoclonus-dystonia: Significance of deletions of the SGCE gene. *Mov Disord* 2007; 22 (Suppl. 16): A442.
2. Fung VSC, Mahant N, Sue CM, **Grünwald A**, Klein C. Autosomal dominant myoclonus dystonia: Unusual phenotype with prominent hypotonia/motor impersistence and positive celiac serology. *Mov Disord* 2007; 22 (Suppl.16): A143.
3. **Grünwald A**, Gegg ME, Taanman JW, Schapira AHV, Klein C. Mitochondriale Funktion und Morphologie bei PINK1-assoziiertem Parkinson-Syndrom. *DGN* 2008.
4. **Grünwald A**, Gegg ME, Taanman JW, Klein C, Schapira AHV. Differential effect of PINK1 nonsense and missense mutations on mitochondrial function and morphology. *DGNG* 2008. Accompanying booklet: P6.

**ORAL PRESENTATIONS**

1. **Grünwald A**, Djarmati A, Lohmann-Hedrich K, Farrell K, Klein C. Phenotypes and genotypes in myoclonus-dystonia: Significance of deletions of the SGCE gene. 11th Annual Congress of the Movement Disorders Society: Highlights of Posters Sessions 1, Istanbul, Turkey, June 2007.

## 9.5 Acknowledgements

The work presented in this thesis was performed in the Neurogenetics Group under the supervision of Professor Christine Klein at the University of Lübeck, Lübeck, Germany. Some of the experiments were carried out in Professor Vincenzo Bonifati's Department of Clinical Genetics at the Erasmus MC, Rotterdam, The Netherlands. Furthermore, a part was conducted at the Department of Clinical Neurosciences at the University College London, London, UK under the supervision of Professor Anthony Schapira.

I would like to begin by thanking Professor Enno Hartmann, the Head of the Institute of Biology, for the representation of this thesis at the Faculty of Natural Sciences of the University of Lübeck.

I am deeply indebted to my supervisor Professor Christine Klein whose support, stimulating suggestions and encouragement helped me throughout my time of research and while writing this thesis. I am very thankful for her critical review of my publications and for the scientific freedom. Furthermore, I would like to thank her for the opportunity to gain international experience at the laboratories of Professor Vincenzo Bonifati and Professor Anthony Schapira.

My colleagues from the Neurogenetics Group in Lübeck greatly supported me throughout my research period. I would like to cordially thank all of them for their continuous interest, patience, help, and valuable hints. Especially, I am obliged to Dr. Katja Lohmann, Dr. Ana Djarmati, Dr. Slobodanka Orolicki and Dr. Norman Kock. Philip Seibler, my Mensa associate, and Aleksandar Raković taught me how to believe in the impossible. I also want to thank Sylwia Dankert, Thora Lohnau, Karin Wieggers, Heike Pawlak and Susen Winkler for their technical assistance, advice and for creating a lovely atmosphere in the lab.

Professor Anthony Schapira I would like to thank for the warm welcome in his department and Dr. Willem Taanman for introducing me to the world of mitochondria. Dr. Matthew Gegg kindly shared all his mitochondria knowledge with me and thoroughly reviewed the final version of this thesis. I thank him for his scientific advice and his incredible patience when teaching me how to perform kinetic assays.

I would like to thank my friends from the “Röntgen-Straße”. Astrid Büchler, Henrike Preis, Michael Glodek, Winfried Schöch, Dennis Pfisterer and Marie-Christine Kuhl: You turned my time in Lübeck into the best period of my entire studies. I cherish our many ventures together and hope that we will be able to stay in touch despite the distances that may come between us.

From Todor Kondić I have learned to always think positive.

I would like to give my special thanks to my parents, grandparents and my godmother who believed in me and whose love enabled me to complete this work.

Finally, of course there are many other co-workers who I collaborated with during my research period, and many dear friends who accompanied me all along, who I am grateful to and I apologize if I may have forgotten to mention them individually.

## 9.6 Declaration

Ich versichere, dass ich die Dissertation ohne fremde Hilfe angefertigt und keine anderen als die angegebenen Hilfsmittel verwendet habe.

Weder vor noch gleichzeitig habe ich andernorts einen Zulassungsantrag gestellt oder diese Dissertation vorgelegt.

Ich habe mich bisher noch keinem Promotionsverfahren unterzogen.

Anne Grünewald

Lübeck, 22.10.2008